NTNU – Trondheim
Norwegian University of
Science and Technology

SIMULATION OF RISER DISCONNECTION IN STOCHASTIC WAVES

Helene Ruth Minet Kinge

Marine Technology
Submission date: December 2014
Supervisor: Carl Martin Larsen, IMT
Co-supervisor: Geir Magnus Knardahl, Aker Solutions

Norwegian University of Science and Technology
Department of Marine Technology

NTNU Trondheim
Norwegian University of Science and Technology
Faculty of Engineering Science and Technology
Department of MarineTechnology

M.Sc. thesis 2014

for

Stud. tech. HELENE KINGE

SIMULATION OF RISER DISCONNECT IN STOCHASTIC WAVES

Planned disconnection of workover risers might become needed due to floater drift- or drive-off, or expectation of unacceptable weather conditions during coming hours. The procedure for disconnection may vary depending on the situation, but the common goal must be to avoid damage of the heave compensation system for riser and drillstring, and also unwanted contact between the lower riser end and the remaining structure on the bottom. Precautions to protect the heave compensators deals with valve operations to control fluid flow in the hydraulic system, while optimum timing of disconnection relative to floater motions is needed to avoid the second type of event. The purpose of the present work is to study the risk of contact between riser end and bottom structure, and propose a strategy for timing that will reduce this risk.

The work might be divided into tasks as follows:

1. Literature study, which should cover the design of a typical workover riser system, operation procedures and procedures for riser disconnection under varying conditions.
2. Simulate a large number of disconnection events under varying wave conditions and random point of time for disconnection. The RIFLEX/SIMA software should be applied in this study.
3. Propose a method for deciding the point of time for disconnection based on information that is available to the operators on the platform, and the time lag between the initiation of disconnection and separation between riser end and bottom structure
4. Simulate a set of disconnections when the proposed procedure is followed, and compare the result in terms of probability of contact for random and planned point of time for initiating disconnection.

The work may show to be more extensive than anticipated. Some topics may therefore be left out after discussion with the supervisor without any negative influence on the grading.

The candidate should in her/his report give a personal contribution to the solution of the problem formulated in this text. All assumptions and conclusions must be supported by mathematical models and/or references to physical effects in a logical manner.

The report should be well organised and give a clear presentation of the work and all conclusions. It is important that the text is well written and that tables and figures are used to support the verbal presentation. The report should be complete, but still as short as possible.

The final report must contain this text, an acknowledgement, summary, main body, conclusions and suggestions for further work, symbol list, references and - if appropriate -appendices. All figures, tables and equations must be identified by numbers. References should be given by author name and year of publication in the text, and presented alphabetically by name in the reference list.

From the report it should be possible to identify the work carried out by the candidate and what has been found in the available literature. It is important to give references to the original source for basic information and applied theories.

The work will be carried out in cooperation with Aker Solutions. Contact person will be Geir Magnus Knardahl.

Supervisor at NTNU is Professor Carl M. Larsen

Trondheim, August 2014

Carl M. Larsen

Submitted: August 2014

Deadline: December 2014

PREFACE

This Master Thesis is a result of finishing my M.Sc. degree at the Norwegian University of Science and Technology fall 2014. My field of study is Marine Technology with a specialization within Hydrodynamics. The Thesis has been carried out in cooperation with Aker Solutions Workover Systems. The scope for this Thesis is to perform a Stochastic Disconnection Analysis of the Workover riser in the computer program RIFLEX. Furthermore the purpose of conducting a disconnection analysis is to study the critical event of collision between the Emergency Disconnect Package and Lower Riser Package.

In advance of working with this Thesis I had written the Project Thesis. This provided me with knowledge about the Workover System, the background theory and the analysis. The relevant theoretical parts from the Project Thesis have therefore been applied in the Master Thesis. The process of writing this Master Thesis has been both challenging and evolving. There does not exist a lot of documentation regarding disconnection. Thus, it has been challenging to retrieve this information. Furthermore, how to conduct the analyses and what to focus on has been challenging to figure out.

I would like express my deepest thanks to my supervisor at NTNU Carl Martin Larsen for very good guidance and help throughout the process. He's door is always open and his knowledge is greatly appreciated. I would also like to thank my supervisor from Aker Solutions Geir Magnus Knardahl, for providing me with information regarding the Workover System and for great feedback and guidance. Additionally I would like to thank Andreas Amundsen from MARINTEK for help in RIFLEX. The RIFLEX model has been provided from a former student Lars Hermanrud, I would therefor like to thank him as well. Finally, I would like to thank my family and fellow students at Tyholt for sharing their experience and knowledge.

Trondheim, 19 December 2014

Helene Ruth Minet Kinge

SUMMARY

Ever since the first oil was discovered in Norway in 1971 the production rates have varied. The development has gone from few wells with high production rates to several wells with lower production rates. It is expected that the production rate will continue to decrease in the future. Taking this into consideration, it is apparent that operations which will enhance the production rate are important. Workover operations are operations where the well is cleaned out, which enhances the production rate. Moreover, Workover operations are conducted with a Workover Riser Systems. The Workover riser system is a long slender structure stretching from the vessel down to the sea bed, which is exposed to loads from the environment and the platform.

If a storm is coming and the operational limits are expected to be exceeded, the system has to perform a planned/normal disconnection. The disconnection takes place between the Emergency Disconnect Package (EDP) and the Lower Riser Package (LRP). This is done to prevent damage to the components, especially the well head. The criteria for conducting disconnection are defined in the operation envelopes. When a planned/normal disconnection is performed there are some critical scenarios that should be avoided. On such scenario is collision between the EDP and the remaining structure at the sea bed, the LRP. The scope of this Master Thesis is to study this event, collision between these two components. The purpose is to study the risk of contact between the Emergency Disconnect Package and the Lower Riser Package and propose a strategy for reducing it.

To study the collision event the computer program RIFLEX has been applied. Two different models have been developed, both are based on the model applied in the Project Thesis. One model on -348m water depth and one model on -996m water depth. Several analyses and disconnection events have been conducted. The first set of analysis conducted is the different disconnection events. These events are disconnection at heave displacement top, heave displacement bottom, half way up the heave displacement (max velocity) and a random in time. The vertical displacement of the EDP after disconnection is studied. Additionally, a mean study has been performed in order to determine the trend for the vertical displacement after disconnect. Based on the different disconnection events, a probability study has been performed to study the frequency of hits. To enable for the probability study a MATLAB script has been developed. This checks if the EDP is within the limits of the LRP.

Moreover, a correlation study has been performed. This has been done to determine if there exists a relation between the vertical velocity 30 seconds in advance of disconnection and at the actual disconnection timing. The reason for studying a 30 seconds time interval is because this is the time it takes for the electrical signal to be sent from the platform down to EDP.

Finally, the last set of analyses which have been completed is disconnection analyses with riser lift up. When the disconnection is done the riser is lifted up 2-4 meters. A set of random disconnection events with retraction for both the shallow and deep water model has been conducted.

The results from the different disconnection events show that when the disconnection is performed at the heave displacement top, the EDP will experience a negative vertical displacement immediately after disconnection. Simultaneously as the EDP is disconnected the riser is locked to the vessel at the top. For disconnection at heave displacement top it is locked at a higher location in the riser, this leads to a longer effective length of the riser underneath the vessel. Thus, the mean vertical displacement is below the location of the LRP. The results from the mean study show that the trend is an immediate negative displacement after disconnect. Additionally, the probability study shows that disconnection at the heave displacement top, has the highest mean percent of time when the EDP is within the LRP limits.

On the other hand, the results from disconnection at the heave displacement bottom show that the EDP will have displacement in positive z-direction, and the mean vertical displacement is above the location of the LRP. The mean percentage of time the EDP is within the limits of the LRP, is zero. When the disconnection is performed in the middle of the heave displacement, the average value of the mean vertical displacement lies at the initial position of the EDP. The mean percent of time the EDP is within the LRP limits is the second lowest. The results from the random disconnection show that the mean percent of time the EDP is within the limits of the LRP, is the second highest. Therefore it can be concluded that the most critical disconnection is the disconnection at the heave displacement top. The second most critical is the random disconnection. However, to avoid collision the most optimal disconnection event is disconnection at the heave displacement bottom.

Finally, riser disconnection analyses with a 0-4 meter lift-up have been performed for the deep and shallow water model. Before the disconnection is performed the riser is retracted 2-4 meters to avoid collision. The results from these analyses show that when the riser is lifted up either two or four meters there is a significant clearance between the EDP and LRP. However, the analysis was also done with zero and one meter retraction, which illustrated that the number of hits is lower for the deep water model than the shallow water model. This may have to do with the length of the riser that is exposed to the current. The deep water model will therefore have a bigger horizontal displacement. From these results it can be concluded that if the riser is lifted up a minimum of two meters, it is likely that the EDP will never collide with the LRP.

SAMMENDRAG

Helt siden oljeeventyret startet i Norge i 1971 har det vært store endringer i produksjonsraten. Utviklingen har gått fra få oljebrønner med høy produksjonsrate, til mange brønner med lavere produksjonsrate. Videre er det forventet at produksjonsraten vil minke ytterligere. Når man tar denne trenden med i betraktning ser man at systemer som øker produksjonsraten er viktig. Brønnoverhalingssystemer gjennomfører operasjoner som øker produksjonsraten. Slike operasjoner blir gjort med arbeidsstigerør som er utsatt for diverse laster fra miljøet og fartøyet.

Hvis en storm er på vei og det er forventet at operasjonsområdet vil bli oversteget er man nødt til å gjennomføre en planlagt frakobling av stigerørsystemet. Dette blir gjort for å beskytte komponenter i stigerøret og hovedsakelig brønnhodet. Kriteriet for å gjennomføre en slik frakobling defineres i et operasjonsvindu. Ved gjennomføring av en frakobling er det noen kritiske scenarier som kan inntreffe. Et av disse scenariene er kollisjon mellom den gjenværende komponenten på havbunnen (LRP) og komponenten som gjennomfører frakoblingen(EDP). Hensikten og målet med denne Masteroppgaven er å studere denne hendelsen, og finne et optimalt tidspunkt for å gjennomføre en frakobling.

For å studere denne hendelsen benyttes dataprogrammet RIFLEX. To ulike modeller på forskjellig vanndyp har blitt utviklet, henholdsvis ved -348m og -996m. Videre er fire ulike frakoblingstilfeller studert; frakobling på toppen av hiv-forskyving, bunnen av hiv-forskyvingen, halvveis opp i hiv-forskyvingen og på et tilfeldig tidspunkt i hiv-forskyvingen. Den vertikale forskyvingen for EDP'en etter frakobling er studert. Basert på de vertikale forskyvningene er et gjennomsnittsstudie utført. Videre har et sannsynlighetsstudie blitt gjort ved hjelp av et MATLAB script. MATLAB scriptet undersøker om bevegelsen til EDP'en er innenfor lokasjonen til LRP'en.

For å undersøke om det eksisterer en relasjon mellom de vertikale hastighetene i tidspunktet ved frakobling og 30 sekunder før, er et korrelasjonsstudie utført. Grunnen til å studere et tidsintervall på 30 sekunder, er fordi det er tiden det tar fra signalet er sendt fra plattformen, til frakoblingen inntreffer. De siste simuleringene som er gjennomført er frakoblingsanalyser med hevning av stigerøret i toppen. Dette blir gjort for å unngå kollisjon mellom EDP'en og LRP'en.

Resultatene fra de ulike frakoblingtilfellene viser at når frakobling intreffer på topp av hiv-forskyvningen vil EDP'en ha en direkte negative vertikal forskyvning. På samme tidspunkt som frakoblingen skjer vil stigerøret låses til plattformen. Når dette skjer på topp av hiv-forskyvingen, vil en lengre del av stigerøret havne under plattformen. Dette medfører at den gjennomsnittlige vertikal forskyvning ligger under lokasjonen til LRP'en. Resultatene fra gjennomsnittstudiet underbygger dette, man ser at det vil være en direkte vertikal forskyvning i negativ z-retning. Videre ser man fra sannsynlighetsstudiet, at frakobling på topp av hiv-bevegelsen fører til høyest gjennomsnittlig prosent av tid hvor EDP'en er innenfor grensene til LRP'en.

På den andre siden viser resultatene fra frakobling i bunn av hiv-forskyvingen at EDP'en vil ha en forskyvning i positiv z-retning direkte etter frakobling. Gjennomsnitts-vertikalforskyvning ligger over lokasjonen til LRP'en og gjennomsnittsprosenten av tid EDP er innenfor grensen til LRP er lik null. Når frakoblingen blir gjennomført halvveis opp i hiv-forskyvingen ligger gjennomsnittsforskyvning for EDP'en ved utgangs-posisjonen til EDP'en. Gjennomsnittsprosenten av tid hvor EDP'en er innenfor LRP'en er nest minst. Videre viser resultatene fra den tilfeldige frakoblingen at gjennomsnitts-prosenten av tiden hvor EDP'en er innenfor grensene til LRP'en er nest størst. Basert på resultatene kan det bli konkludert med at den mest kritiske frakoblingen skjer på topp av hiv-forskyvingen og den minst kritiske skjer i bunn av hiv-forskyvingen.

Til slutt har frakoblinghendelsene blitt studert med hevning av stigerøret. Stigerør-systemet heves vanligvis 2-4m samtidig som frakobling. Analyser med hevning av stigerørsystem har derfor blitt gjennomført for begge vanndypsmodellene. Resultatene viser at når riseren heves enten to eller fire meter er det en signifikant klaring mellom EDP'en og LRP'en. Analysene har også blitt gjennomført for null og èn meter hevning. For disse hendelsene vil kollisjon inntreffe. Imidlertid, viser resultatene at gjennomsnittlig prosent av tid hvor EDP er innenfor grensene til LRP er lavere for modellen på dypt vann enn på grunt vann. Grunnen til dette er at strømningen som virker på stigerøret vil ha en lengre del å virke på for dypt vann enn for grunt. Dette vil gi en større horisontal forskyvning for dypt vann. Basert på dette kan det konkluderes med at hvis stigerøret er løftet opp enten to eller fire meter er det liten sannsynlighet for kollisjon.

TABLE OF CONTENTS

LIST OF FIGURES

LIST OF TABLES

ABBREVIATIONS

AKSO	Aker Solutions
BOP	Blow Out Preventer
CTTF	Coiled Tubing Tension Frame
DNV	Det Norske Veritas
DPLS	Drill Pipe Landing String
EDP	Emergency Disconnect Package
EQD	Emergency Quick Disconnect
FEM	Finite Element Method
GRA	Global Riser Analysis
LRP	Lower Riser Package
NPD	Norwegian Petroleum Department
RP	Recommended Practice
SFT	Surface Flow Tree
SLS	Simplified Landing String
SSTT	Subsea Test Tree
TH	Tubing Hanger
VIV	Vortex Induced Vibrations
WH	Well Head
WOS	Workover Systems
XMT	Christmas Tree
XTAC	Christmas Tree Adaptor Connector

1. INTRODUCTION

Since the oil adventure started in Norway in 1971 the production rates have changed over time, see (Norwegian Petroluem Directorate , 2014). The trend in the beginning was few fields with high production rates. This trend has developed into many fields with significantly lower production rates, seen in **Figure 1**. Additionally, the old fields have moved into a mature stage where the production rates are declining.

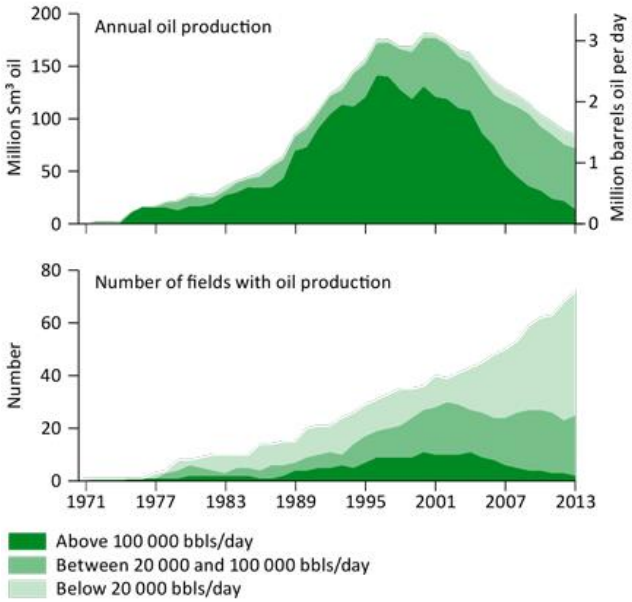

Figure 1: Production rates over time (Norwegian Petroluem Directorate , 2014)

The production rates are in general decreasing and it is expected that they will continue to decrease.

Taking this into consideration, it is apparent that operations which increase the production rates are essential. The main purpose of conducting a Workover Operation is to increase the production rate of the well. Hence, Workover Operations becomes more important. Workover Operations are conducted with a Workover Riser which is exposed to loads from vessel motions and the environment. When designing a Workover system a Global Riser Analysis is conducted. In the Global Riser Analysis the operational limits for the riser is determined.

If a storm is coming and the operational limits are expected to be exceeded, the Workover Riser has to perform a Planned/Normal disconnect. This is done to prevent damage to the equipment, especially the well head. The scope of this Master Thesis is to study the Planned/Normal disconnection event. The disconnection is conducted by releasing the EDP. Furthermore the critical scenario of collision between the Emergency Disconnect Package (EDP) and the Lower Riser Package (LRP) is studied. The purpose of this Thesis is to study the risk of this scenario and to propose a strategy for the timing that can reduce this risk.

1.1.PREVOIUS WORK

Workover systems is a fairly new concept, thus the existing research within this area is limited. However, Workover riser is quite similar to drilling riser. Thus this research is also of interest.

- Project Thesis (Kinge, 2014). In the spring of 2014 the Project Thesis was completed. In this Thesis a Global Riser Analysis was conducted, in addition to a literature study. The literature study included a comprehensive part about the Workover System in addition to detailed part of the theory. Some parts of this Thesis are either partly or fully included in this Master Thesis to create a more holistic perspective of the topic.
- Master Thesis (Grønevik, 2013). In this Thesis the riser recoil scenario, in addition to the disconnection timing were studied. However, the analyses were conducted for a drilling riser rather than a Workover Riser.
- In the Spring of 2014 Lars Hermanrud wrote a Master Thesis about the Workover System. In the Thesis the critical scenario of lock up of the heave compensation system for a Workover riser was studied (Hermanrud, 2014).
- Doctoral Thesis (Sten, 2012), the Thesis discuss the modelling aspects of deep water risers related to dynamic analyses, with a focus on the heave compensation system.
- Geir Magnus Kardahl Master Thesis, (Knardahl, 2012). The Thesis is about vortex induced vibrations on the Workover riser.

1.2.ORGANIZATION OF THE THESIS

The structure of this Master Thesis has been developed in order to provide the reader with a clear overview of the topic. It is divided into four parts.

- **Part I:** Part I contain information regarding the Workover System. In this part there is an overall description of the system and the system components including their functions. Part I also contain information regarding the rules and regulations which applies for the Workover system.
- **Part II:** In Part II the theory is described. The first part is a description of the disconnection theory. It is followed by the background theory for the analysis, which includes static analysis, dynamic analysis and stochastic analysis.
- **Part III:** The third part of the Thesis contains information about the method applied to conduct the analysis. The program used to perform the analyses is RIFLEX. A description of the modelling of the riser system and the input is also included.
- **Part IV:** In Part IV the results from the analysis are presented. The results are further outlined in discussion, conclusion and further work.

PART I: SYSTEM DESCRIPTION

2. WORKOVER SYSTEMS

2.1.DESCRIPTION OF WORKOVER SYSTEM

As described in (Aker Soltuions, 2013), WOS (Workover systems) are temporary systems applied to perform workover operations. Moreover, workover operations are completion of the well or well intervention activities. The entire Workover system stretches from the top sight down to the seabed.

Well interventions are maintenance operations in the well, see (Aker Solutions , 2008). The maintenance operations can typically be repair or stimulation of existing well in order to increase production of hydrocarbons. Additionally, workover operations can be major maintenance operations to replace or repair tubing. Well intervention also include through tubing with coiled tubing operations.

Well completions are workover operations to install tubing hanger, XMT and upper completion, see (Aker Solutions , 2008). The installation of XMT is conducted with a drill pipe on a dead well.

There are three different systems to perform workover operations, these are categorized in the following way;

- Category A; Riser-less system
- Category B; Open Water system (Light workover system)
- Category C; In-riser system (Heavy workover system)

2.2.CATEGORY A, RISER-LESS SYSTEM

The riser-less system is a workover system where the operations are performed without a riser. The operations are however performed with a wireline (Aker Solutions, 2014).

2.3.CATEGORY C, IN-MARINE RISER SYSTEM

The In-Marine riser system, also called landing string system, is applied to conduct heavy workover operations. It is used to do well completion and well intervention. The information about the In-Marine Riser system described in (Aker Soltuions, 2013).

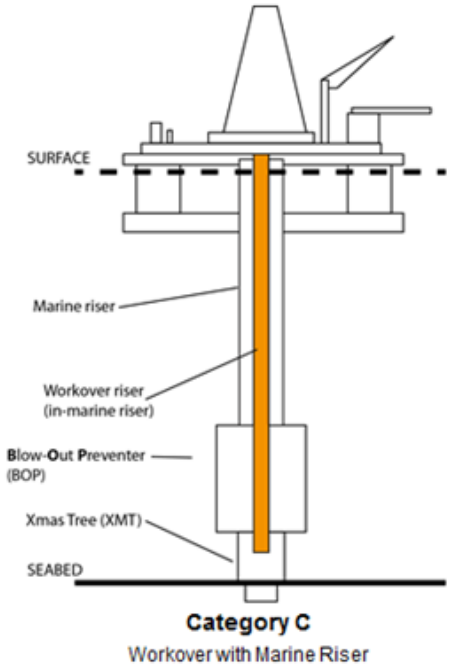

Figure 2: In-Marine Riser System (Aker Soltuions, 2013)

The In-Marine riser system is named after the set up, see **Figure 2**. The system has a riser inside a marine riser. The components in this system as seen in **Figure 3** are briefly described below. The marine riser is exposed to loads from the environment, like waves and current.

There are two catecories within the In-Marine Riser system.What differenciate the two systems, is whats inside the marine riser. There is either a simplified landing string (SLS)/drill pipe landing string(DPLS) or a Landing string. These two systems perform different type of workover operations and are described below.

The simplified Landing String is applied to perform completion of well by installing tubing hanger(TH). This is done on a dead well. Therefore there are no valves in the string.

The system consist of riser joints, pup-joints and the SLS at the lower end. The SLS runs inside the BOP (blow out preventor) and is connected to a tubing hanger running tool (THRT). The THRT is a component which runs the tubing hanger. The BOP is a component consisting of powerful cutting and sealing valves and acts as a safety barrier. Furthermore the DPSL is applied in the same way as the SLS. The only difference is that it is made up by a drill pipe instead of casing.

The Landing string is located inside the marine riser. This system is applied to perform well intervention activities. The landing string consists of riser joints, pup joints, special joints, valves, connections and at the lower end of the landing string the SSTT (subsea test tree). The SSTT acts as a safety barrier consisting of several valves. The SSTT runs inside the BOP and is connected to the TH as seen in **Figure 3**. The tubing hanger carries the weight from the tubing and is landed in the XMT.

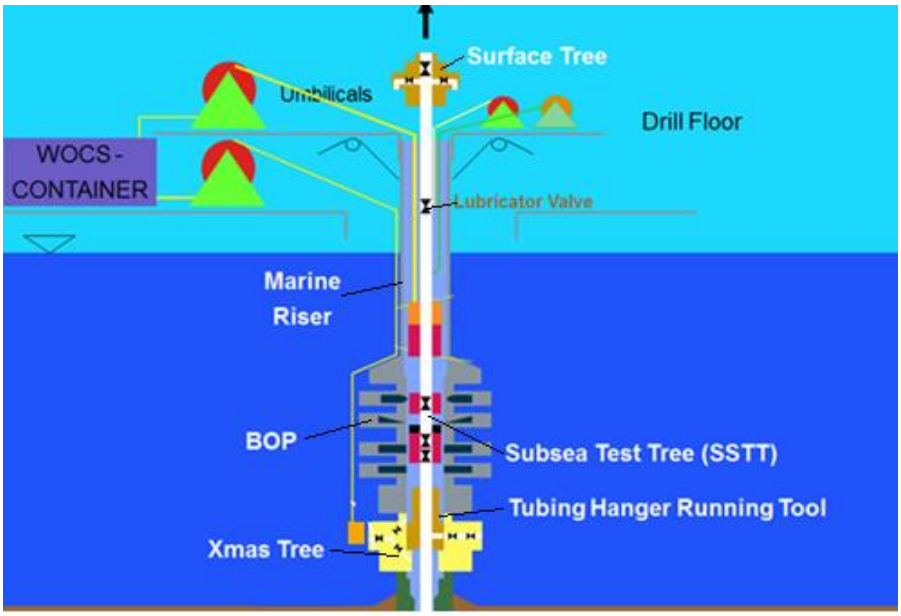

Figure 3: In-Marine Riser system (Aker Soltuions, 2013)

2.4.CATEGORY B, OPEN WATER SYSTEM

The Open Water system is a system which can conduct well intervention through an Open Water riser. Information regarding the Open Water System is obtained from (Aker Soltuions, 2013). The type of intervention activity performed with an Open Water system is milling (removal of blockage) and coiled tubing (cleaning, logging and cementing). The system can also be applied to conduct test production. As seen in **Figure 4** there is no marine riser protecting the workover riser, hence it is directly exposed to loads from the environment like waves and current.

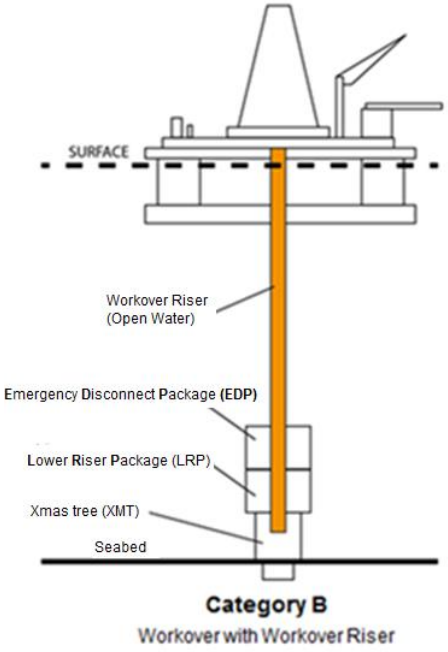

Figure 4: Open Water System (Aker Soltuions, 2013)

Furthermore, the system analyzed in this Master Thesis is the Open Water system. Therefor a more detailed description of the system is appropriate. The components including the system stack-up are illustrated in **Figure 5**. All components are described in this section. This is done in terms of their location and function in the system.

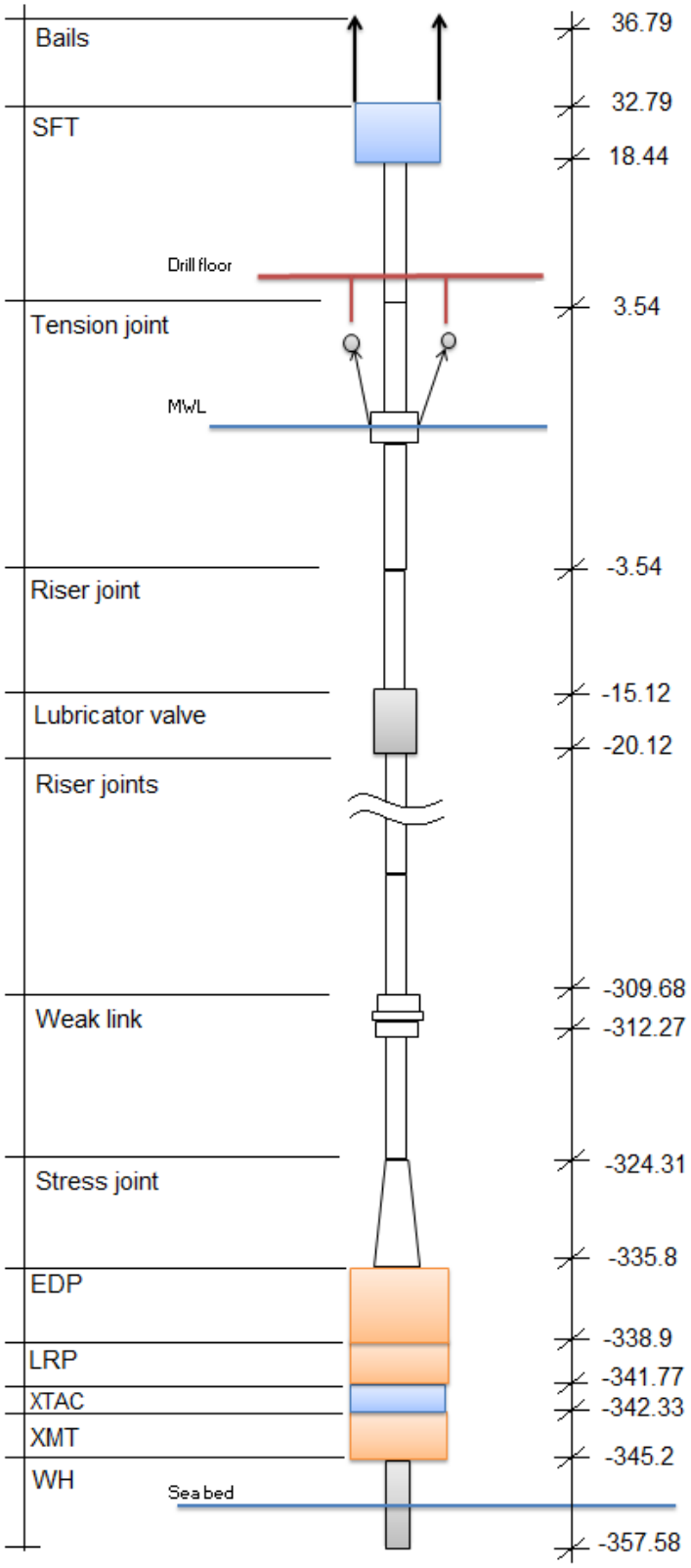

Figure 5: System stack-up based on drawing from (Aker Soltuions, 2013)

2.4.1. COMPONENT DESCRIPTIONS

In this section the components of the Open Water riser system are found, most of them are further outlined in (Aker Soltuions, 2013) or stated otherwise.

BAILS; Bails are attached to the top of the Surface flow tree, the top tension is applied in these, see (Kirkvik & Berge, 2011).

COILED TUBING TENSION FRAME; CTTF (Coiled tubing tension frame) is a component which is used when conducting operations with coiled tubing, information received from (Aker Solutions, 2014). The component is a frame with pressure control equipment. The frame is connected to the heave compensation system and bails.

SURFACE FLOW TREE; The SFT (surface flow tree) works as the last safety barrier of the system. It is located on top of the workover riser and consists of valves. The SFT acts as a sluice for tools to be lowered and hoisted in to the well.

LANDING JOINT; The landing joint is the top joint of the workover riser and connects the SFT to the workover riser. The landing joint may have an extra heavy slick wall pipe to withstand large tensile and bending moments. The landing joint passes through the rotary table (drilling floor which can rotate) during heave motions of the rig.

Since the landing joint passes through the drill floor it will be exposed to point loads. These point loads will generate moments with its maximum at the end of the joint.

TENSION JOINT; The tension joint is located below the landing joint. Approximately half of the joint is below the water surface and the other half is in air. The tension joint is attached to the rig by a tension system, in order to add tension to the riser. It is designed to carry the weight of the riser, LRP, XTAC and the XMT.

LUBRICATOR VALVE; The lubricator valve is located under water but close to the surface. The Lubricator valve acts as an additional safety barrier since it isolated the surface with a valve, and enable for pressure testing of the upper part of the Workover riser.

To isolate the top section of the riser from the well, the lubricator valve is closed during building and installation of tools, information received from (Aker Solutions, 2014).

STANDARD RISER JOINT; The standard riser joint is a pipe with a connector at the end. It has a certain standard length and inner diameter which makes it possible for tools and plugs to be run down to the well. In addition to the pup joints the standard joints make up the length from the lubricator valve down to the weak link.

PUP JOINT; Pup joints are the same as standard riser joints except for the length. The pup joints have tailor-made lengths in order to get the correct length of the riser.

WEAK LINK; The weak link is located low in the workover riser, close to the seabed. The weak link is designed to be the weakest component in the system. Of all the components

in the riser system it will therefore break first. The purpose is to prevent damage of EDP, LRP, XTAC, XMT and the Well Head in case of extreme tension loads.

Explained by (Aker Solutions, 2014) the reason for the weak link is located low in the riser is to control that it breaks due to pure tension, and not due to bending moments.

STRESS JOINT; The stress joint is the last component in the riser before the EDP. In this part of the riser large bending moments will occur. Hence, the stress joint must withstand bending moments. The function of the stress joint is to provide axial support, pressure transition and bending transition. This ensures that the localized stresses will be reduced, hence the fatigue life is increased.

The stress joint has a tapered cross section, which means that it has different cross sectional thickness along the length (Bai & Bai, 2012). This is to control curvature and reduce local bending stresses.

EDP (EMERGENCY DISCONNECT PACKAGE); The EDP is a component which can disconnect from the well in case of an emergency (Bai & Bai, 2012). It is connected to the stress-joint and on top of the LRP.

In addition to conducting disconnections due to emergencies it also performs planned/normal disconnects.

LRP (LOWER RISER PACKAGE); The LRP is located between the EDP and XTAC and acts as a safety barrier. It consists of valves which can close the well (American Petroleum Institute, 1998).

XTAC (Xmas Tree Adaptor Connector); The XTAC is a connection between LRP and XMT. Its function is to connect the LRP and the XMT since they have different interfaces, information received from (Aker Solutions, 2014).

XMT (X-MAS TREE); The XMT mainly consist of a valve system which can be controlled. It works as an interface between the well and the production system (Bai & Bai, 2012). The valves are used for testing, servicing, regulation, or choking the stream of production oil, gas, and liquid coming from the well.

The XMT is located on top of the wellhead.

WH (WELL HEAD); The wellhead is located at the seabed. The WH's function is to be a structural and pressure-containing anchoring point on the sea bed (Bai & Bai, 2012). In the WH there are internal profiles, to support the casing strings and isolate the annulus. In addition, the WH enables guidance, mechanical support and connection of the systems applied for completion of the well.

3. RULES AND REGUALTIONS

In addition to local laws and legislations, it is common practice that the customer has certain requirements when purchasing a Workover System. Information for rules and regulations regarding WOS are received from (Aker Solutions, 2014). Typical requirements are that the system must be designed according to a certain standard. In this case the analysis needs to be performed in compliance with the standard. In this perspective, the standard rules and regulations applying for workover system are presented in the following section.

As described in (Det Norske Veritas, 2010) the difference between service specification, standards and recommended practices is:

- *"Offshore Service Specification. Provide principle and procedures of DNV (Det Norske Vetitas) classification, certification, verification and consultancy services."* (Den Norske Veritas, 2010)
- *"Offshore Standards. Provide technical provisions and acceptance criteria for general use by the offshore industry as well as the technical basis for DNV offshore service."* (Den Norske Veritas, 2010)
- *"Recommended Practices. Provide proven technology and sound engineering practice as well as guidance for the higher level Offshore service specifications and offshore standards."* (Den Norske Veritas, 2010)

In addition to the requirements to the system, the standards and recommended practices also contain several guidelines for performing calculations and analysis and not to mention descriptions about functions and the entire system itself.

3.1.HIERARCHY

There are several existing documents with rules and regulations. The documents in this section are presented in terms of their level of priority for Workover systems as shown in **Figure 6**. The following information has been provided by (Aker Solutions, 2014).

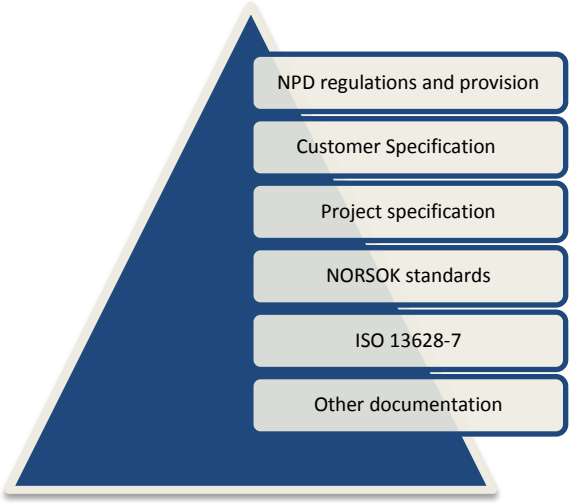

Figure 6: Hierarchy for rules and regulations regarding WOS based on info in appendix A.6

The hierarchy presented in **Figure 6** has been obtained from an ongoing project in Aker Solutions, the description is found in appendix A.6 . In consequence this is only an example case. However the rules and regulations are similar for all projects.

1. **Norwegian Petroleum Department's(NPD);** The NPD has the highest priority. They defines the rules and regulations which apply for the Norwegian shelf.
2. **Customer Specification;** In the customer specification the requirements for the system from the customer are defined. The customer specification refers to the standard ISO 13628-7. However, it usually contains more information and is therefore regarded as more conservative. The customer specification is a general specification for the system and not specific for each project.
3. **Project specification;** The project specification on the other hand is specific for the project. It is provided by the customer and gives a detailed description of the requirements for the particular project.
4. **Standards;** Out of the standards, NORSOK is the one with the highest priority. *"NORSOK standards are as far as possible intended to replace oil company specifications and serve as references in the authorities regulations."* (Standard, 2014). The NORSOK only applies for projects on the Norwegian shelf, and it is considered to be conservative.
5. **ISO 13628-7 Design and operation of subsea production system-Part 7: Completion/Workover systems;** The ISO 13268-7 is the most important for Workover Systems in terms of application. It is always applied when designing a Workover System, and the customer often requires that the entire system has to be designed according to it. As a consequence this standard will have a more detailed description than the others in the following sections.

6. **Other documentations;** includes different standards and recommended practices in order to give additional information and guidance.

Following in the next sections there is description of the most commonly applied standards and recommend practices for Workover Systems.

3.2.ISO 13628-7 DESIGN AND OPERATION OF SUBSEA PRODUCTION SYSTEMS- PART 7: COMPLETION/WORKOVER SYSTEMS

In this section the ISO 136287 will be presented. The information obtained from (Technical Comittee ISO/TC 67, 2005). ISO (the International Organization for Standardization) is an international federation which develops standards. This is conducted by a technical committee. As already mentioned the ISO 13628-7 is the most commonly applied standard for the WOS and is therefore described in more detail than the others.

"This part of the ISO 13628 gives requirements and recommendations for the design, analysis, materials, fabrication, testing and operation of subsea completion/workover (C/WO) riser system run from a floating vessel" (Technical Comittee ISO/TC 67, 2005)

The standard can be applied for both new riser systems and for modifications. This standard consists of several parts described briefly here.

- **System requirements;** in this part the requirements to the entire system are specified. It consists of a description of the system, system engineering, system definition, system design and system review. There is a part including the operation modes and a part describing design principle, operation principle and safety principle.
- **Functional requirements;** specifies the functional requirements of the system in general, followed by specific functional requirements for the components.
- **Design requirements;** specifies the design requirements, in terms of methods for design, the effects from the loads and which loads the system must withstand.
- **Material and fabrication**; describes the requirements and guidelines for material selection, manufacture, testing, corrosion, protection, fabrication and documentation for the system.
- **Testing;** consists of the minimum requirements for testing of the system and components.
- There is also a part consisting of information about storing and shipping of the system and components. Further there is a part consisting of information about inspection and maintenance.
- **Documentation;** describes the necessary documentation regarding the design basis, analysis, drawing and other relevant documentation.
- **Appendices;** contain relevant information such as standardization of the riser interface , operation modes and global riser analysis, fatigue analysis, structural resistance methods, example calculations and some more. The most relevant part for this thesis is however the operation envelopes and global riser analysis.

In the appendices there is an separate chapter regarding the Global Riser Analysis and how this should be performed. The appendices also contain information about operating envelope further described in detail in section 4.2. Operational envelopes are operating limits (operating windows) for the riser. The part about operation envelopes is of high importance for this Master Thesis, since it defines when the riser should perform a disconnection.

3.3.DNV-OS F201 DYNAMIC RISERS

The DNV offshore standard for Dynamic Risers is developed by DNV(Det Norske Veritas). The information in the following section is found in (Det Norske Veritas, 2010).

"This standard gives criteria, requirements and guidance on structural design and analysis of riser systems exposed to static and dynamic use in the offshore petroleum and natural gas industries. " (Det Norske Veritas, 2010)

The purpose is to provide an international standard of safety for steel risers and a technical reference document in contractual matters. It is also a guideline for riser design and analysis. It applies for all new built risers, but can also be used for modifications. The standard is divided into two parts. The first part is the main part and describes the minimum requirements for explicit criteria including necessary external functional requirements. The second part consists of appendices providing guidance and background on topical issues.

3.4.DNV-RP-C203 FATIGUE DESIGN OF OFFSHORE STEEL STRUCTURES

This DNV RP (recommended practice) contains information about fatigue calculations for the workover system, further outlined in (Den Norske Veritas, 2010). It provides recommendations for fatigue analyses based on fatigue tests and fracture mechanisms. Furthermore, the RP contains information about fatigue analysis based on S-N data, stress concentration factors, calculations of hotspot stress, simplified fatigue analysis, improvement of fatigue life and uncertainties in fatigue life predictions.

3.5.DNV-RP-C205 ENVIRONMENTAL CONDITION AND ENVIRONMENTAL LOADS

"This new Recommended Practice gives guidance for modelling, analysis and prediction of environmental conditions as well guidance for calculating environmental loads acting on structures (Det Norske Veritas, 2007)*."*

As described in (Det Norske Veritas, 2007) the environmental loads taken in to consideration in this RP are due to wind, current and waves. The first part of the RP consists of information regarding environmental conditions. Included in this part are wind conditions, wave conditions, current conditions and tide conditions. The second part consists of environmental loads. Included in this part is wind loads, wave and current induces loads on slender members, wave and current induced loads on large structures, air gap and slamming and vortex induced oscillations. Finally, the last part consists of hydrodynamic model testing. The appendices contains information about

Torsethaugen two-peak spectrum, nautic zones, scatter diagrams, added mass coefficients, drag coefficients and physical constants.

This document is the only document that describes the environmental conditions and how to calculate the loads including VIV (vortex induced vibrations). Hence this RP is applied to calculate the environmental loads on the structure.

PART II: THEORY

4. DISCONNECT THEORY

4.1.INTRODUCTION

When conducting Workover operations the riser will experience several loads. Information in this section is mainly received from (Aker Solutions, 2014), or specified otherwise. These loads are;

- Loads caused by the motion of the platform. The riser is connected to the well head at the seabed and to the vessel at top. Hence, when the vessel moves the riser will experience loads. It can move in the horizontal direction. However, due to the heave compensation system which will prevent vertical motion. The riser system will not experience vertical motion.
- Wave and current loads. The riser is exposed to the environment and will therefore directly experience these loads.

In the Global Riser Analysis the limit for how big loads the riser and its components can withstand are calculated. This is defined in the operation envelopes which are further outlined in section 4.2.

"A C/WO riser is classified as a temporary riser and normally has a limited operating envelope. In situations where operating conditions are expected to exceed the allowable, the riser shall either be disconnected and hung-off or retrieved." (Technical Comittee ISO/TC 67, 2005)

As stated in the quote above, if it is expected that the operation limits will be exceeded, the riser should perform a safety maneuver. It exists mainly two types of disconnection events of a Workover Riser, either *normal/planned disconnect* or *Emergency Quick Disconnect (EQD)*. These scenarios are defined below.

Normal or planned disconnect: The weather forecast predicts how big the waves and wind are in the future. If a storm is predicted, and it is expected that the loads are going to exceed the operation limits, a safety measure needs to be done. This can be done by conducting a normal/planned disconnect. Additionally, if it is observed that the system already has exceeded the normal operation limit but the conditions are not so severe, a normal disconnect should be performed. In this case the Workover riser is disconnected and put in a safe "Hang-off" mode, this is further described in section 4.3.

Emergency Quick Disconnect (EQD): Emergency Quick Disconnect is the scenario which is done when an emergency which leads unsafe loads in the riser or well head occur. These emergencies can be; drift/drive-off, incident with the heave compensation

system, lack of control of the tensioners, stroke out of the compensation system, large angle at the EDP/LRP or other emergencies.

As defined in (Technical Comittee ISO/TC 67, 2005) drift-off and drive-off are;

- **Drift-off;** is the scenario when the dynamically positioned vessel moves unintendedly off its intended position over the wellhead. This happens due to lack of station-keeping control or propulsion.
- **Drive-off;** is the scenario when the dynamically positioned vessel moves unintendedly off its intended position driven by the thrusters of main propulsion.

When an EQD is conducted, there is no time to remove the tension applied in the riser. The riser system will therefore experience an imbalance of tension causing it to accelerate upwards. This physical phenomenon is called Riser Recoil (ISO Technical commtee, 2009).

The riser can also experience the recoil effect due to high internal pressure.

4.2.OPERATING ENVELOPES

The criteria for conducting both EQD and planned disconnect is determined by the operation envelopes. This information in this section is further outlined in (Technical Comittee ISO/TC 67, 2005).

The operation limits for the riser system are defined in terms of operation envelopes. The components in the system have different strengths, and therefore also different operation limits. These operation limits are called operation envelopes and are presented as graphs. The operating envelopes are presented in terms of significant wave height and mean vessel offset from wellhead extension as seen in **Figure 7**. Hence, the operation envelopes define how big offset the vessel can have, and still have an acceptable operation limit. Furthermore the operation envelopes define the criteria for disconnect and are applied by the operators on the vessel.

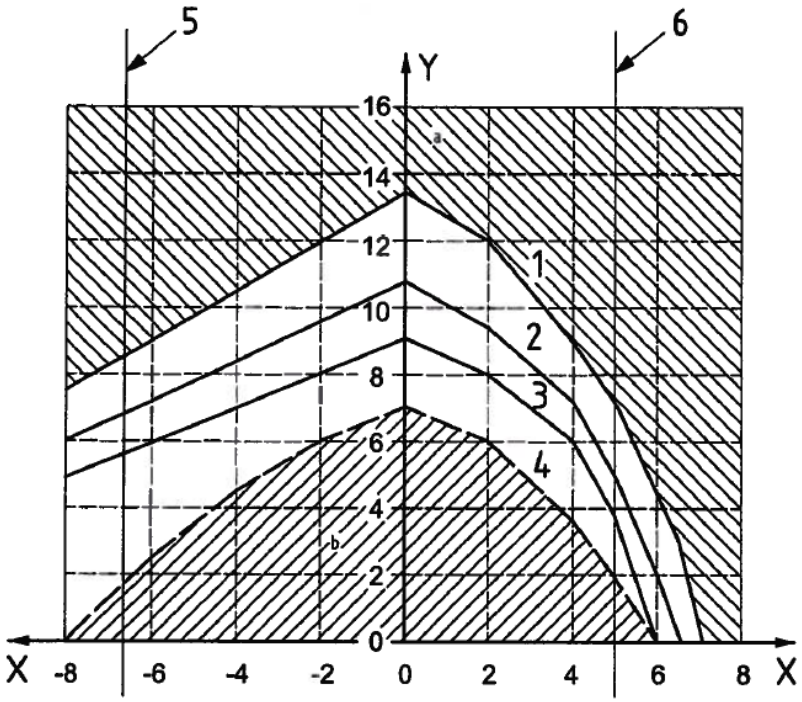

Figure 7: Operation envelope graph (Technical Comittee ISO/TC 67, 2005)

X vessel offset from wellhead
Y significant wave height
1 strength limit: accidental
2 strength limit: extreme
3 strength limit: normal
4 stroke limit
5 EDP angle limit (upstream)
6 EDP angle limit (downstream)
a unsafe operating area
b safe operating area

As seen in **Figure 7** the safe zone is in area ***b***, thus this area is within the operating limits. Further, area ***a*** is the unsafe area of operation which means that an EQD shall be performed.

The limitations which define the operation limits for the riser system are;

- Strength
- Riser stroke
- Riser clearance
- Maximum allowable disconnection angle
- Vessel drift considerations

In the operating envelope shown in **Figure 7** all these factors have been taken into consideration and the effects have been combined. To make sure the operation is carried out in a safe manner, the parameters as shown in **Figure 7** should be monitored.

According to (Technical Comittee ISO/TC 67, 2005) the design of the workover riser shall include an appropriate design factor or safety factor, to ensure appropriate safety. One such method is the working stress design method as shown in (Eq. 4.1). It is a method where the safety is assured by using design factors to the resistance of the component.

$$S_d \leq R_d = R_{uc} \times F_d \qquad \text{(Eq. 4.1)}$$

Where the variables in (Eq. 4.1) are;

S_d	design load effect
R_d	design capacity (resistance)
R_{uc}	ultimate capacity (resistance)
F_d	design factor

Furthermore, in the design factor also called *usage factor* or *allowable stress factor,* the integrated uncertainty and possible bias in the load effects and resistance is considered.

4.3.DISCONNECTION PROCEDURE

In section 4.2 the operating envelopes are explained. The operating envelopes set the criteria for when to conduct disconnection, both an EQD and normal disconnect. The information regarding the disconnection procedure is provided by (Aker Solutions, 2014). It has become apparent during the work with this Thesis that there exists no standard procedure for conducting a disconnection. However, it exists a significant amount of information about the Workover Riser system including information about operation envelopes in (Technical Comittee ISO/TC 67, 2005).

The riser is added top tension to prevent it from buckling. For the workover systems it is normal that there is an "overpull" at the EDP of about 25 tons in connected mode. The purpose of the overpull, is to make sure the EDP does not collide with the LRP when an EQD is conducted. If disconnection is performed with overpull, the tension makes the riser accelerate upwards, and the riser will experience recoil. This is however not the case for normal/planned disconnect since the tension in the riser is reduced before a disconnection is performed.

The event studied in this Master Thesis is the normal/planned disconnection. Moreover, the purpose is to determine the ideal moment to perform a disconnection to make sure the EDP and LRP does not collide. A description of the disconnection sequence is therefore found below.

1. **Remove tension:** Tension in the workover riser is often applied at two locations, in the top drive and the main tension system. The high tension in the riser is reduced before disconnecting. The tension is reduced sufficiently to avoid recoil effect. When this is done there is approximately zero tension at the LRP. However the rest of the riser has positive tension to avoid buckling.
2. **Positioning the rig:** The most optimal scenario is to conduct the disconnection with a small disconnection angel. Thus, the rig is positioned to achieve the smallest possible disconnection anlge.
3. **Disconnection:** The disconnection is initiated when the operators on the platform send an electric signal to the EDP. It takes approximately 30 seconds from the signal is sent until it reaches the EDP, and the disconnect takes place. In order to prevent a collision between the EDP and the LRP, seen in **Figure 5** the entire riser is lifted up about 2-4 meters. At the same time the riser is locked to the vessel. The EDP therefore has the same heave displacement as the vessel.
4. **Hang-off:** After the disconnection is performed the riser is in Hang-off mode. The rig will first sail away from the well head center to prevent collision. When the riser is in hang-off mode the riser will hang in the spider, top-drive or a separate hang-off joint, see figure in appendix A.5 . It is required that the riser shall be able to be in hang-off mode for a while. Therefore a fatigue analysis has to be conducted. As seen in appendix A.7 the requirement can be ten years.

4.4.DISCONNECT TIMING

There exist critical scenarios when performing an EQD. These scenarios are as follows, and further outlined in (Lang , Real, & Lane, 2009);

- Collapse of the telescopic joint which leads to high loads transmitted to the drillfloor. This is a high risk for the personal at the drillfloor.
- The tension lines become slack which can lead to the tension wires to jumps out of their sheaves or the telescopic joint outer barrel can lift of the tension ring.
- If the riser accelerates upwards due to recoil, the riser might buckle due to compression.
- When the vessel experience heave motions the EDP and the LRP can collide if the EDP does not lift high sufficiently from the LRP.

The latter scenario is also a critical scenario when performing normal/planned disconnection. Furthermore, the purpose of this Master Thesis is to study this, collision between the EDP and LRP. When studying this event, a method for determining the optimal timing for performing a disconnection shall be proposed. A description of disconnection timing is therefore presented in this section.

Disconnection timing, is the time incident when the actual disconnection between the EDP and the LRP takes place. As mentioned in section 4.3 it takes approximately 30 seconds from the signal is sent until the actual disconnection occurs.

The time incident when the disconnection happens is important when studying the collision scenario. The riser is locked to the vessel simultaneously as the disconnection takes place. Hence, the riser system will follow the heave displacement of the vessel after disconnect. Where, heave displacement is displacement in z-direction.

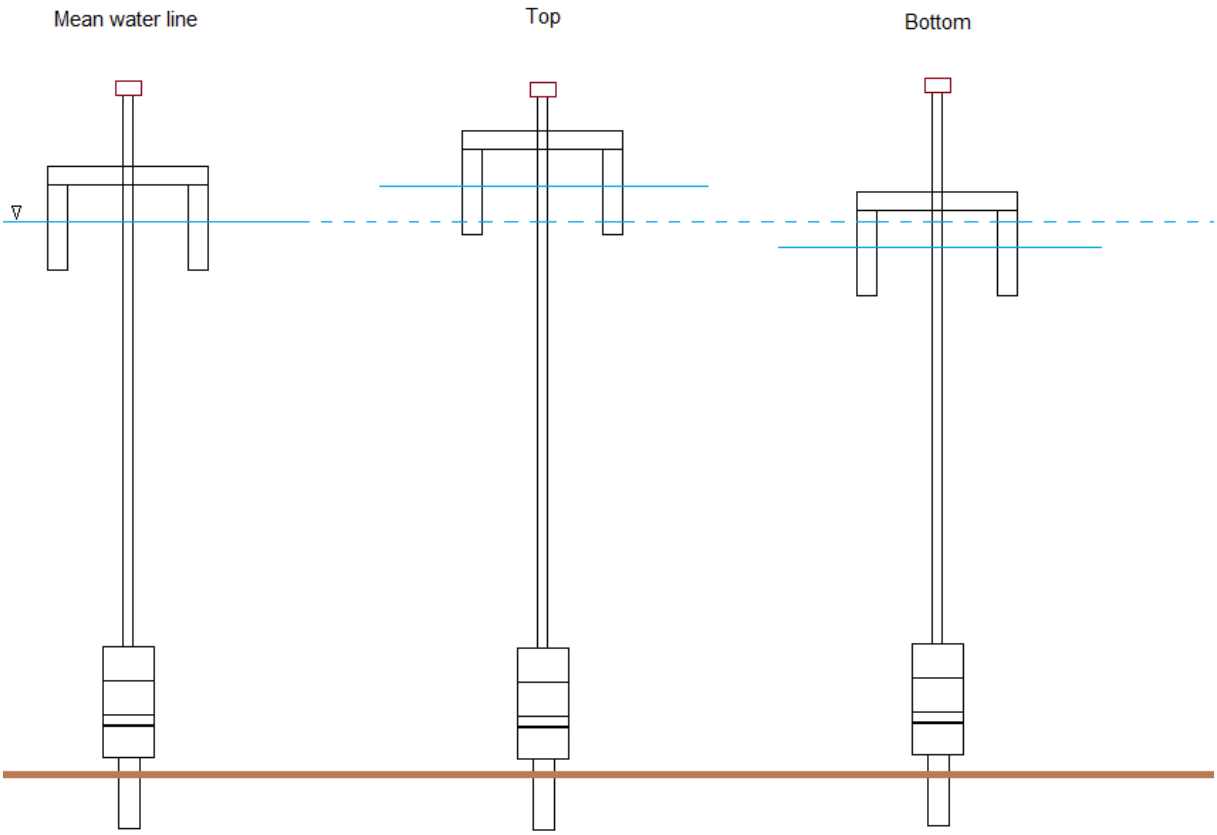

Figure 8: Different disconnection events

Top of the heave displacement: If the disconnection is performed when the vessel is at the heave displacement top, the riser will be locket to the vessel when it has a negative velocity and it is displaced downwards. Additionally, it will also be locked at higher position at the riser, leading to a longer length of riser is below the vessel as seen in **Figure 8**.

Bottom of the heave displacement: On the other hand, if the riser is disconnected when the vessel is at bottom of the heave displacement it will immediately experience a velocity which pulls it in positive z-direction. Additionally, the riser is locked at a lower point and the length underneath the vessel is therefore shorter, see **Figure 8**.

Half way up the heave displacement: If a disconnection of the riser is performed when the vessel is at half way up the heave displacement, it will take place at the moment with highest positive vertical velocity. However, there will be no change in the riser length underneath the vessel, since it will lock at the initial position.

Random Disconnect: When the disconnection is performed at random time incident, it cannot be predicted where in the heave displacement the disconnection will be. Thus, it cannot be foreseen what the consequence may be.

5. STATIC ANALYSIS

5.1.INTRODUCTION

The purpose of the static analysis is to determine the nodal displacements so that the total system is in equilibrium. This is done by considering the external and internal forces acting on the system (MARINTEK, 2013).

$$F^S(r) = F^E(r) \qquad \text{(Eq. 5.1)}$$

F^S	Internal structural reaction force vector
F^E	External force vector assembled from all elements
r	Is the nodal displacement vector

The static equilibrium as seen in (Eq. 5.1) is found by applying incremental loading procedure with equilibrium for each load step (MARINTEK, 2012).

As described in (Larsen, Marine Riser Analysis, 2008), the axial forces are found by adding the vertical forces together, buoyancy, weight and tension. When the forces are found the total stiffness matrix can be formulated, which is based on the stiffness matrices from the elements.

5.2.OUTLINE OF THE FINITE ELEMENT METHOD

In this section an outline of how the Finite Element Method (FEM) is conducted in the static analysis is described. The step by step sequence is retrieved from (Larsen, Marine Riser Analysis, 2008). However, some of the information and equations are from other sources, as stated.

The Global stiffness matrix can be expressed as shown in (Eq. 5.2) (Larsen, Response Modelling of Marine Risers and Pipelines, 1990).

$$K = \sum_i a_i^T T_i K_i T_i^T a_i \qquad \text{(Eq. 5.2)}$$

The global stiffness matrix is established by considering the internal work for the system.

a_i	Connectivity matrix
T_i	Transformation matrices
K_i	Element stiffness matrices

$$k_{tot} = k_M + k_G \qquad \text{(Eq. 5.3)}$$

The stiffness matrix (Eq. 5.3) is a result of both geometric and material stiffness (Larsen, Finite Element Modelling lecture notes, 2007). For the 3-dimensional case the non-

linearities need to be taken into consideration due to large displacements. This is described in detail in section 5.3.

(Larsen, Finite Element Modelling lecture notes, 2007) describes that the work done by higher order strains due to lateral displacement in axial stresses, is used to find the effect on lateral stiffness from axial tension in a beam element. Furthermore, the geometric stiffness matrix can be expressed in terms of strain energy.

The displacement *r* (Eq. 5.4) can be expressed in term of the equilibrium equation.

$$r = K^{-1}R \qquad \text{(Eq. 5.4)}$$

As described in (MARINTEK, 2012) the load vector $\boldsymbol{R}$ contains the external forces. The forces included in the load vector are;

- Volume forces, weight and buoyancy.
- Specified displacements
- Specified forces (nodal point loads)
- Position dependent forces (current forces)

The structural weight and the effects of top tension are taken into account when calculating geometric stiffness. The external loads on circular structures from waves and current can be described by Morison's equation (Eq. 5.5).

$$F = \frac{1}{2} \cdot \rho \cdot \ C_D \cdot d \cdot l \cdot v|v| + \rho C_M \frac{\pi D^2}{4} a \qquad \text{(Eq. 5.5)}$$

Morison's equation is retrieved from (Faltinsen, 1990).

When the element displacement vectors have been determined and refer to the local base vector $\boldsymbol{i_i}$ further described in section 5.3, the strains stresses, forces and stiffness can be calculated according to conventional beam theory (Larsen, Response Modelling of Marine Risers and Pipelines, 1990).

When the displacement vector $\boldsymbol{r}$ is found, the node displacements (Eq. 5.6) and stresses can be calculated from the equations below.

$$v_j = a_j \cdot r \qquad \text{(Eq. 5.6)}$$

The internal stress resultants can then be found as (Eq. 5.7).

$$s_j = k_j \cdot v_j \qquad \text{(Eq. 5.7)}$$

$\boldsymbol{v_j}$ is the node displacements vector, $\boldsymbol{k_j}$ is the element stiffness including geometric stiffness and $\boldsymbol{s_j}$ is the stress resultant.

5.3.NON-LINEARITY

There are mainly three non-linearites that are considered; Geometric non-linearity due to large displacement, material non-linearity and non-linearity caused by interaction between the construction and the environments (Sigbjörnsson & Langen, 1979).

The following information about the non-linearities are presented in (Larsen, Response Modelling of Marine Risers and Pipelines, 1990). The geometric non-linearity is taken into account by applying a co-rotated ghost reference system.

"Rotations in the 3-dimensional space need to be handled with care, because large rotations are not true vectors that may be expressed by vectorial components in a base coordinate system" (Larsen, Response Modelling of Marine Risers and Pipelines, 1990).

The co-rotated ghost reference system applies a coordinate system where the base vector $\bar{\iota}_i$ is frozen to the nodal point and the coordinate system follows the movement of the node.

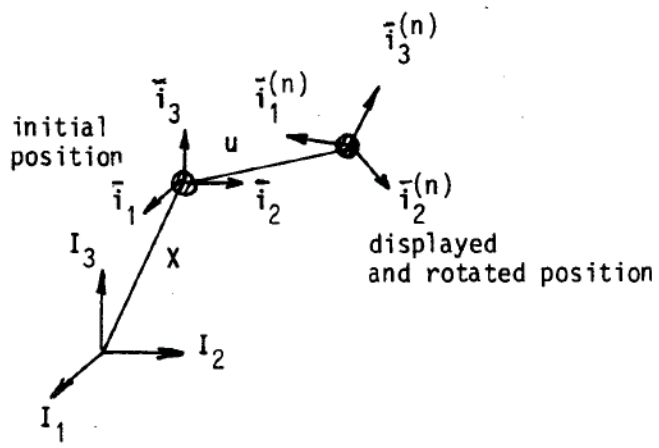

Figure 9: Nodal point translation and rotation degrees of freedom (Larsen, Response Modelling of Marine Risers and Pipelines, 1990)

The coordinate system is parallel to the global base vectors $\boldsymbol{I_i}$ as can be seen in **Figure 9**.

$$\overline{\iota_\iota^{(n)}} = T_{ij}^{(n)} I_j \qquad \text{(Eq. 5.8)}$$

T *Rotation matrix with direction cosines for the* $\bar{\boldsymbol{\iota}}$ *vector relative to* $\boldsymbol{I}$

The nodal point orientations in space described in (Eq. 5.8), are uniquely defined by the base vector transformation. The rotations of the node are given by the transformation matrix $\boldsymbol{T_{ij}}$ which is orthogonal, hence by rotations and not by angles. Thus, the general motion of the nodes is given by three dimensional components $\boldsymbol{u_i}$, and the nine elements of rotation matrix $\boldsymbol{T_{ij}}$.

5.4.EFFECTIVE TENSION

The axial force in a beam structure is a result of integrating stresses in the cross-section (Sævik, 2014).

The theory behind effective tension is described in (Larsen, Marine Riser Analysis, 2008). The effective axial force is used when calculating the geometric stiffness. Risers are exposed to internal pressure, pressure forces from buoyancy and the weight of the internal fluid. Hence, when calculating the tension, the effects of buoyancy and internal weight need to be taken into consideration. From Archimedes; the buoyancy of a submerged body is equal to the weight of the submerged volume of the body. However, for a riser the ends are connected so there are no pressure forces acting on them.

The buoyancy force can be decomposed. The resulting buoyancy is equal to the vertical component minus the axial force. The buoyancy will depend on the displacement, the orientation of the riser. However, by applying the method described below, it is possible to obtain an orientation independent description. **Figure 10** illustrates contributions from forces on the riser that need to be considered when it is displaced.

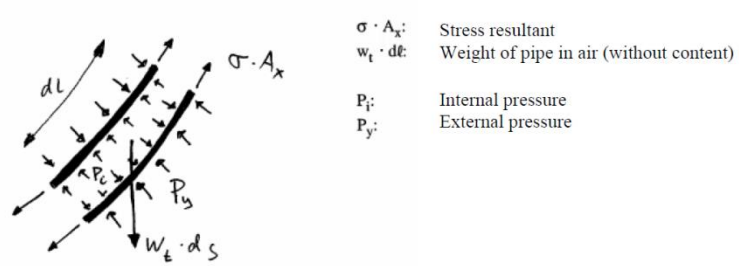

Figure 10: Forces in a pipe (Larsen, Aspects of Marine Riser Analysis, 2008)

The contribution to the tension can be represented in another way as shown in **Figure 11**.

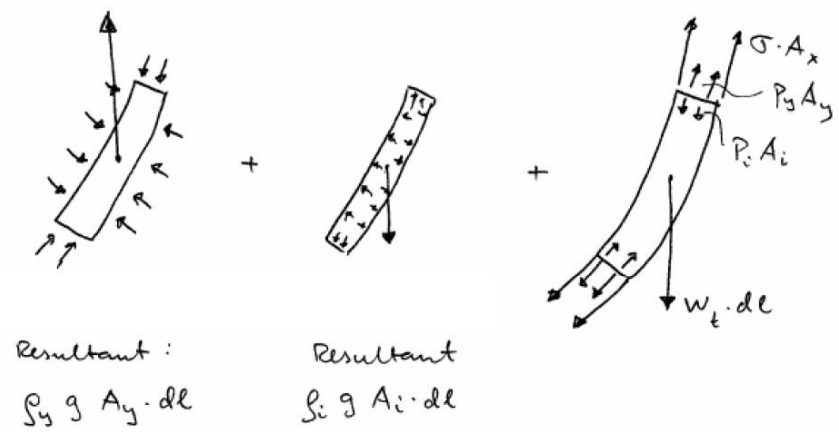

Figure 11: Force contributions from external and internal pressure (Larsen, Aspects of Marine Riser Analysis, 2008)

Figure 11 illustrates how the forces from the buoyance can be represented by external pressure P_y, the internal pressure P_i together with the internal weight can be added

together to represent tension in the riser. Thus, the effective tension can be calculated as seen in (Eq. 5.9).

$$T_e = T_\sigma + p_e A_e - p_i A_i \quad \text{(Eq. 5.9)}$$

T_e	*Effective tension*
p_e	*External pressure*
A_e	*External cross section area*
p_i	*Internal pressure*
A_i	*Internal cross section area*

In the same way when the weight of the riser is calculated it is necessary to take the internal and external pressure into account. Thus the effective weight is calculated in the following way.

$$w_e = w_t - \rho_e g A_e + \rho_i g A_i \quad \text{(Eq. 5.10)}$$

In (Eq. 5.10) w_t is the weight per unit length of the pipe, the ***e***-subscript is external and the ***i***-subscript is internal.

6. DYNAMIC ANALYSIS

6.1.INTRODUCTION

It is necessary to perform a dynamic analysis in order to study the displacement and forces in the structure when it moves. The analysis is conducted by solving the dynamic equilibrium equation which is shown below. The external forces are balanced by the inertia, damping and restoring forces as seen in equation (Eq. 6.1) (Larsen, Response Modelling of Marine Risers and Pipelines, 1990).

$$M\ddot{r} + C\dot{r} + Kr = Q(t) \qquad \text{(Eq. 6.1)}$$

As described in (MARINTEK, 2012) the vectors in the dynamic equilibrium equation (Eq. 6.1) are a result of element contributions and specified discrete nodal forces. The mass matrix $\boldsymbol{M}$ considers the structural mass, internal fluid mass and hydrodynamic mass matrix. The external forces $\boldsymbol{Q(t)}$ considers weight, buoyancy, forced displacements due to vessel, specified discrete nodal forces and the Morison's equation. The damping matrix $\boldsymbol{C}$ has contributions from internal structural damping, hydrodynamic damping and specified discrete dashpoint dampers which may be displacement dependent. The global stiffness matrix $\boldsymbol{K}$ was found in the static part. Nonlinear effects should also be taken in to consideration when conducting a dynamic analysis. These are;

- Geometric stiffness
- Nonlinear material properties
- Hydrodynamic loading according to Morison's equation
- Integration of loading to actual surface elevation
- Contact problems

According to (MARINTEK, 2012), if the hydrodynamic loading is the dominating nonlinear effect, it can be sufficient to conduct a linearized time domain analysis. This is desirable since the computation time is significantly reduced. Both the linearized, and the nonlinear time domain analysis are conducted by step by step numerical integration. In the next part the numerical integration methods, nonlinear time domain analysis, linear time domain analysis and the description of how the mass and damping matrix are presented.

6.2.NUMERICAL INTEGRATION

Numerical integration is a step by step numerical integration method. Furthermore it is applied to solve the dynamic equilibrium equation, see (MARINTEK, 2012).

(Sigbjörnsson & Langen, 1979) explains that the numerical integration method is based on the time interval being divided into time steps with equal length. When the start value is known, in this case the displacement and velocity in the beginning of the interval, the solution at the end of the interval can be found by assuming the shape of the motion during the interval. The result is used as the start value for the next interval. By doing this step by step, the solution is achieved. The accuracy of the solution depends on the size of the time steps.

As described in (Larsen, TMR4182 Marin Dynamikk, 2012), if the numerical method is not stable the calculated results will deviate from the correct solution. The stability of the system is controlled by the length of the time steps, and not by the damping. If the numerical integration procedure is unconditionally stable, it means that it cannot become unstable. However some procedures might become unstable, with the consequence that the length of the time step needs to be shorter, compared to the eigenperiod of the system.

Newmarks-β family and the Wilson method are methods that can be applied to conduct numerical integration (MARINTEK, 2012). Both these methods can be used to solve the dynamic equilibrium equation by numerical integration, and can be applied for linear as well as non-linear analysis. Further the most frequent applied method is the Newmarsk-β method.

In Newmarsk-β method equation (Eq. 6.2) and (Eq. 6.3) are the basic equations for velocity and displacement (Sigbjörnsson & Langen, 1979).

$$\dot{r}_{k+1} = \dot{r}_k + (1-\gamma)h\ddot{r}_k + \gamma h\ddot{r}_{k+1} \qquad \text{(Eq. 6.2)}$$

$$r_{k+1} = r_k + h\dot{r}_k + \left(\frac{1}{2} - \beta\right)h^2\ddot{r}_k + \beta h^2\ddot{r}_{k+1} \qquad \text{(Eq. 6.3)}$$

Where $h = \theta\Delta$ and$\theta \geq 1$.

The parameters γ, β and θ define the functional change in displacement, velocity and acceleration vectors over the time step Δt.

6.3.NONLINEAR ANALYSIS

The non-linear effects are described in the introduction to dynamic analysis in section 6.1. Furthermore these non-linearities must be taken into consideration in the dynamic analysis. In this section, the methodology for how a non-linear dynamic analysis is conducted with numerical time integration is found, further outlined in (Sigbjörnsson & Langen, 1979).

The non-linear dynamic equilibrium equation can be written in the following way (Eq. 6.4).

$$F^I(t) + F^D(t) + F^S(t) = Q(t, r, \dot{r}) \quad \text{(Eq. 6.4)}$$

F^I	Inertial forces
F^D	Dissipation forces
F^S	Elastic forces

In the numerical integration method the time space is divided into intervals with length h, the desired solution is at the discrete times *t=kh* and k is the number of time steps. The dynamic equilibrium equation is obtained on the incremental form in (Eq. 6.6) by considering the dynamic equilibrium equation with a time interval, seen in (Eq. 6.5).

$$(F^I_{k+1} - F^I_k) + (F^D_{k+1} - F^D_k) + (F^S_{k+1} - F^S_k) = (Q_{k+1} - Q_k) \quad \text{(Eq. 6.5)}$$

$$\Delta F^I_k + \Delta F^D_k + \Delta F^S_k = \Delta Q_k \quad \text{(Eq. 6.6)}$$

To linearize the dynamic equilibrium equation, the tangential slopes calculated at the start of the interval is applied as incremental damping and stiffness. These are applied instead of the average values, since they are dependent on the unknown velocity and displacement. By doing so, the dynamic equilibrium equation is written as;

$$M\Delta\ddot{r}_k + C_{Ik}\Delta\dot{r}_k + K_{Ik}\Delta r_k = \Delta Q_k \quad \text{(Eq. 6.7)}$$

When applying the Newmark-β method the solution at the end of the interval for (Eq. 6.7) is found, this gives (Eq. 6.8);

$$\begin{aligned} r_{k+1} &= r_k + \Delta r_k \\ \dot{r}_{k+1} &= \dot{r}_k + \Delta\, \dot{r}_k \\ \ddot{r}_{k+1} &= \ddot{r}_k + \Delta\ddot{r}_k \end{aligned} \quad \text{(Eq. 6.8)}$$

The linearization of each time step leads to an error which will accumulate. When these equations are applied at the end of the time step, there will no longer be equilibrium between the internal and external forces but a set of residual forces will occur.

$$\Delta F_{k+1} = Q_{k+1} - (F^I_{k+1} + F^D_{k+1} + F^S_{k+1}) \quad \text{(Eq. 6.9)}$$

To prevent this error from accumulating a correction is performed by adding the residual forces to the external forces at the next time step to the equilibrium equation. When this correction is accounted for, the dynamic equilibrium equation becomes.

$$M\Delta\ddot{r}_k + C_{Ik}\Delta\dot{r}_k + K_{Ik}\Delta r_k = Q_{k+1} - [F_k^I + F_k^D + F_k^S] \qquad \text{(Eq. 6.10)}$$

(Eq. 6.10) is an approximation to the total dynamic equilibrium equation for the time t_{k+1}.

Furthermore, for the Newmarks-β method, the velocity and acceleration on incremental form are;

$$\Delta\ddot{r}_k = \frac{1}{\beta h^2}\Delta r_k - \frac{1}{\beta h}\dot{r}_k - \frac{1}{2\beta}\ddot{r}_k$$
$$\Delta\dot{r}_k = \frac{\gamma}{\beta h}\Delta r_k - \frac{\gamma}{\beta}\dot{r}_k - \left(\frac{\gamma}{2\beta} - 1\right)h\ddot{r}_k \qquad \text{(Eq. 6.11)}$$

By inserting (Eq. 6.11) into equation (Eq. 6.10) the following equations are obtained.

$$\widehat{K}_k\Delta r_k = \Delta\hat{Q}_k$$

Where

$$\widehat{K}_k = K_{Ik} + \frac{\gamma}{\beta h}C_{Ik} + \frac{1}{\beta h^2}M \qquad \text{(Eq. 6.12)}$$

Which gives the following solution;

$$\Delta\hat{Q}_k = Q_{k+1} - [F_k^I + F_k^D + F_k^S] + \left(\frac{\gamma}{\beta}\dot{r}_k + \left(\frac{\gamma}{2\beta} - 1\right)h\ddot{r}_k\right)C_{Ik} + \left(\frac{1}{\beta h}\dot{r}_k + \frac{1}{2\beta}\ddot{r}_k\right)M \qquad \text{(Eq. 6.13)}$$

Improvements can be made to the displacement increment. However this will not be further outlined her. A description on how this is done is found in (Sigbjörnsson & Langen, 1979).

6.4.LINEAR ANALYSIS

(MARINTEK, 2012) describe that the linear time domain approach of the dynamic analysis is a simpler method. As a consequence, the computational time will be reduced significantly. The method is based on linearization of the dynamic equilibrium equation (Eq. 6.14). The system matrices are therefore constant throughout the analysis.

$$M\ddot{r} + C\dot{r} + Kr = Q(r, \dot{r}, t) \quad \text{(Eq. 6.14)}$$

$\boldsymbol{M}$, $\boldsymbol{C}$ and $\boldsymbol{K}$ are tangential mass, damping and stiffness matrix respectively. The dynamic displacement vector r and the dynamic load vector are expressed as;

$$r = r_{tot} - r_{stat} \quad \text{(Eq. 6.15)}$$

$$Q = Q_{tot} - Q_{stat} \quad \text{(Eq. 6.16)}$$

The dynamic load vector R expresses the difference between the total load vector and the load vector in static equilibrium. The dynamic equilibrium equation is solved by introducing equation (Eq. 6.11).

6.5.DAMPING

Damping is a term which describes the constructions ability to dissipate energy. In a real life damping will always exist (Sigbjörnsson & Langen, 1979).

"The tangential damping matrix is in the global Rayleigh damping formation established as a linear combination of the global tangential mass- and stiffness matrices (MARINTEK, 2012) *".*

$$C = \alpha_1 M + \alpha_2 K \quad \text{(Eq. 6.17)}$$

$\alpha_1 \, and \, \alpha_2$ are mass- and stiffness proportional damping coefficients (MARINTEK, 2012).

6.6.LOADS

When the riser is connected to both the sea bed and to a moving platform, it will experience several load effects. In addition, it will also be exposed to the environmental loads such as waves and current. When conducting a dynamic analysis these load effects will change over time. These loads are included in the dynamic equilibrium equation (Eq. 6.1) described in (MARINTEK, 2012).

- Weight and inertia
- Hydrostatic forces
- Hydrodynamic forces
- Forced motion of the line

The hydrostatic forces for risers have already been discussed in section 5.4 in terms of effective tension. Moreover, the wave loads and hydrodynamic loads will be further described in the following sections.

6.6.1. WAVE LOADS

6.6.1.1. REGULAR WAVES

The regular waves are modelled as Airy Linear waves which assume that the gravity wave can be described by harmonic functions (Larsen, Response Modelling of Marine Risers and Pipelines, 1990).

The boundary conditions for linear waves are valid at the mean water level. Hence, linear theory is only valid at for small wave amplitudes (MARINTEK, 2012).

$$\varphi = \frac{g\zeta_a}{\omega}\frac{\cosh k(z+h)}{\cosh kh}\cos(\omega t - kx) \qquad \text{(Eq. 6.18)}$$

Equation (Eq. 6.18) shows the wave potential for shallow water retrieved from (Faltinsen, 1990).

Predictions of acceleration and velocities in the wave crest are important. However as already mentioned, the wave potential is only valid for the mean water level. Further it exists methods for predicting this. These are;

- Extrapolation of potential
- Use of surface value in the wave crest
- Parallel move of potential
- Stretched or modified potential
- Use of higher order wave theory

These methods will not be further outlined here. However a detailed description is found in (Larsen, Response Modelling of Marine Risers and Pipelines, 1990).

6.6.1.2. IRREGULAR WAVES

In RIFLEX the irregular sea state is described as a sum of two wave spectra (MARINTEK, 2012).

$$S_{\zeta TOT}(\beta,\omega) = S_{\zeta 1}(\omega)\varphi_1(\beta-\beta_1) + S_{\zeta 2}(\omega)\varphi_2(\beta-\beta_2) \quad \text{(Eq. 6.19)}$$

In (Eq. 6.19), $S_{\zeta 1}$ and $S_{\zeta 2}$ describe the frequency distribution of the wind and the swell, $\varphi_1 and\ \varphi_2$ describes the directionality of the waves and β as shown below in **Figure 12** describes the direction of the wave propagation.

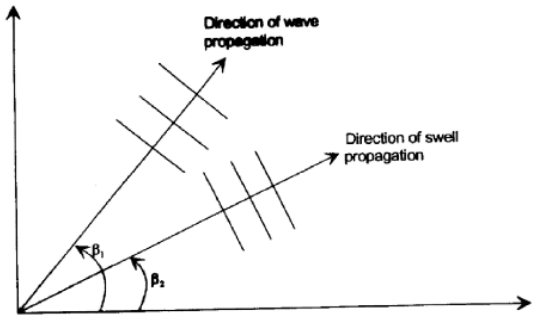

Figure 12: Wave direction (MARINTEK, 2012)

In this Master Thesis the analysis is conducted with irregular waves and a stochastic analysis is done. A detailed description of irregular waves and spectra is therefore found in chapter 7.

6.6.2. HYDRODYNAMIC LOADS

In this section the hydrodynamic loads acting on the riser are described. These are further outlined in (Larsen, Response Modelling of Marine Risers and Pipelines, 1990).

The inertia forces in y- and z-direction can be expressed as shown below. Furthermore, the inertia forces are linear and can therefore be decomposed as seen in (Eq. 6.20).

$$F_y = dx[(\rho A + A_{yy})a_{w'y} - A_{yy}\ddot{y}]$$
$$F_z = dx[(\rho A + A_{zz})a_{w'z} - A_{zz}\ddot{z}] \quad \text{(Eq. 6.20)}$$

As seen from (Eq. 6.20) the inertia forces are dependent on the orientation.

A	Cross section area
$A_{yy}$and A_{zz}	Added mass in respectively y- and z-direction

The inertia forces can also be found by the equation (Eq. 6.21).

$$F_y = \rho(C_M - 1)\frac{\pi D_H^2}{4}\ddot{y} + \rho C_M \frac{\pi D_H^2}{4}a_w \quad \text{(Eq. 6.21)}$$

C_M are the inertia coefficient and C_M=2 for circular cylinders. D_H is the hydrodynamic diameter for the cross-section. It should also be mentioned that by applying (Eq. 6.21) there is a risk of errors. However, by applying (Eq. 6.20) such errors can be avoided.

Drag forces are expressed in terms of Morison's equation as shown below.

$$F_{DRAG} = \frac{1}{2}\rho C_D D|v_r|v_r \quad \text{(Eq. 6.22)}$$

v_r is the relative structure –fluid velocity, C_D is the drag coefficient.

7. STOCHASTIC THEORY

7.1.INTRODUCTION TO STOCHASTIC THEORY

As described in (Myrhaug, 2007), by studying the sea surface it can be seen that the wave picture is quite chaotic and the shapes of the waves seem random. Hence, the proper description of waves is not obtained by describing them as a single sinusoidal wave. However, by describing the waves as irregular, it is possible to obtain what seems like random wave description. The disconnection analyses in this Thesis are conducted with irregular waves. Thus a proper description of irregular waves and how these are modelled is appropriate.

Irregular waves can be modelled by a stochastic process. (T.Moan-N.Spidsøe-S.Haver, 1980) explains that a stochastic process is a process which develops in time and space. It cannot be foreseen which value a stochastic process will have at a given time and space. However, based on statistics, it is possible to describe the probability of an incident wave in that space and time.

Since waves are a modelled as a stochastic process, a stochastic analysis is preferred. Information in the following part is obtained from (Larsen, Response Modelling of Marine Risers and Pipelines, 1990), or specified otherwise. The basic assumptions behind stochastic analysis are as follows;

- The sea surface is a Gaussian process seen in **Figure 13**, with a mean equal to zero and a constant variance (Myrhaug, 2007).
- The sea surface is an ergodic wave process, meaning that one single time series is representative for the wave process (Myrhaug, 2007).
- The waves are stationary within its time limits, which is approximately three hours.

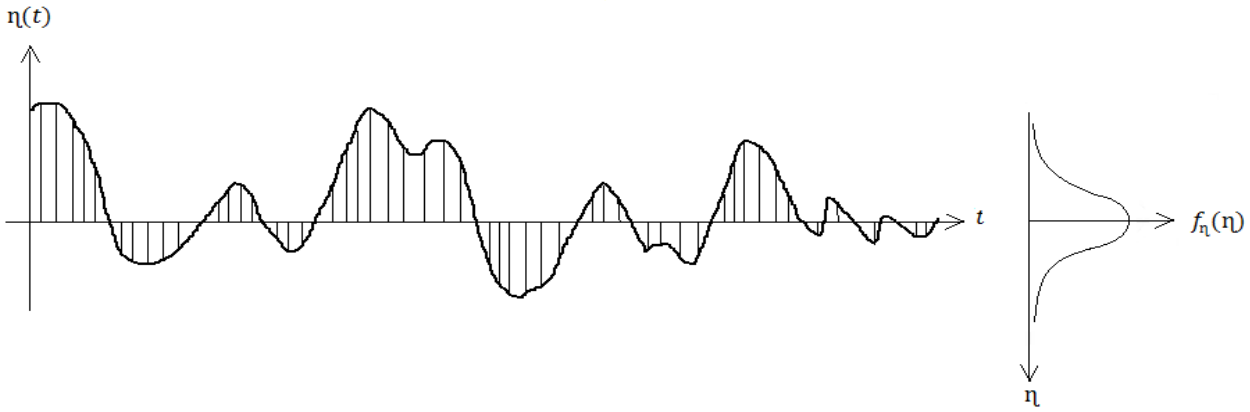

Figure 13: Gaussian Process based on graph in (Larsen, Response Modelling of Marine Risers and Pipelines, 1990)

Described in the stochastic wave process is assumed to be Gaussian distributed. This means that if sampling a process at a random time increment, t_i, the wave elevation is Gaussian distributed, seen in **Figure 13**.

If a certain set of requirements are satisfied the response becomes Gaussian distributed, these requirements are described in (Larsen, Stochastic Analysis of Marine Structures, Lecture notes, 2013). When this is the case the system is called a linear system.

7.2.SPECTRUM

As described in (Larsen, Stochastic Analysis of Marine Structures, Lecture notes, 2013),(Eq. 7.1) expressed the energy content in a harmonic wave per unit area of the surface. This description is based on linear wave theory.

$$E_i = \frac{1}{2}\rho g \zeta_{0i}^2 \qquad \text{(Eq. 7.1)}$$

$$\frac{E_i}{\rho g} = \frac{1}{2}\zeta_{0i}^2 \qquad \text{(Eq. 7.2)}$$

(Eq. 7.2) describes the energy content of a wave component, expressed in term of the wave amplitude.

A different way of describing the energy in the wave is by a wave spectrum (Eq. 7.3). The energy in the wave in a frequency interval Δω, represent the area of the wave spectrum for the same interval, seen in **Figure 14** (Larsen, Stochastic Analysis of Marine Structures, Lecture notes, 2013). Thus, the spectrum as seen in **Figure 14** is a description of the energy distribution of the wave components.

$$\frac{1}{2}\zeta_{0i}^2 = S_x(\omega_i)\Delta\omega_i \qquad \text{(Eq. 7.3)}$$

Where (Eq. 7.3) describe the wave spectrum.

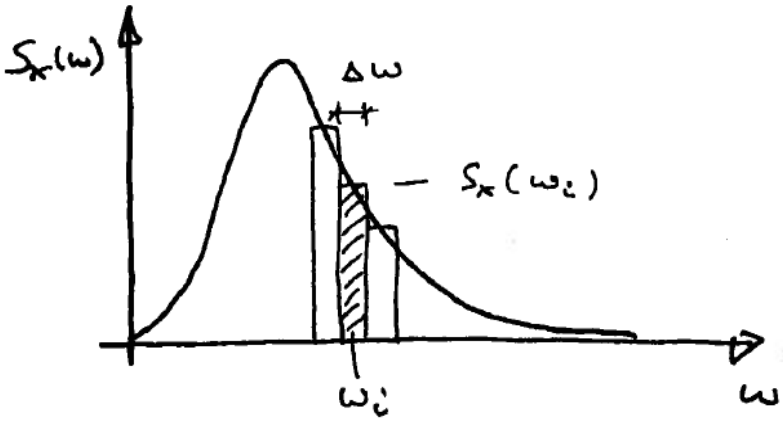

Figure 14: Spectrum based on graph in (Larsen, Response Modelling of Marine Risers and Pipelines, 1990)

Several spectrums have been developed based on measurements from different areas at sea. These spectrums are called standardized spectra.

As explained in (Myrhaug, 2007), a standardized wave spectrum is a "mean" spectrum expressing the mean response in the wave condition. When applying standardized spectra the actual spectrum for the area of study is not known. However, by applying standardized spectra it is possible to achieve a good estimate.

The statistical properties such as variance and standard deviation for the Gaussian process can be described by the wave spectra, seen in the equations (Eq. 7.4) and (Eq. 7.5), see (Larsen, Response Modelling of Marine Risers and Pipelines, 1990).

$$m_n = \int_0^\infty S_x(\omega)\omega^n d\omega \qquad \text{(Eq. 7.4)}$$

$$m_0 = \int_0^\infty S_x(\omega)d\omega = \sigma_x^2 \qquad \text{(Eq. 7.5)}$$

(Eq. 7.4) is the general equation for the spectral moments, and (Eq. 7.5) is the equation for the standard deviation.

The spectral moments can be applied to find the significant wave height (Eq. 7.6).

$$H_s = 4\sigma_x \qquad \text{(Eq. 7.6)}$$

7.2.1. *PIERSON-MOSKOWITZ SPECTRUM*

The Pierson- Moskowitz is a standardized spectrum further outlined in (Myrhaug, 2007). The Pierson-Moskowitz (PM) spectrum is a single parameter fully developed specter at open sea. A fully developed spectrum is a spectrum that has had sufficient time and space to fully develop the waves. The PM spectrum is based on measures taken in the North Atlantic Sea. The equations below describe the spectrum.

$$S(\omega) = \frac{A}{\omega^5}\exp[-\frac{B}{\omega^4}] \quad \text{(Eq. 7.7)}$$

(Eq. 7.7) is the equation for the PM spectra, A and B are constants which are defined below.

$$A = 0.0081g^2 \quad \text{(Eq. 7.8)}$$

$$B = 0.74(\frac{g}{V})^4 \quad \text{(Eq. 7.9)}$$

Moreover, the most relevant moments to the PM spectra are defined as follows.

$$m_0 = \frac{A}{4B} \quad \text{(Eq. 7.10)}$$

$$m_1 = 0.306\frac{A}{B^{3/4}} \quad \text{(Eq. 7.11)}$$

$$m_2 = \frac{\sqrt{\pi}}{4}\frac{A}{\sqrt{B}} \quad \text{(Eq. 7.12)}$$

For the PM spectrum the mean frequency (Eq. 7.13), zero up-crossing period (Eq. 7.14) and significant wave height (Eq. 7.15) are given by the following relationships, see (Larsen, Stochastic Analysis of Marine Structures, Lecture notes, 2013).

$$\omega_1 = 1.14\frac{g}{v} = \frac{m_1}{m_0} \quad \text{(Eq. 7.13)}$$

$$T_z = 2\pi^{\frac{3}{4}}B^{-\frac{1}{4}} = 2\pi\sqrt{\frac{m_0}{m_2}} \quad \text{(Eq. 7.14)}$$

$$H_s = 0.21\frac{v^2}{g} = 4\sqrt{m_0} \quad \text{(Eq. 7.15)}$$

Furthermore, in the analyses performed in this Master Thesis the Pierson-Moskowitz spectra is applied to generate the irregular waves.

7.2.2. JONSWAP SPECTRUM

The JONSWAP spectrum which is short for Joint North Sea Wave is a standardized spectrum. Information in this section is based on (Myrhaug, 2007). The JONSWAP spectrum is based on measures performed in the south-east part of the North Sea in 1968-1969.

The difference in the standardized spectrums is where the energy in the spectrum is distributed over the frequencies. In the JONSWAP spectrum there is more energy around the top frequency and less energy away from the top frequencies.

Moreover it should be mentioned that the JONSWAP spectrum is measurements from quite shallow water depths and close to shore. Additionally, the JONSWAP describes spectrum for not fully developed sea states. This leads to a stronger top than fully developed spectra. Consequently, it is discussed whether or not this specter should be used. However, it is a quite common spectrum to use on shallow water depths.

$$S(f) = \alpha g^2 (2\pi)^{-4} f^{-5} \exp\left[-\frac{5}{4}\left(T_p f\right)^{-4}\right] \gamma^{exp\{\frac{(T_p f - 1)^2}{2\sigma^2}\}} \quad \text{(Eq. 7.16)}$$

(Eq. 7.17) show the range where the JOSNWAP spectrum is assumed to be good.

$$3.6\sqrt{H_{m0}} \leq T_p \leq 5\sqrt{H_{m0}} \quad \text{(Eq. 7.17)}$$

7.3.STOCHASTIC ANALYSIS

Based on the spectrum function $S_\zeta(\omega)$ the harmonic stochastic waves can be generated by applying inverse Fourier transformation, further explained in (Larsen, TMR4182 Marin Dynamikk, 2012). The amplitude can be expressed in terms of the wave spectrum (Eq. 7.19).

$$x(t) = \sum_{i=1}^{N} x_{0i}\cos(\omega_i - \varepsilon_i) \qquad \text{(Eq. 7.18)}$$

$$x_{0i} = \sqrt{2S_x(\omega_i)\Delta\omega_i} \qquad \text{(Eq. 7.19)}$$

x_{0i} is the amplitude and ε_i is the random phase angle made by a random number generator. When estimating the wave realization in this way, it means going from the frequency domain where the process is fully described, to the time domain where it is not.

As described in (Larsen, Response Modelling of Marine Risers and Pipelines, 1990) the interval for the phase angle is between [0,2π]. The quality of the random number generators can vary leading to the generation of $x(t)$ not being Gaussian. If the quality of the generator is poor, it does not generate random numbers. Furthermore, when applying a random number generator the time series will be periodic. Hence, the time series will repeat itself after a given time T. This time period is defined by (Eq. 7.20).

$$T = \frac{2\pi}{\Delta\omega_{min}} \qquad \text{(Eq. 7.20)}$$

Further outlined in (Larsen, TMR4182 Marin Dynamikk, 2012), by applying Fourier Transformation it is possible to achieve an estimate for the spectrum over time. This is done by applying the following equation in (Eq. 7.21).

$$\omega_i = i\frac{2\pi}{T}\ , i = 1,2,,,,,N \qquad \Delta\omega = \frac{2\pi}{T}$$

$$a_i = \frac{2\pi}{T}\int_0^T x(t)\sin(\omega_i t)dt \qquad b_i = \frac{2\pi}{T}\int_0^T x(t)\cos(\omega_i t)dt \qquad \text{(Eq. 7.21)}$$

$$x_i = \sqrt{a_i^2 + b_i^2} \qquad \varepsilon_i = arctg(\tfrac{a_i}{b_i}) \qquad S_x(\omega_i) = \frac{1}{2\Delta\omega}x_i^2$$

When applying these equations (Eq. 7.21) directly several thousand time steps are generated. The computation time for this process is extensive. However, by applying Fast Fourier Transforms (FFT) the computation time can be significantly reduced.

FFT is an alternative way to the Fourier Transformation, and it is always applied when considering long stochastic time series, see (Larsen, Response Modelling of Marine Risers and Pipelines, 1990). The generation of cosine and sine is very time consuming. However, by applying FFT this is avoided. In this method, $\Delta\omega$ and Δt are fixed as seen in (Eq. 7.22), and the time series are generated in one shot.

$$N_{\Delta t} = 2N_{\Delta\omega} \qquad N_{\Delta t} = \frac{T}{\Delta T} = \frac{\omega_p}{\Delta\omega}\ 2$$

$$T = \frac{2\pi}{\Delta\omega} \qquad T_{min} = \frac{2\pi}{\omega_p} \qquad \text{(Eq. 7.22)}$$

(Larsen, Response Modelling of Marine Risers and Pipelines, 1990) describe that the stochastic process when considering the dynamic equilibrium equation is the external forces R(t). When applying (Eq. 7.23), the non-linearities further described in section 6.1 are also considered.

$$M\ddot{r} + C\dot{r} + Kr = R(t) \qquad \text{(Eq. 7.23)}$$

The dynamic equilibrium equation (Eq. 7.23) is solved by using the direct use of numerical time integration as further described in section 6.2. Moreover, it should be mentioned that the response is a result of the stochastic process. Hence, the mean variance and extremes should be estimated.

7.4.EXTREME STATISTICS

If the individual maxima of the process is statistical independent, it will be described by either the Rayleigh- or the Rice distribution. Information presented in this section is obtained from (Larsen, TMR4182 Marin Dynamikk, 2012).

For the general Gaussian process the Rice distribution describes the individual maxima. Moreover, the Rice distribution is defined by two parameters, the bandwidth and the standard deviation.

Where the bandwidth is;

$$\varepsilon = 1 - \frac{m_2^2}{m_0 m_4} \qquad \text{(Eq. 7.24)}$$

ε	Bandwidth
m_0, m_2, m_4	Spectral moments

However, if the bandwidth is $\varepsilon = 0$, it means that the process is narrow banded, and the individual maxima can be described be the Rayleigh distribution instead. Furthermore, a narrow-banded process is a process where there only exist positive maxima, seen in the top graph in **Figure 15**.

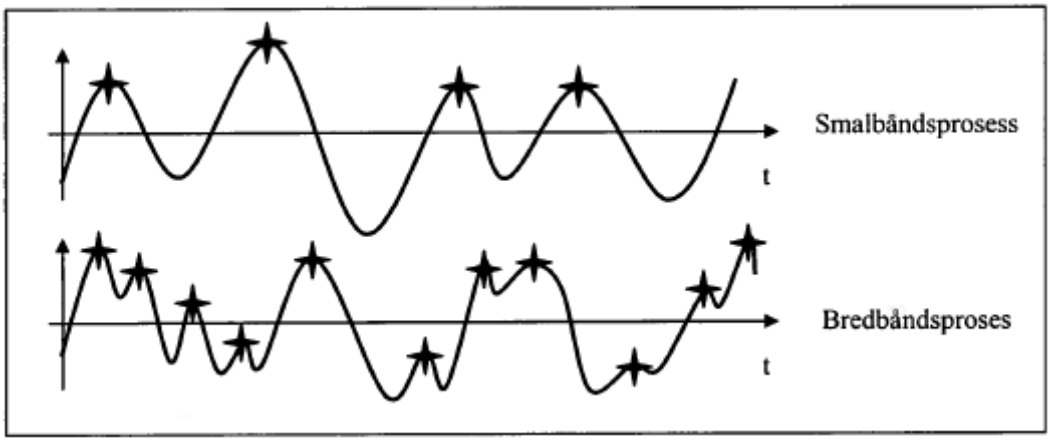

Figure 15: Narrow-banded and Broad-banded processes (Larsen, TMR4182 Marin Dynamikk, 2012)

If $\varepsilon = 1$ it means that the process is broad-banded. In this case the individual maximum is described by the Gaussian distribution rather than the Rice distribution. Furthermore, in the broad-banded process there exist both positive and negative maxima, as seen in bottom graph in **Figure 15**.

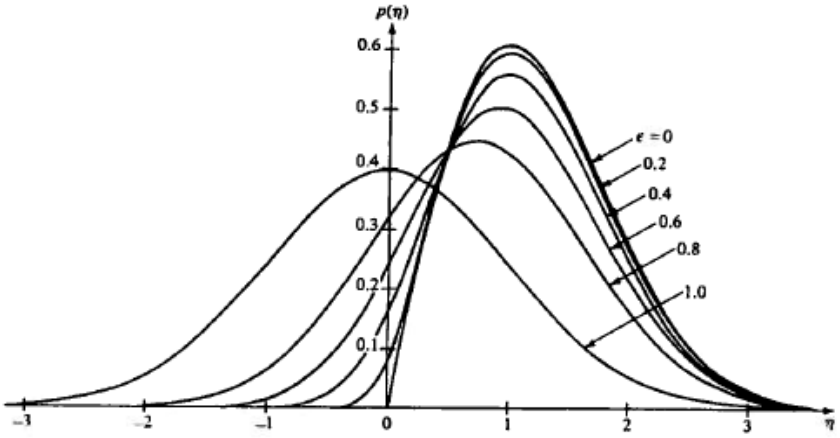

Figure 16: Transition between the distributions (Larsen, TMR4182 Marin Dynamikk, 2012)

Seen in **Figure 16** is the transition between the different distributions, illustrated with the bandwidth.

PART III: METHOD

8. MODELLING

8.1.INTRODUCTION TO RIFLEX

The analysis in this thesis is conducted with the modeling program RIFLEX. Information regarding RIFLEX is further outlined in (MARINTEK, 2013).

RIFLEX is an analysis program which is based on the Finite Element Method to conduct static and dynamic analyses. The program has been developed by MARINTEK to be applied on flexible marine risers but may also be used on other slender structures.

The analyses which can be conducted in RIFLEX are;

- Static analysis
- Static parameter variation analysis
- Dynamic analysis
- Frequency domain analysis

8.2.MODELLING IN RIFLEX

The initial model was provided by a fellow student (Hermanrud, 2014) who wrote his Master Thesis on a similar system in the spring of 2014. This model was converted and changed in order to achieve the correct size and setup in the Project Thesis. Furthermore, the modified model has then been further changed into to two models with different water depth, approximately 350m and 1000m.

As described in (MARINTEK, 2013), the system in RIFLEX is modelled with a number of lines which are connected by supernodes as seen in **Figure 17**. The boundary conditions for the system are given by classifying the supernodes as free or fixed. When the supernodes are fixed it is due to modelling support at fixed structures or sea bed connection.

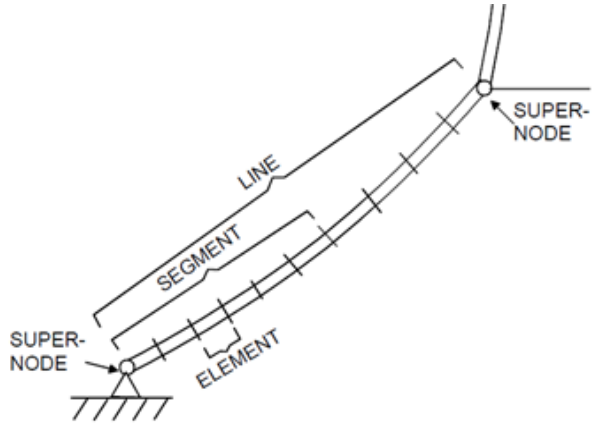

Figure 17: System definition RIFLEX (MARINTEK, 2013)

A line is a linear structural element between two supernodes as seen in **Figure 17**. Each line is given a line number and consists of several segments. A single line can applied several times during the model which makes the modelling efficient. Each segment in the line are provided with a certain cross-section which describes the properties of the segment. The segments represent the different components in the system. Hence, the cross-sectional properties for each segment represents the component.

As mentioned each segment represents a type of a component in the system, and the properties of the component are characterized by the cross-sectional properties. Some of the components in the system have cross-sections which are not circular, like the LRP and EDP. However, in RIFLEX a global cross-section is applied, thus the properties such as axial-, bending-, and torsional stiffness have to be specified as input. Hence, all components are modelled as circular cylinders.

In this analysis all components are modelled by using CR01 cross-section in RIFLEX. The stress joint is modelled by a built in line type in RIFLEX where it is divided in three as seen in **Figure 18**.

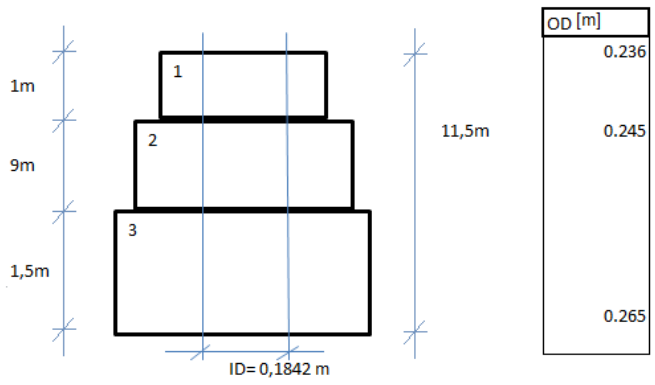

Figure 18: Dimensions stress joint

Moreover the wellhead is modelled as a circular cylinder. The total length is 12.38 meters where 2.403 meters are above the sea bottom and the rest below.

8.3.MODELLING DISCONNECTION

To model the disconnection event a master-slave relationship has been applied. The method is based on a similar event that was conducted in (Grønevik, 2013). The disconnection takes place between the EDP and the LRP as seen in **Figure 5**.

Initially, Node 12's boundary condition was set as free. However, it is not possible to set a node free when it already is. In consequence, the master-slave relationship has been applied between Node 12 and Node 13 to enable for disconnection. The master-slave relationship means that the slave-node will be fully dependent on the master-node. Thus, when the master-node moves, so does the slave. As seen from **Figure 19** Node 12 is the slave-node and Node 13 is the master-node. To enable for disconnection, the slave-node is exposed to a boundary condition change from fixed to free. This will release the EDP from the LRP and the riser will hang free from the vessel.

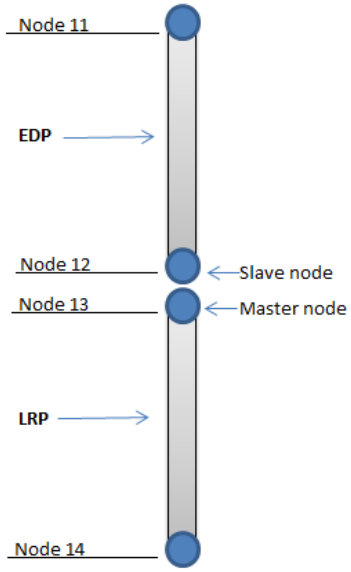

Figure 19: Master-Slave relationship EDP-LRP

At the same time as the disconnection takes place the riser is locked to the vessel and will follow the motion of the vessel. To model this, a boundary change has been applied. The boundary condition of Node 1 changes from free to fixed. When it is set as fixed, it is fixed to the vessel motions. This is done simultaneously as the disconnection.

8.4.MODELLING RISER RECTRACTION

To prevent collision between the EDP and the LRP the riser is lifted-up at the top. This retraction is performed simultaneously as the EDP disconnects from the LRP. It is considered to be conservative to assume that the retraction length is approximately 2-4m. In RIFLEX the retraction is modelled by applying the *Segment Length Variation* in the dynamic calculations. This length variation is done in Line1, thus in the top of the riser. This function will change the length of the riser at a given time interval. In the retraction analyses performed in this Thesis, the segment length variation is changed over a time interval of one second. This is done at the same time as the disconnection is performed.

Lift-up	Velocity [m/s]
1m	-1
2m	-2
4m	-4

Table 1: Lift-up velocity

To obtain the different lift-up events, the variation is changed with the rate as seen in **Table 1**.

8.5.HEAVE DISPLACMENT VESSEL

In order to find the heave (vertical) displacement of the vessel an independent line has been defined. The line is attached to the vessel, this is done by setting the boundary condition for the node fixed to the vessel. The line is attached to the vessel throughout the simulations in order to get the results for the heave (vertical) displacement for the vessel. The initial position of the studied node is 25 meter. Hence, when studying the heave displacement results the displacement is subtracted by a number of 25 for each value.

8.6.SHALLOW WATER MODEL

The shallow water model is similar to the model applied in the Project Thesis seen in **Figure 20**. The main modification that has been made is the master-slave relationship described in section 8.3.

The shallow water model consists of the components illustrated in **Figure 20**. The length the components are presented below.

Component	Length [m]	Number of lines
Surface Flow Tree	1.851	1
Landing Joint	14.8990	1
Tension joint section 3	2.7990	1
Tension joint section 2	0.2860	1
Tension Joint section 1	4.0090	1
Open Water Lubricator Valve	4.9960	1
Safety joint	3.048	1
standard joint	11.5820	27
Stress joint (tapered)	11.5000	1
Non-circular cross sections		
EDP	3.1630	1
LRP	2.2980	1
XTAC	1.0600	1
XMT	2.8700	1
WH	12.3800	1
Total Length of the system		377.873

Table 2: Lengths Shallow water model

As can be seen from **Table 2** the entire length of the system is 377.873 m. However, this includes the parts above the water line. The water depth is 348m.

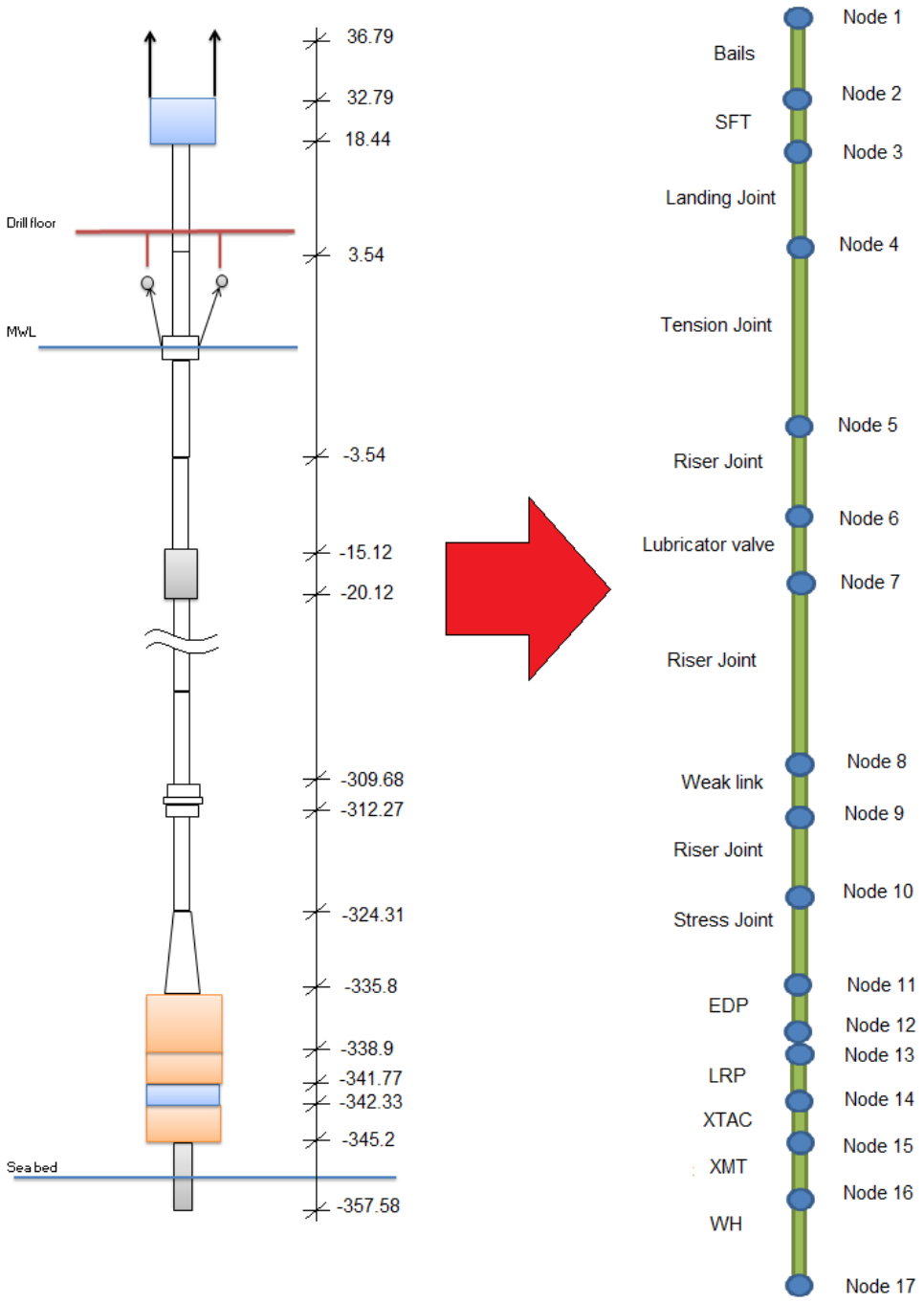

Figure 20: System modelling RIFLEX shallow water depth

In **Figure 20**, the modelling of the Workover Riser, which is applied in this Thesis is illustrated. The stack-up at left, shows the actual model and its length. The figure at right, shows the RIFLEX modelling of the system.

To model the Workover Riser 15 lines have been applied. Some are applied several times in order to model the correct length. As seen, the system is modelled with 17 super nodes which connect these lines.

Furthermore, the EDP and LRP are connected by two nodes to enable the disconnection event.

8.7.DEEP WATER MODEL

The deep water model is basically the same as the shallow water, except for its length. The length has been adapted in order to have a water depth of approximately 1000m.

Component	Length [m]	Number of lines
Surface Flow Tree	1.851	1
Landing Joint	14.8990	1
Tension joint section 3	2.7990	1
Tension joint section 2	0.2860	1
Tension Joint section 1	4.0090	1
Open Water Lubricator Valve	4.9960	1
Safety joint	3.048	1
standard joint	11.5820	83
Stress joint (tapered)	11.5000	1
Non-circular cross sections		
EDP	3.1630	1
LRP	2.2980	1
XTAC	1.0600	1
XMT	2.8700	1
WH	12.3800	1
Total Length of the system		1026.465

Table 3: Lengths deep water model

As can be seen from **Table 3** the length of the entire system is 1026m. The length of the water depth is 996.19m, thus almost a 1000m.

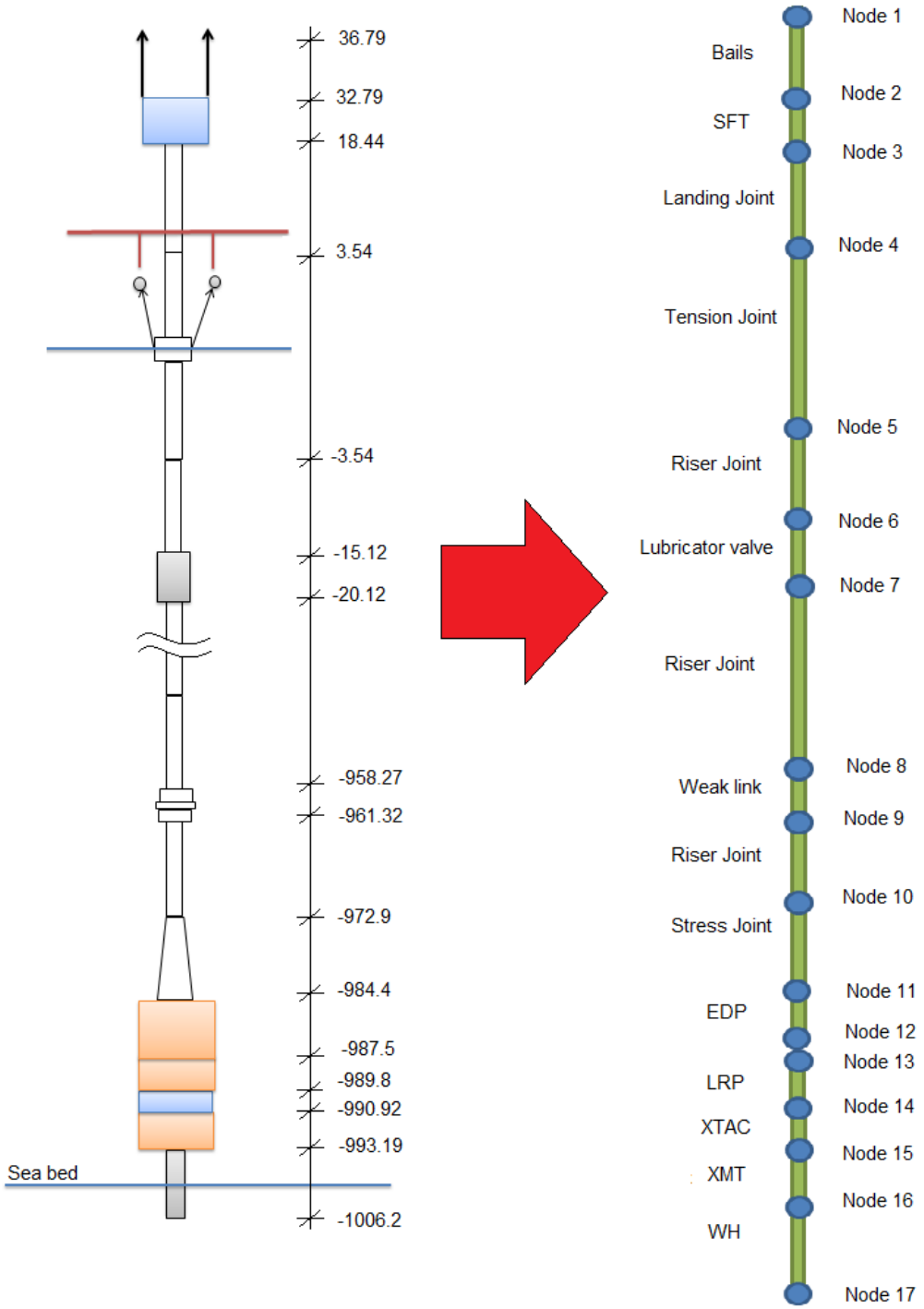

Figure 21: System modelling RIFLEX deep water model

As for the shallow water model, **Figure 21** illustrates the system set-up for the modelling. Where the system to the left is the Workover System for deep water and the system to the right is the modelling in RIFLEX. The set up for the two models are identical. The only difference is the water depth.

9. INPUT

The system input for this Thesis has been provided by Aker Solutions. It is meant as an example for typical values and is not a specific project. Furthermore, the stack-up for both the shallow water and the deep water model have been developed in order to fit the different water depths. The following properties have been provided, seen in **Table 4**.

- System components
- Length of components
- Inner diameter at start and end of each component
- Outer diameter at start and end of each component
- Material density
- E-modulus
- Ultimate Yield Strength
- Yield Strength

Component	Length	OD_start	ID_start	OD_end	ID_end	Width (non-circular sections)	rho	E-modulus	YS (Yield strenght)	UTS(Ultimate Tensile Strength)
Unit	m	m	m	m	m	m	kg/m^3	N/m^2	MPa	MPa
Surface Flow Tree	1.851	0.4320	0.1797	0.4320	0.1797	-	7850	2.05E+11	550	690
Landing Joint	14.8990	0.2530	0.1842	0.5080	0.1842	-	7850	2.05E+11	550	690
Tension joint section 3	2.7990	0.2530	0.1930	0.2530	0.1930	-	7850	2.05E+11	550	690
Tension joint section 2	0.2860	0.5400	0.1930	0.5400	0.1930	-	7850	2.05E+11	550	690
Tension Joint section 1	4.0090	0.2530	0.1930	0.2530	0.1930	-	7850	2.05E+11	550	690
Open Water Lubricator Valve	4.9960	0.2445	0.1930	0.2445	0.1930	-	7850	2.05E+11	550	690
Safety joint	3.048	0.2445	0.1930	0.2445	0.1930	-	7850	2.05E+11	550	690
standard joint	11.5820	0.2508	0.1944	0.2508	0.1944	-	7850	2.05E+11	655	818.75
Stress joint (tapered)	11.5000	0.2650	0.1842	0.2360	0.1842	-	7850	2.05E+11	550	690
Non-circular cross sections										
EDP	3.1630	0.6858	0.1873	0.6858	0.1873	4.500	7850	2.05E+11	550	690
LRP	2.2980	0.7366	0.1778	0.7366	0.1778	4.198	7850	2.05E+11	550	690
XTAC	1.0600	0.7366	0.1778	0.7366	0.1778	4.000	7850	2.05E+11	550	690
XMT	2.8700	0.7366	0.1873	0.7366	0.1873	4.100	7850	2.05E+11	550	690
WH	2.4030	0.7630	0.7112	0.7630	0.7112	-	7850	2.05E+11	550	690

Table 4: Input provided by Aker Solutions

As mentioned in section 8.2 each component is defined by their cross-sectional properties. The cross-sectional properties that each segment in RIFLEX needs are; axial stiffness, bending stiffness, buoyancy, moment of inertia and hydrodynamic diameter. These properties are calculated based on the given input, as seen in the following equations. The calculations for both the shallow water model and the deep water model are presented in appendix A.1 .

$$Axial\ Stiffness = AE \quad \text{(Eq. 9.1)}$$

$$Bending\ Stiffness = EI \quad \text{(Eq. 9.2)}$$

$$B = (W_{air} - W_{water})g \quad \text{(Eq. 9.3)}$$

$$I_x = I_y = \frac{\pi}{64}(D_o^4 - D_i^4) \quad \text{(Eq. 9.4)}$$

$$D_H = \sqrt{\frac{4B}{\rho_w g L} + D_i^2} \quad \text{(Eq. 9.5)}$$

A_e	External are
E	E-modulus
$W_{air,}$ W_{water}	Weight in air and Weight in water
D_o,D_i	Outer diameter and inner diameter
D_H	Hydrodynamic diameter
L	Length
ρ_w	Density water

The components are all modelled with a global circular cross-section even though some of them are not circular. Because of that, the components with non-circular cross-sections have to be given a hydrodynamic diameter. By doing so RIFLEX takes the different geometry into consideration when conducting the analysis or calculations. In (Eq. 9.5) the hydrodynamic diameter is calculated. This equation has been retrieved from (Knardahl, 2012) and is further described in (Det Norske Veritas, 2010).

The RAO which has been applied is the same as (Hermanrud, 2014) used, based on recommendations from Aker Solutions. The RAO is for a drilling platform “Deepsea Atlantic”, which is a dynamically positioned semi-submersible vessel.

9.1.CURRENT PROFILE

The current profile applied in the simulations in this Thesis was provided by (Aker Solutions, 2014) and are shown in the table below.

	NE	0.99998	0.999	0.995	0.99	0.95	0.9	0.5	0.1
	Prob	0.001	0.004	0.005	0.040	0.050	0.400	0.400	0.100
Water Depth	0	124	89	73	66	48	40	18	6
	20	124	89	73	66	48	40	18	6
	50	110	80	67	60	45	38	17	6
	100	102	73	60	55	40	33	14	5
	200	92	68	57	52	39	33	14	3
	300	79	60	51	47	36	31	15	5
	400	78	60	51	47	36	31	15	5
	500	62	48	41	38	30	25	13	4
	600	50	40	35	33	26	23	12	4
	800	50	40	35	33	26	23	12	4
	1000	46	37	32	30	24	21	12	4
	1200	49	39	33	31	24	21	11	4
	1300	44	34	30	28	22	19	9	3

Table 5: Current profiles provided by (Aker Solutions, 2014).

Table 5 illustrates the current profiles with different velocities. The column on the left shows the water depth.

The current profiles applied for the shallow water depth and deep water depth in this Thesis are shown in **Table 6**.

Depth [m]	Shallow water current [m/s]	Deep water current [m/s]
0	0.4	0.4
20	0.4	0.4
50	0.38	0.38
100	0.33	0.33
200	0.33	0.33
300	0.31	0.31
400	0.31	0.31
500		0.25
600		0.23
800		0.23
1000		0.21

Table 6: Current profiles applied in analyses

10. CORRELATION STUDY

A correlation study has been performed in order to check if there exist a relation between the vertical velocity at the time of disconnection and 30 seconds in advance. It takes 30 seconds to send the signal from the vessel to the EDP before the disconnection takes place. This is why the time interval is 30 seconds.

The velocities are calculated as shown in equation (Eq. 10.1) in accordance with (Larsen, Guidance Master Thesis, 2014). To study the correlation these values are plotted in a scatter diagram.

$$\frac{dH_i}{dt} = \frac{h_{i+1} - h_i}{\Delta t} \qquad \text{(Eq. 10.1)}$$

H1 Vertical displacement at 30 seconds in advance of disconnection
H2 Vertical displacement at Disconnection

The criteria for correlation is, if a relation between the two velocities exists, the values in the scatter diagram should form a linear pattern.

Excel is applied to plot and calculate the correlation coefficient. The equation for calculation coefficient is presented below.

$$Correl(X,Y) = \frac{\sum(x-\bar{x})(y-\bar{y})}{\sqrt{\sum(x-\bar{x})^2 \sum(y-\bar{y})^2}} \qquad \text{(Eq. 10.2)}$$

The correlation coefficient (Eq. 10.2) is calculated in accordance with (Microsoft Office, 2014).

11. MATLAB CODING

Three MATLAB scripts has been developed in order to retrieve results and to do calculations. In this section a description of these MATLAB scripts are found, shown in appendix A.4 .

In section 10 there is a description the correlation study. To complete this study a MATLAB script was needed to calculate the vertical velocities. The MATLAB script is presented in appendix A.4 .Firstly the script reads in all the results from all the analyses and stores it in a three dimensional matrix. Secondly it defines a matrix for the vertical velocities. Finally, the calculations are performed and stored in the velocity matrix.

The next script is the probability script. It has been developed to check for collision between the EDP and LRP. Firstly it reads in the displacements from the file. A counting parameter set as zero, and starting parameters are defined. Furthermore, a criteria is set, and the results from the displacements are checked. If the criterion for collision is satisfied the counter is added by a value of one. Finally the result for the counter is returned.

The next script has been developed to post-process the results for the displacements. First the script read in the results to a matrix called x. Further it defines the heave displacement, the time and displacement for the EDP. Finally these results are plotted.

PART IV: RESULTS, DICUSSION AND FUTHER WORK

12. RESULTS

12.1. INTRODUCTION TO RESULTS

The purpose of this Thesis is to study the critical scenario of collision between the EDP and LRP. To study this event several disconnection analyses have been conducted. Furthermore, a method for deciding the optimal point in time to perform a disconnection should be proposed. In this chapter all results from the analyses are presented. This is performed in the following way:

Different disconnection events: To study the displacement of the EDP, several disconnection events have been completed for the shallow water model. The disconnection events are conducted at heave displacement top, heave displacement bottom, in the middle of the heave displacement and at random disconnection timing.

Mean study: Based on the results from the disconnection events a mean displacement study has been conducted. The results in this section are presented in terms of graphs.

Probability: To study the probability of collision between the EDP and LRP for the disconnection events a MATLAB script are developed. The results are presented in terms of the mean percent of time the EDP is within the limits of the LRP.

Correlations study: Several random disconnections have been completed for three different T_p. Based on the displacement results, the vertical velocity is calculated. Moreover, a correlation study has been conducted from the vertical velocities.

Riser Lift-up: Simultaneously as the disconnection is conducted the riser is lifted up 2-4 meters. Riser retraction (lift-up) analyses have therefore been conducted to study how this will influence the displacement.

The results presented in the following sections are presented in the same sequence as presented above. Moreover, all the analyses are performed with irregular waves based on the Pierson-Moskowitz Zero spectrum explained in section 7.2.1. The simulation length applied in all the analyses is 500 seconds. The time step is 0.03. However, the storage step is 2, therefore the results are presented with a time step of 0.06.

Furthermore, the top tension applied in Node 1 in the systems is 1500kN for the shallow water model and 2100kN for the deep water model. These values were chosen so that the effective tension is positive in the entire riser system. However, they will not influence the results for the displacement, since the riser is locked to the platform at the same time as disconnected.

12.2. DISCONNECTION EVENTS

To study the difference in disconnection timing four different disconnection events are analyzed. For each of these events several analyses have been conducted. The disconnection events studied for the shallow water model are;

- Disconnection at the top of the heave displacement
- Disconnection at the bottom of the heave displacement
- Disconnection half way up the heave displacement (at maximum velocity)
- Disconnection at a random time incident

All the analyses are run with a significant wave height H_s=5.5m, and the peak period is T_p=10sec. The reason for running the analysis with H_s=5.5m is because this is a typical requirement for performing a normal disconnection with the Workover Systems, as seen in appendix A.7 .

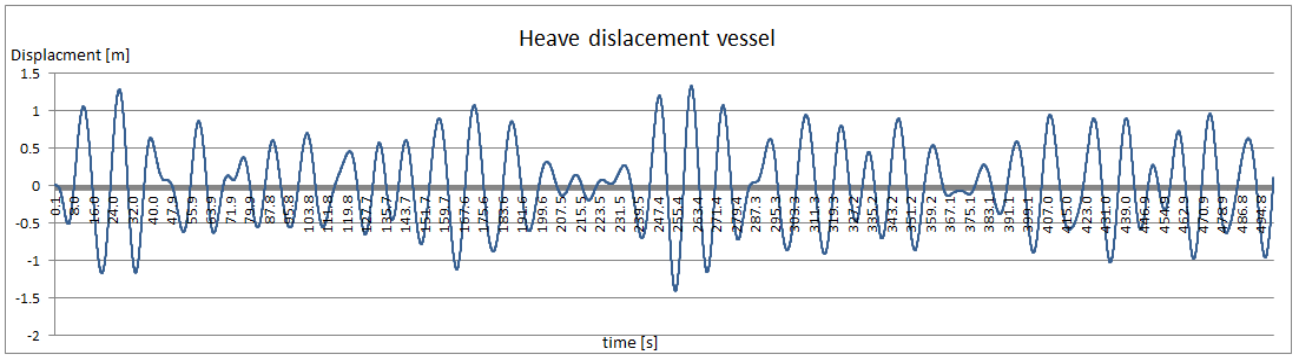

Figure 22: Heave motion vessel

Figure 22 shows the heave displacement for the vessel. By studying this, the disconnection timings for the top, bottom and half way up the heave displacement are determined. The different disconnection timings for each sea state are presented in **Table 7**.

Number	Seed	Top [s]	Bottom [s]	Middle [s]	Random [s]
1	87685	408.419983	416.2799988	422.0999756	380.48
2	43739	388.97998	395.5799866	398.9400024	380.48
3	76599	359.339996	368.039978	371.3999939	380.48
4	87698	360.359985	367.019989	370.2599792	380.48
5	50414	325.97998	333.8399963	337.6799927	380.48
6	49126	363.47998	370.6799927	374.9400024	380.48
7	48482	360.720001	367.6199951	371.4599915	380.48
8	48160	342.539978	351.3599854	356.4599915	380.48
9	47999	393.359985	400.7399902	404.3399963	380.48
10	87634	355.380005	361.9199829	365.3399963	380.48

Table 7: Table with seed numbers and disconnection timings

After the disconnection timings were found each scenario was run. The four different disconnection scenarios have been completed. This has been done for 10 different sea states, thus the 40 different analyses have been run.

12.2.1. DISCONNECTION EVENTS FOR SHALLOW WATER MODEL

In **Figure 22** the heave displacement for the vessel for a particular sea state is presented. Based on this heave displacement, the disconnection timings for this sea state are determined. The sea state for this case is run with a seed=87685, T_p=10s and H_s=5.5m. Furthermore, the model considered here is the shallow water model, thus the water depth is -348 meter. The displacements presented in the following graphs show the displacement for the bottom of the EDP with the initial position at -338.96 meter. Moreover, the location of the top part of the LRP also is -338.96 meter.

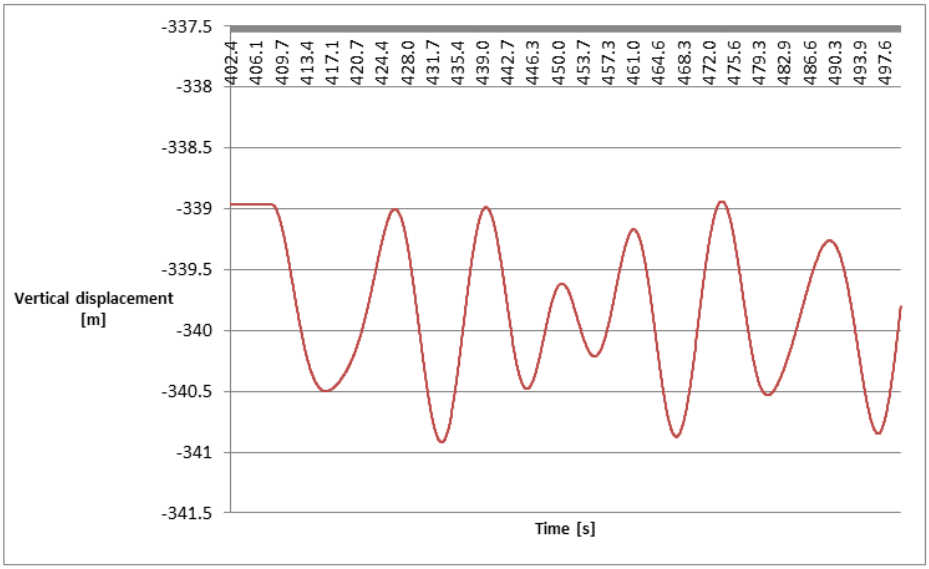

Figure 23: Vertical displacement of EDP, disconnection at top of heave displacement

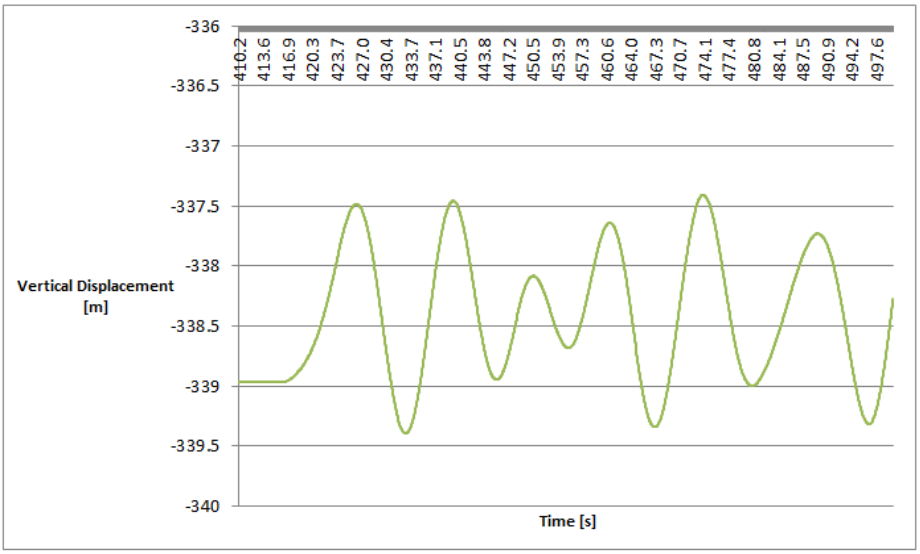

Figure 24: Vertical displacement of EDP, disconnection at bottom of heave displacement

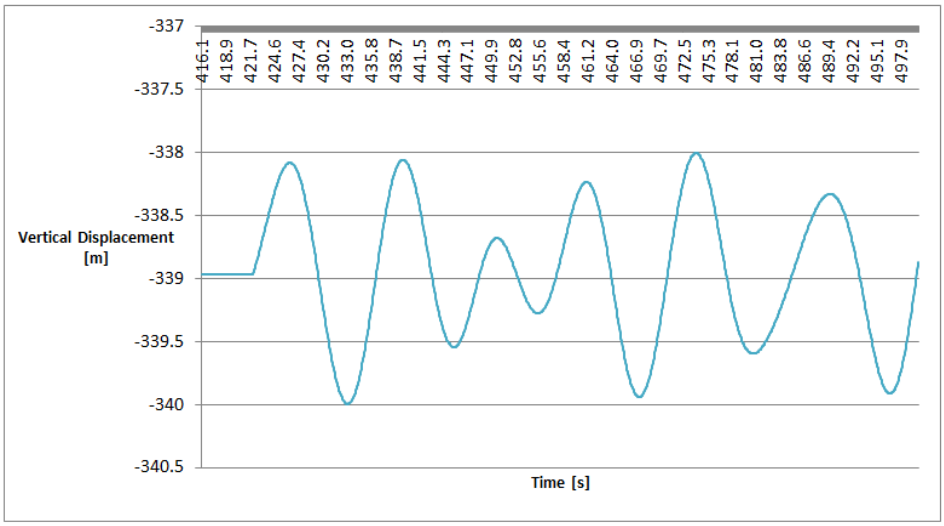

Figure 25: Vertical displacement, disconnection half way up the heave displacement

Presented in **Figure 23**, **Figure 24** and **Figure 25** are the vertical displacement for the different disconnection events performed at top, bottom and half way up the heave displacement respectively. A certain time interval is presented to emphasize the displacement after disconnection.

The graph in **Figure 23** shows the vertical displacement for the EDP when the disconnection is performed at the top. In this case the disconnection is done at 408.41s. When the disconnection is activated the boundary condition is set as free. As observed the EDP immediately has a displacement in negative z-direction when disconnection is performed. Moreover, it is seen that the mean displacement after disconnect is below its initial position.

Figure 24 shows the vertical displacement when the disconnection is performed at the bottom. After disconnection the EDP will have a displacement in positive z-direction as observed in the graph. Compared to disconnection performed at top, seen in **Figure 23**, it is seen that the mean vertical displacement for disconnection at the bottom is above the initial position of the EDP.

The graph in **Figure 25** shows the results for disconnection conducted half way up the heave displacement at 422.09s. This is the time incident with highest positive vertical velocity. The velocity has its maximum when the derivative of the velocity is equal to zero, which is half way up the heave displacement. As observed the EDP has a vertical displacement in positive z-direction for a short time interval, followed by a negative. Furthermore the mean displacement is at its initial position. As observed the EDP will first have a small vertical displacement in positive z-direction, followed by displacement in negative z-direction.

12.3. MEAN DISPLACEMENT

In **Table 7** the different analyses are presented. A mean displacement study has been conducted based on the results from these events. The vertical displacement for the EDP after disconnection has been retrieved and exported from MATLAB to excel. The mean displacement has been calculated in the following way.

$$x(t) = \frac{\sum_{i=1}^{n} z_i(t)}{n} \qquad \text{(Eq. 12.1)}$$

x(t) is the mean displacement at time t and $z_i(t)$ is the displacement for each sea state at time t. n is the total number of analyses for the different scenarios. These results have been plotted and are presented in the following part.

The graphs presented in this section illustrate the EDP's mean vertical displacement for the different disconnection events. The time interval shows the time after disconnection is performed. The displacements presented in the graphs show the displacement for the bottom part the EDP. The initial position for this is -338.96 meters, which is also the top of the LRP.

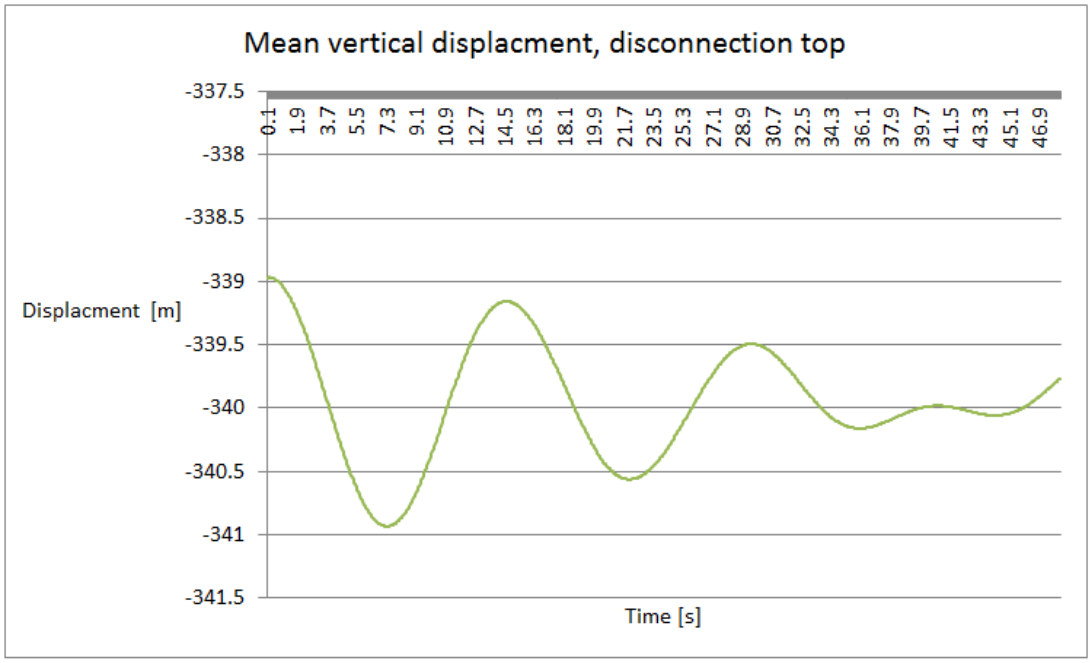

Figure 26: Mean vertical displacement for EDP, disconnect at heave top

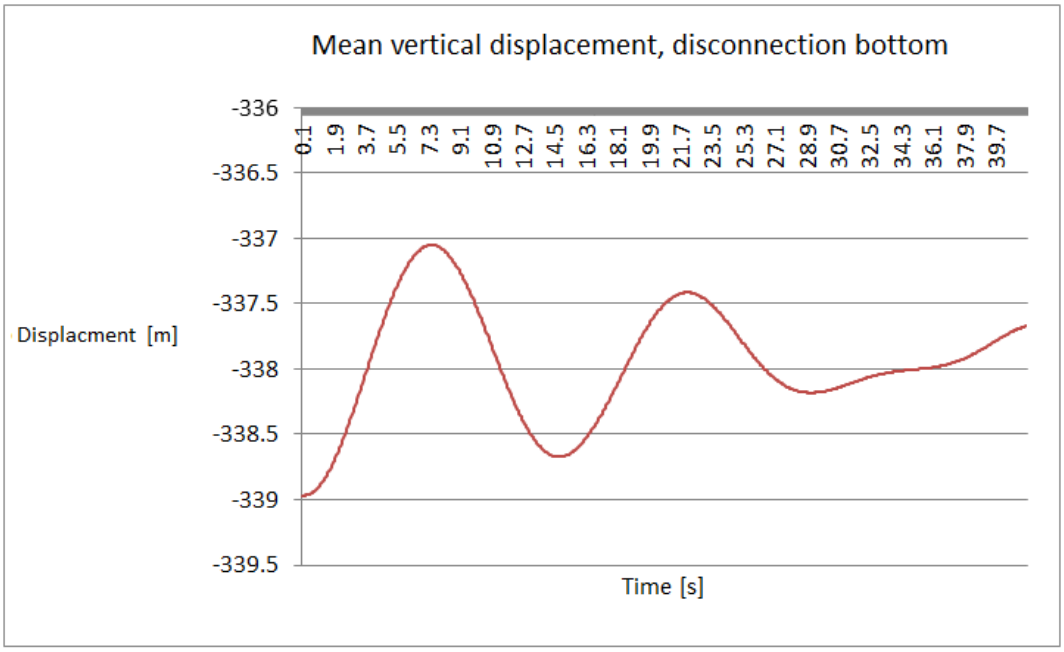

Figure 27: Mean vertical displacement for EDP, disconnection at heave bottom

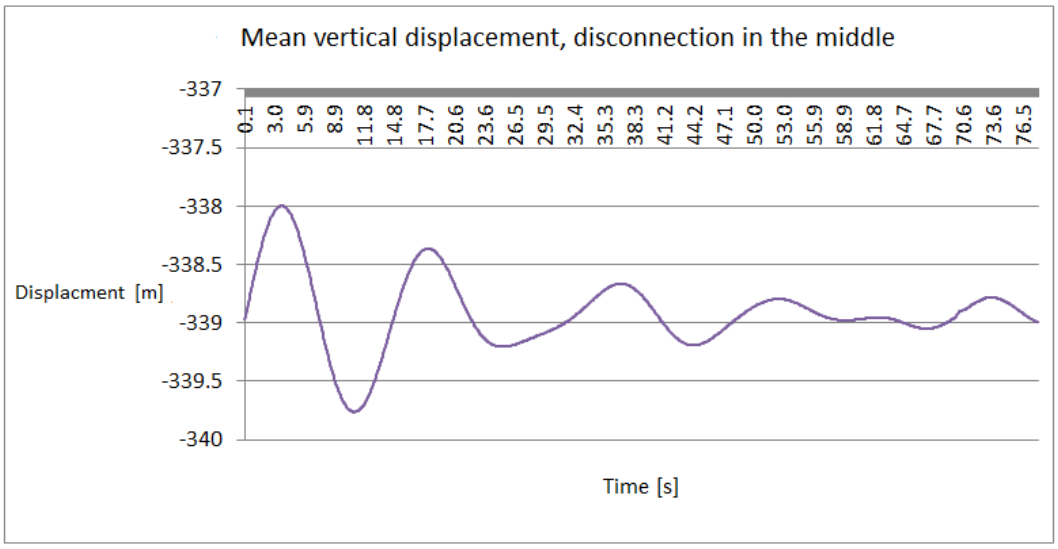

Figure 28: Mean vertical displacement for EDP, disconnect half way up the heave displacement

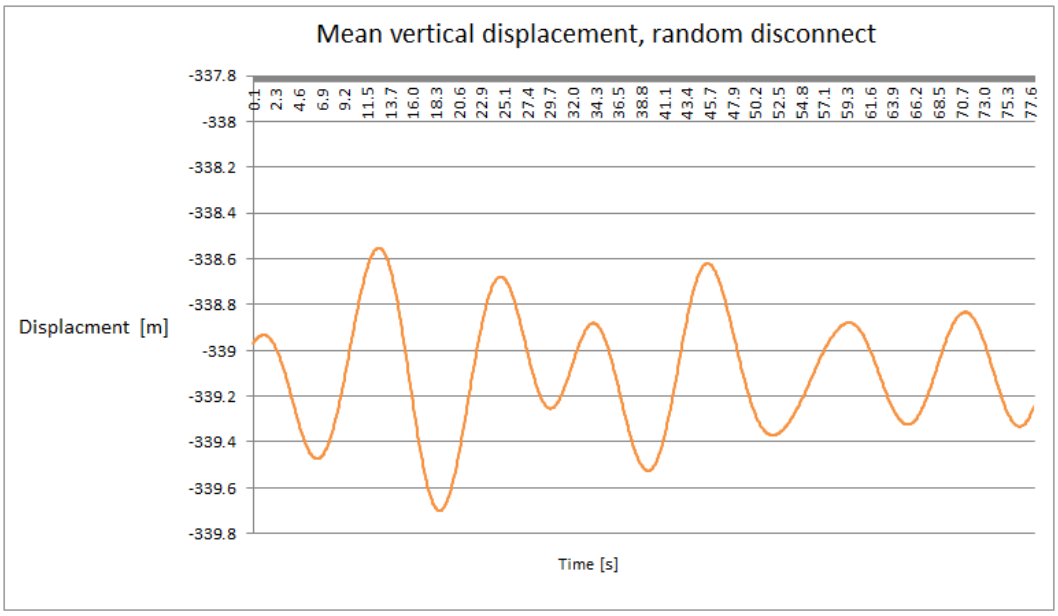

Figure 29: Mean vertical displacement for EDP, random disconnection

The first graph presented in **Figure 26** is the mean vertical displacement when disconnection is performed at the heave displacement top. As seen the trend is that the EDP immediately has a displacement in negative z-direction. It is also observed that the average value of the mean vertical displacement is approximately -340 meter and thus below its initial position.

In **Figure 27** the results from the mean vertical displacement for the EDP when disconnected at the bottom of the heave displacement are presented. Illustrated in the graph is the trend for the vertical displacement, which is that the EDP is displaced directly in positive z-direction. Compared to **Figure 26** average value of the mean vertical displacement is above its initial position at approximately -338m rather than -340m.

Figure 28 illustrates the mean vertical displacement when the disconnection is performed half way up the heave displacement, which is the time incident with highest velocity. As observed the EDP has a vertical displacement in positive z-direction after disconnection. Additionally the average value of the mean vertical displacement is approximately the same as the initial position.

Shown in **Figure 29** is the mean vertical displacement for the EDP after disconnection at a random time incident. As the graph indicates the average value of the mean vertical displacement is below is original position. The trend shows that the EDP first experience a small displacement in positive z-direction, it changes rapidly and then is displaced in negative z-direction.

12.4. PROBABILITY

To further study the difference between the disconnection events a MATLAB script has been developed. The MATLAB script checks for collision between the EDP and the LRP. This is done by reading in the results from the displacement of the EDP after disconnection. This is done for the 40 different analyses.

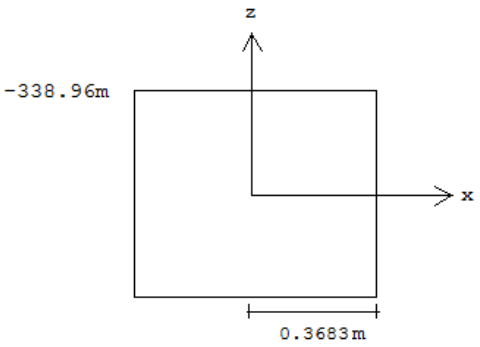

Figure 30: LRP dimensions

The LRP is located at -388.96 meters and has a width of 0.7366 meters. In RIFLEX the LRP is modelled as a circular cylinder. However, in real life the LRP has a shape similar to a square. Therefore the criteria for collision is set as shown in **Figure 30**. The MATLAB script runs through the results after disconnection and check if the displacement of the EDP is within the area of the LRP in z,- and x-direction. The results from disconnection at top of the heave displacement, bottom of the heave displacement, half way up the heave displacement and random time incident are presented in the following section.

Disconnect	Number of hits	Total nr. rows	Fraction of hits	Percent hits
Top1	70	1527	0.045841519	4.5841519
Top2	98	1851	0.052944354	5.2944354
Top3	70	2344	0.029863481	2.9863481
Top4	52	2328	0.02233677	2.233677
Top5	64	2901	0.022061358	2.2061358
Top6	71	2276	0.031195079	3.1195079
Top7	76	2321	0.032744507	3.2744507
Top8	45	2625	0.017142857	1.7142857
Top9	69	1778	0.038807649	3.8807649
Top10	70	2410	0.029045643	2.9045643

Table 8: Disconnection at heave top

In **Table 8** the results from the disconnections performed at heave displacement top are presented. Presented in column two are the number of times in the time series after disconnections the criterion shown in **Figure 30** is satisfied. Each time the criterion for collision is satisfied, the number of hits will be added by one. In column three are the total number of rows after disconnection. In column four is the fraction which is calculated by dividing number of hits by total number of rows. Finally, the percent is the

fraction multiplied by a hundred to get percent of time. Thus, the percent illustrates the percent of time the EDP is within the limits of the LRP after disconnection.

Disconnect	Number of hits	Total nr. rows	Fraction of hits	Percent hits
Bottom1	0	1396	0	0
Bottom2	0	1741	0	0
Bottom3	0	2200	0	0
Bottom4	0	2217	0	0
Bottom5	0	2769	0	0
Bottom6	0	2155	0	0
Bottom7	0	2206	0	0
Bottom8	0	2478	0	0
Bottom9	0	1655	0	0
Bottom10	0	2302	0	0

Table 9: Disconnection at heave bottom

In **Table 9** are the results from the disconnection events performed at the heave displacement bottom. As seen when the disconnection is performed at the bottom, the EDP is never within the limits of the LRP.

Disconnect	Number of hits	Total nr. rows	Fraction of hits	Percent hits
Middle1	0	1299	0	0
Middle2	0	1684	0	0
Middle3	1	2143	0.000466636	0.0466636
Middle4	20	2163	0.009246417	0.9246417
Middle5	0	2705	0	0
Middle6	0	2084	0	0
Middle7	0	2143	0	0
Middle8	0	2393	0	0
Middle9	27	1595	0.0169279	1.69279
Middle10	0	2244	0	0

Table 10: Disconnection in the middle of the heave displacement

Table 10 presents the results from the disconnection events performed half way up the heave displacement, thus at the time incident with highest vertical velocity. The criterion for collision between the EDP and the LRP is satisfied for some analyses.

Disconnect	Number of hits	Total nr. rows	Fraction of hits	Percent hits
Random1	44	1992	0.022088353	2.2088353
Random2	50	1992	0.025100402	2.5100402
Random3	0	1992	0	0
Random4	0	1992	0	0
Random5	36	1992	0.018072289	1.8072289
Random6	70	1992	0.035140562	3.5140562
Random7	62	1992	0.031124498	3.1124498
Random8	97	1992	0.048694779	4.8694779
Random9	50	1992	0.025100402	2.5100402
Random10	0	1992	0	0

Table 11: Random disconnection

Finally **Table 11** presents the results when the disconnection is performed at a random time incident in the heave displacement. As seen from the table, number of hits varies for this scenario. Furthermore, total numbers of rows are constant since all the disconnections are conducted at the same time incident in the simulations.

Disconnection	Mean percent
Top	3.2198
Bottom	0
Middle	0.2664
Random	2.0532

Table 12: Mean percentage of the time the EDP is within the limits of the LRP

The mean percent presented in **Table 12** is the mean of the percent calculated for each disconnection event. The values are calculated by summing up the percent and dividing them by the total number of analyses, ten for these cases. As shown, the disconnection at the heave displacement top has the highest mean percent of hits. Moreover the random disconnection has the second highest mean percent of hits, followed by disconnection half way up the heave displacement. Finally, the mean percent for the bottom has the value zero, there are no values within the LRP limits for this case.

12.5. CORRELATION STUDY

The disconnection analysis has been run for 75 different seeds, meaning that 75 different sea states have been generated. To perform the random disconnect, the disconnection timing has been constant for all the different sea states. The disconnection has been performed at 258.48 seconds as seen in **Figure 31**. The time interval illustrated in the graph is chosen to highlight the relevant time interval. The seeds for these analyses are shown in appendix A.8 .

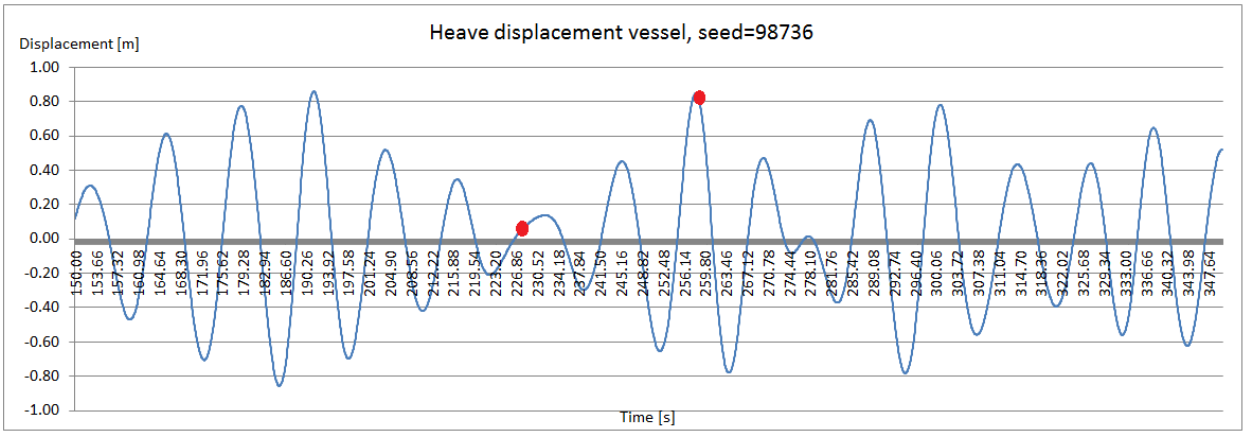

Figure 31: Heave displacement vessel for Tp=8sec and seed=98763

Shown in **Figure 31** is the heave displacement for the vessel for one of the analyses. The two red dots illustrate the disconnection timing at the right (258.48s) and 30 seconds in advance (228.48) at the left. Based on the results from the vertical displacement from the different sea states a correlation study has been performed, described in section 10. The results from the correlation study are presented in this section. As mentioned been performed 75 times altogether, 25 times for each following peak periods T_p.

- T_p=8 seconds
- T_p=10 seconds
- T_p=15 seconds

All analyses are conducted with the same significant wave height H_s=5.5m.

The MATLAB script described in section 11 is applied to calculate the vertical velocities. In the correlation study the vertical velocity at the moment of disconnection and 30 seconds in advance are studied. **Figure 31** shows the heave displacement from one of the studied sea states.

The velocity results have been exported from MATLAB to Excel where they have been plotted. The results from the velocities are found in appendix A.3 . In Excel the correlation coefficients were calculated, these are found in **Table 13**.

H1 Vertical velocity at 30 seconds in advance of disconnection

H2 Vertical velocity Disconnection

Presented in the graphs are the vertical velocities H1 at the horizontal axis and H2 at the vertical axis for T_p=8s, T_p=10s and T_p=15s. If correlation exists between the two velocities a linear pattern should be formed.

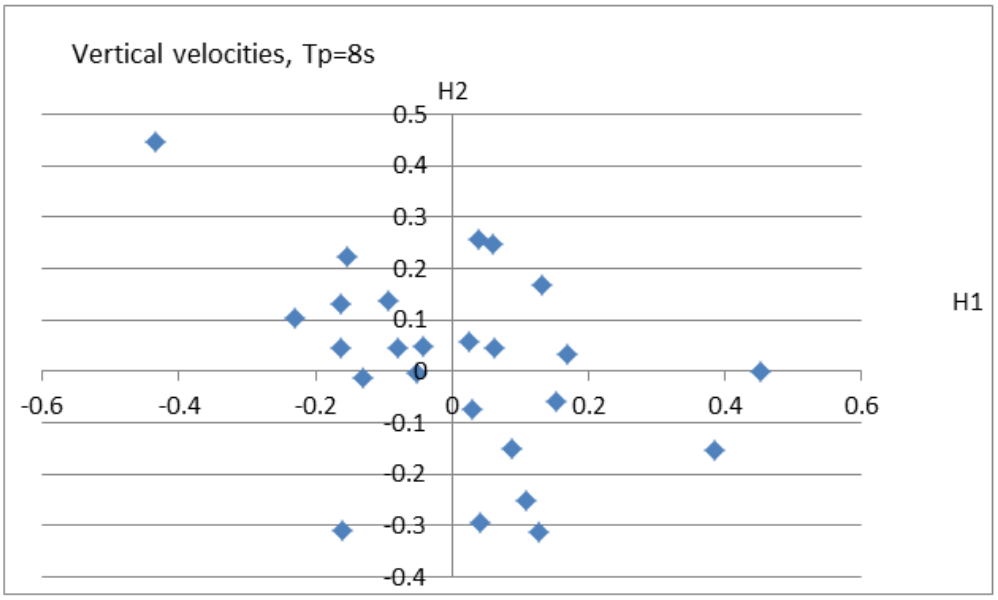

Figure 32: Vertical velocity H1 and H2 plot Tp=8sec

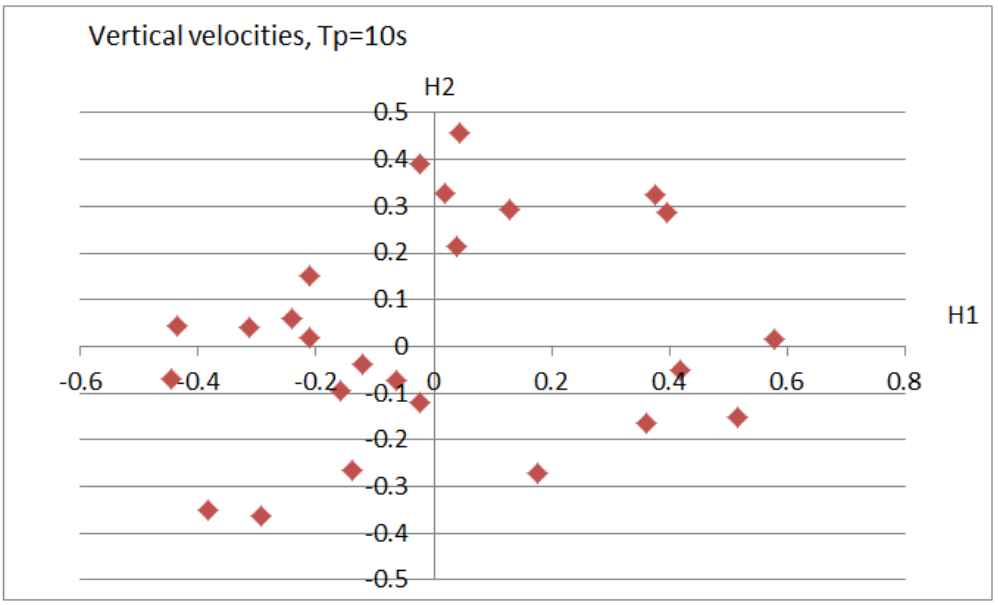

Figure 33: Vertical velocity H1 and H2 plot Tp=10sec

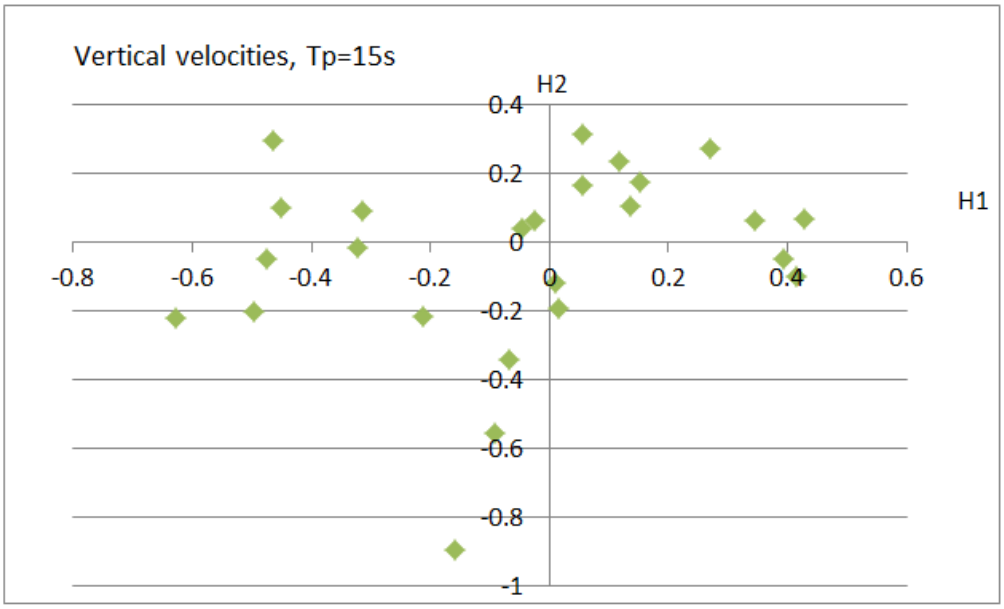

Figure 34: Vertical velocity H1 and H2 plot Tp=15sec

The graph presented in **Figure 32** shows the two vertical velocities H1 and H2 for T_p=8s plotted versus each other. As seen in the graph the velocities do not form a pattern, but seem to be spread randomly around the origin.

The graph in **Figure 33** shows the vertical velocities from the analyses conducted with T_p=10 seconds. The graph does not show a linear pattern for this case either. However, the dots seem to shape a more linear pattern than in **Figure 32**.

Figure 34 presents the results from the correlation study for T_p=10s. Comparing the graph to the other cases, neither in this case does it exist a clear pattern for the vertical velocities.

Tp [s]	Correlation coeff.
8	-0.4184827
10	0.2124362
15	0.2045246

Table 13: Correlation coefficients

Table 13 presents the result from the correlation coefficient for the three different periods. The correlation coefficient in excel is calculated according to (Eq. 10.2). For peak period T_p=8s the correlation is negative. For T_p=10s and T_p=15s the correlation coefficient shows small improvements. However the correlation is low for all periods.

12.6. DISCONNECTION ANALYSIS WITH RISER LIFT-UP

In section 4.3 a description of the disconnection sequence is found. Simultaneously as the disconnection is performed the riser is raised (lift-up) at the top to prevent collision between the EDP and LRP. In this section the results from analyses performed with riser retraction are presented.

All the analyses are performed with H_s=5.5m and T_p=10s. In addition, the analyses have been run for both the shallow water and the deep water model. Random disconnection has been performed. Hence, the disconnection timing is the same for all the sea states, seen in **Table 14** and **Table 15**. The graphs from the analyses performed with zero retraction are foun in appendix A.2 . As mentioned in section 8.4 the lift-up is done over a time interval of one second. The lift-up velocities are therefor, -1[m/s],-2[m/s] and -4[m/s].

First in this section there is a presentation of disconnections with the shallow water model for subsequently disconnection with 1,2 and 4 meter lift-up. Following is a presentation of the mean displacement for the shallow water model and the deep water model. Finally is a presentation of the mean percent of time the EDP is within the limits of the LRP for both water depths.

Shallow				
Seed	No retraction	1 [m] retraction	2 [m] retraction	4 [m] retraction
48160	380.48 s	380.48 s	380.48 s	380.48 s
48161	380.48 s	380.48 s	380.48 s	380.48 s
48162	380.48 s	380.48 s	380.48 s	380.48 s
48163	380.48 s	380.48 s	380.48 s	380.48 s
48164	380.48 s	380.48 s	380.48 s	380.48 s

Table 14: Seed numbers and disconnection timings shallow water model

Deep				
Seed	No retraction	1 [m] retraction	2 [m] retraction	4 [m] retraction
48160	380.48 s	380.48 s	380.48 s	380.48 s
48161	380.48 s	380.48 s	380.48 s	380.48 s
48162	380.48 s	380.48 s	380.48 s	380.48 s
48163	380.48 s	380.48 s	380.48 s	380.48 s
48164	380.48 s	380.48 s	380.48 s	380.48 s

Table 15: Seed numbers and disconnection timings shallow water model

Presented in **Table 14** and **Table 15** are the different seed numbers and disconnection timings for each completed retraction scenario. For the shallow water model and the deep water model four different scenarios have been run for five different sea states. The different scenarios are zero retraction, 1 meter retraction, 2 meters retraction and 4 meters retraction. When the EDP disconnects, it will be lifted up minimum two or four meter. The zero and one meter retraction cases are only presented to study the effect of less retraction and be a base of comparison.

12.6.1. SHALLOW WATER DISCONNECTION SEED=48161

Presented in this section are the results from the analyses conducted with different retractions of the riser for the shallow water case. The graphs presented in the following section show the vertical displacement for the EDP at a relevant time interval after disconnection. The displacements presented in the following graphs show the displacement for the bottom part of the EDP. The initial position for this is -338.96 meters for the shallow water model. Furthermore the location at the bottom of the EDP is also the top of the LRP. The graph showing the case with zero retraction is not presented in this section. However it is found in appendix A.2 .

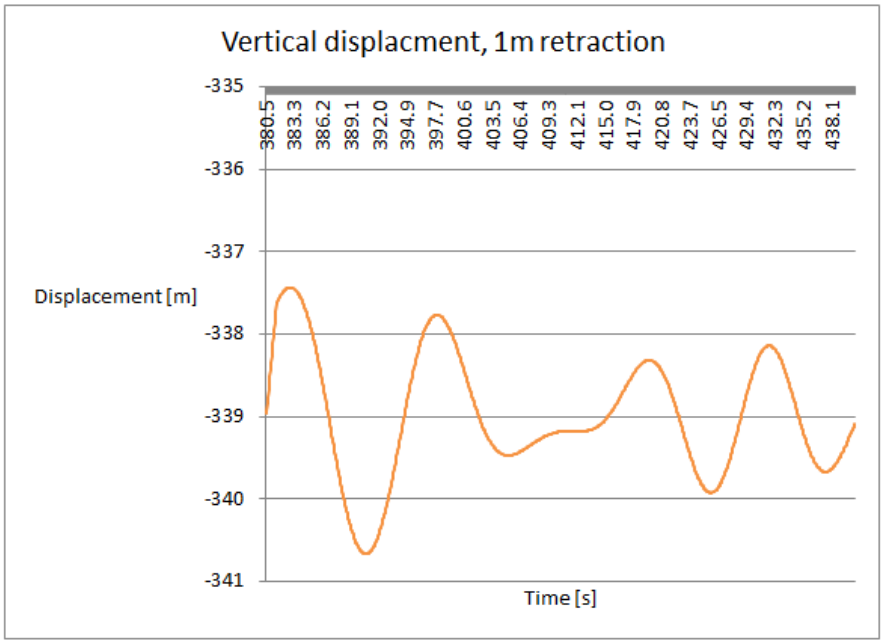

Figure 35: Vertical displacement 1m retraction, shallow water model seed=48161

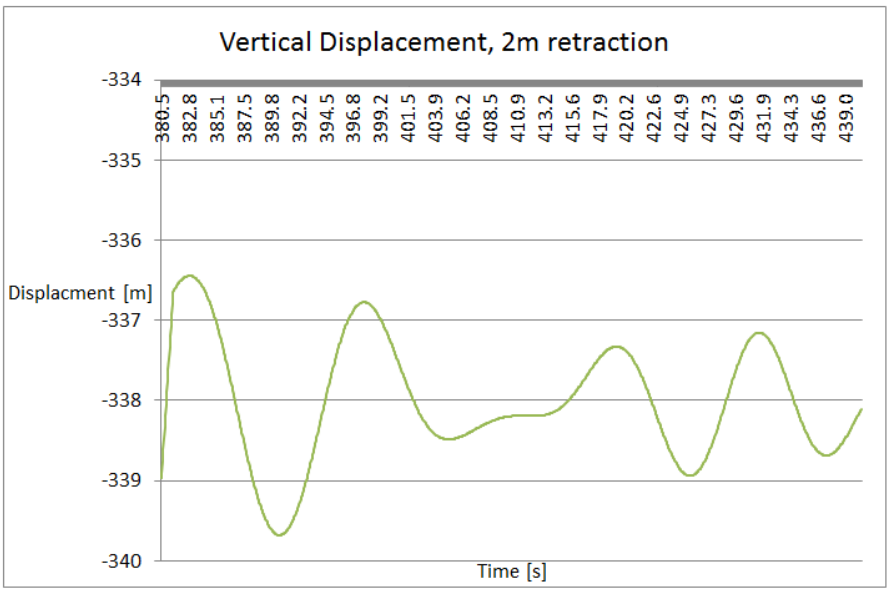

Figure 36: Vertical displacement 2m retraction, shallow water seed=48161

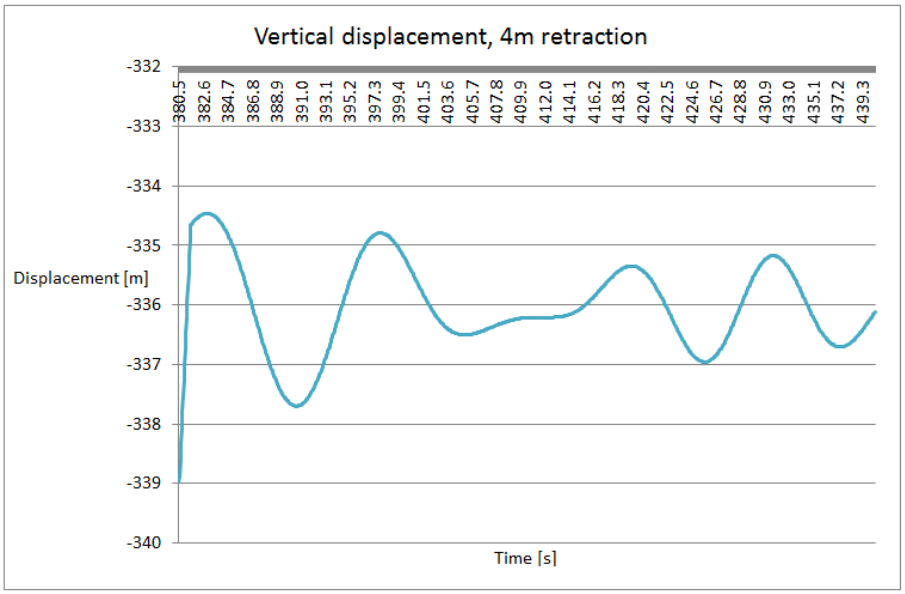

Figure 37: Vertical displacement 4m retraction, shallow water seed=48161

The first graph presented in **Figure 35** illustrates the vertical displacement after disconnection is performed with one meter lift up. As the graph indicate the EDP is first lifted up one meter.

The graph in **Figure 36** shows the vertical displacement of the EDP after a random disconnect with a retraction of 2 meter. By comparing it to **Figure 35** it is seen that the riser has a larger lift-up. After the EDP has been retracted it stabilizes.

Presented in the graph in **Figure 37** is the vertical displacement of the EDP after disconnection done with 4 meter retraction. Compared to the two other events it is seen that the retraction is significantly higher.

12.6.2. SHALLOW WATER MODEL MEAN DISPLACEMENT

Based on the results for each event a mean vertical displacement is calculated. This has been done for both the shallow water model and the deep water model. Presented in this section are the results from the retraction analyses conducted with the shallow water model. As already mentioned the location of the LRP is at -338.96m. The graphs presented show the displacement of the bottom part of the EDP, with initial position at -338.96m.

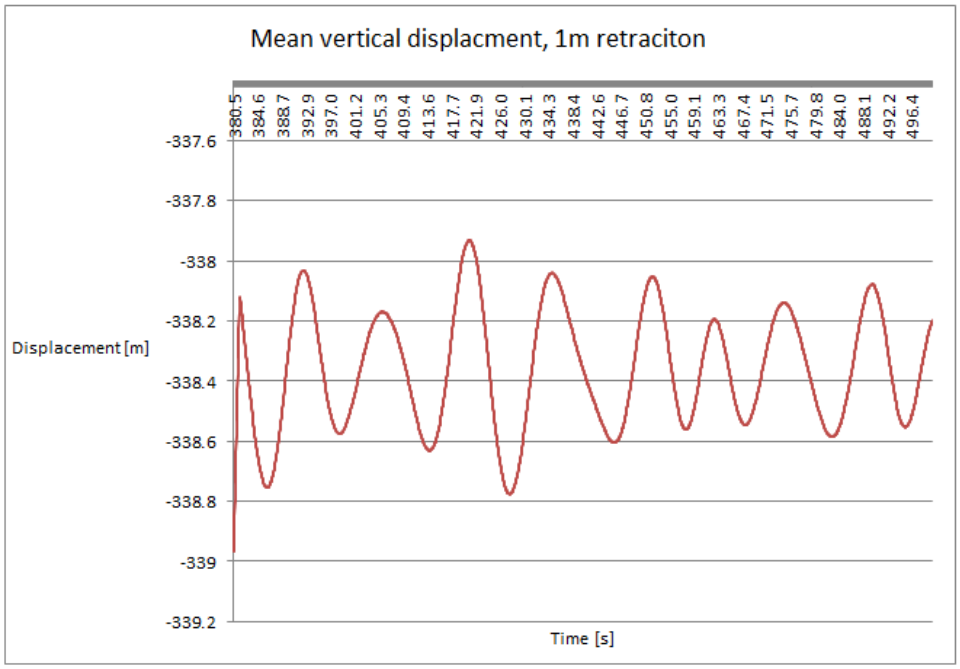

Figure 38: Mean vertical displacement, 1 meter retraction

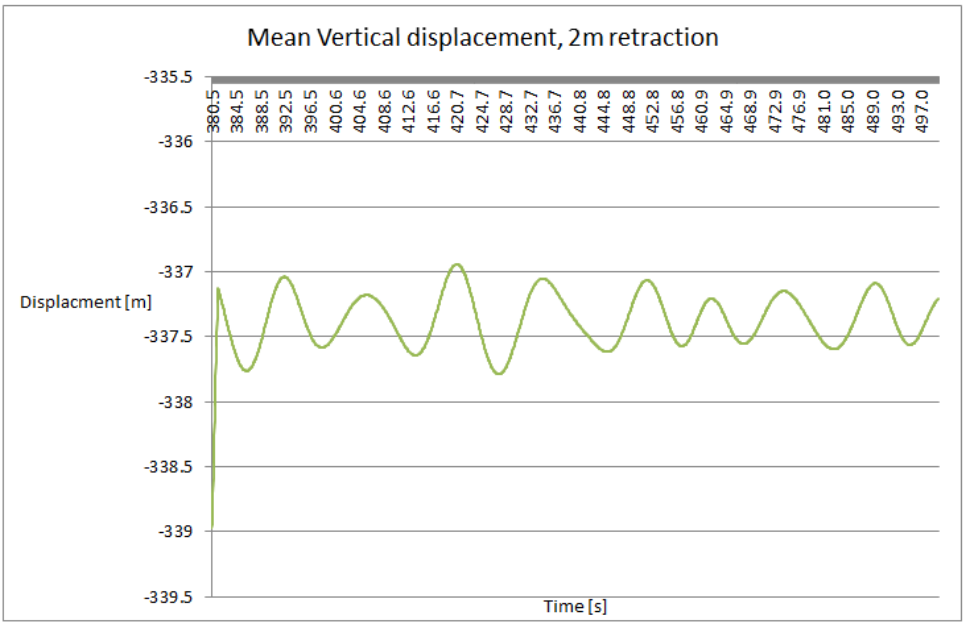

Figure 39: Mean vertical displacement, 2 meter retraction

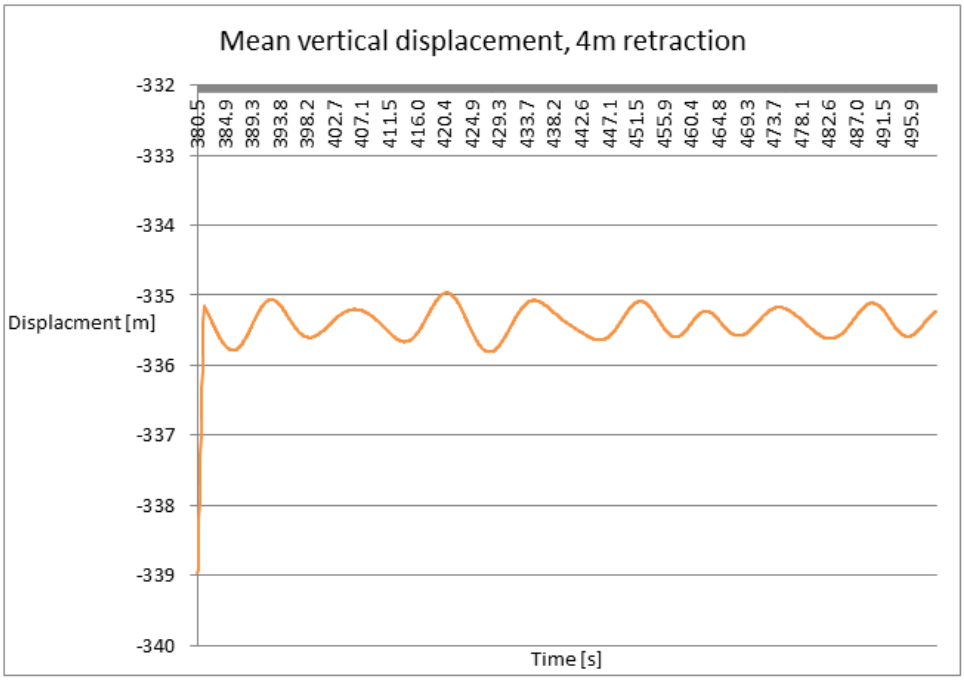

Figure 40: Mean vertical displacement, 4 meter retraction

The graphs presented in **Figure 38**, **Figure 39** and **Figure 40** are the vertical displacement for the EDP after disconnect with one, two, and four meters retraction respectively. As can be seen, the trend for all of them is that the EDP has a positive vertical displacement. Moreover, they all have an average value of the mean vertical displacement above the initial position of the EDP which is at -339.96m. Additionally it is observed that the retraction event with four meter lift-up, **Figure 40**, has a higher average displacement than the others. The two meter retraction also has a higher mean displacement than the one meter retraction event.

12.6.3. DEEP WATER MODEL

Presented in this section are the results from for the mean vertical displacement for the deep water model when the analyses are performed with retraction. The mean is based on the five analyses presented in **Table 15**. The disconnections are random disconnect, thus the disconnection is performed at 380.48 seconds. The time interval presented in these graphs is the time after disconnection. The position of the LRP for the deep water model is -987.56m. Furthermore the graphs presents the vertical displacement of the bottom part of the EDP, with an initial position of -987.56m.

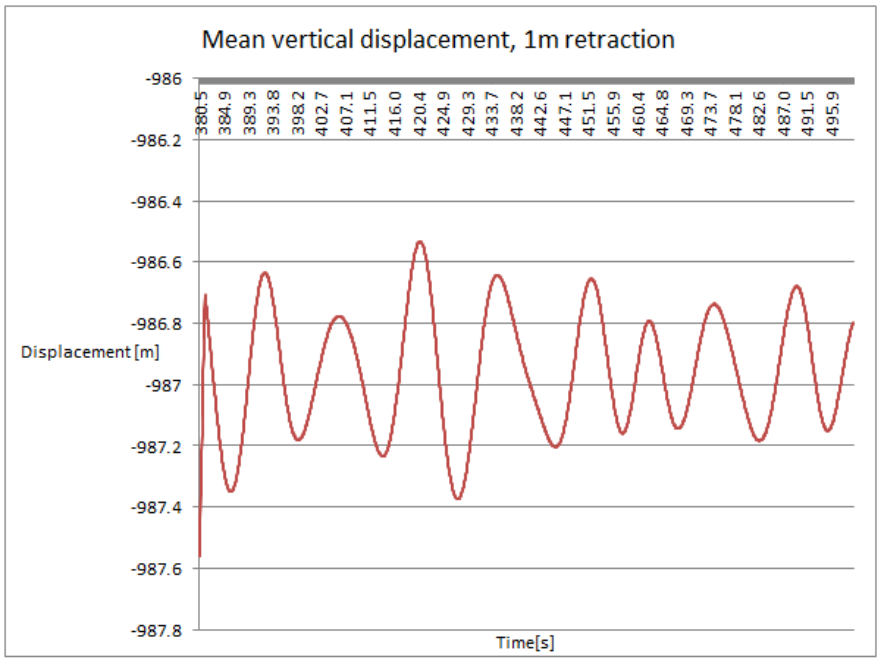

Figure 41: Mean vertical displacement, with 1 meter retraction

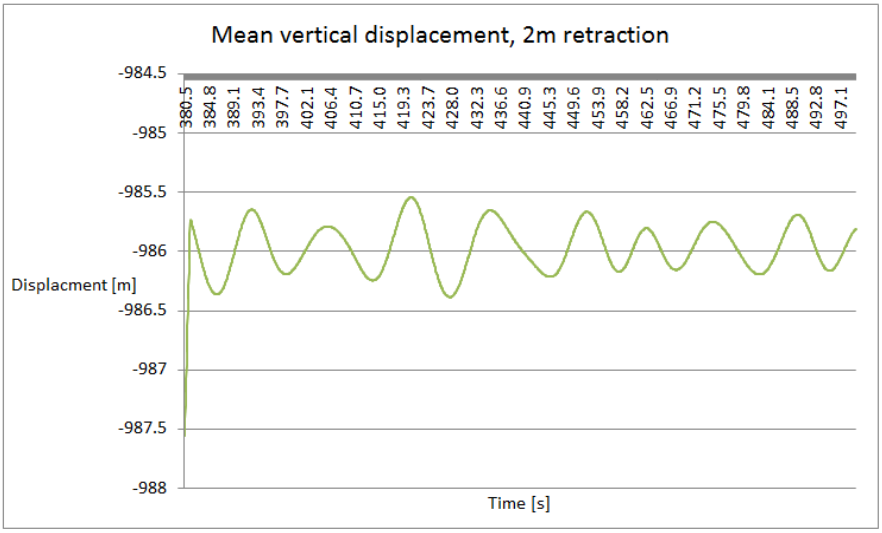

Figure 42: Mean vertical displacement, 2 meter retraction

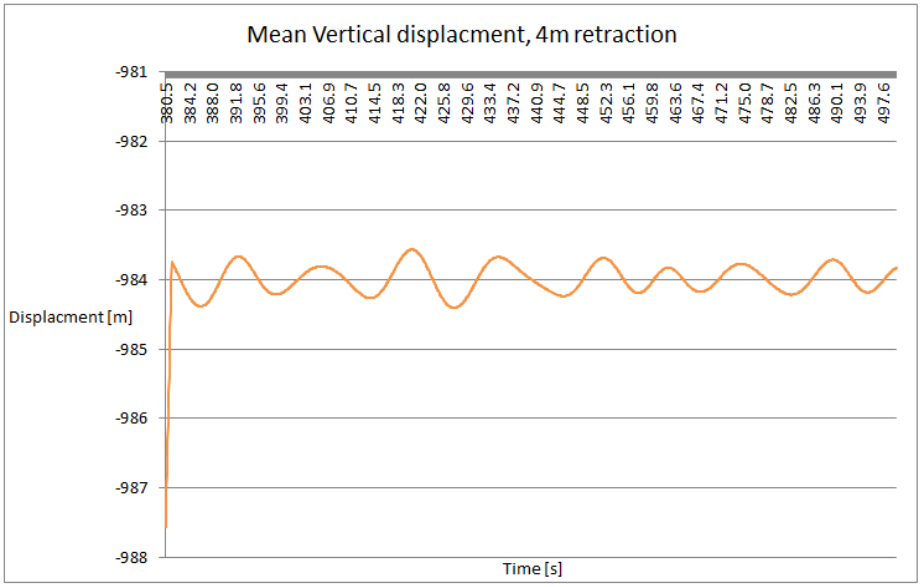

Figure 43: Mean vertical displacement, 4 meter retraction

The graphs presented in this section, seen in **Figure 41**, **Figure 42** and **Figure 43** shows the results from the disconnection analyses performed with one, two and four meters retraction respectively for the deep water model. As seen the trend for all the events is that the EDP is first lifted up immediately after disconnection. How big the displacement is, will vary depending on the retraction. Additionally they have average value of the mean vertical displacement higher than the initial position of the EDP. By comparing the mean for the one meter retraction to the two other events, it is seen that the EDP is closer to the LRP than for the two others. After the retraction is performed, vertical displacement stabilizes for all the events.

12.6.4. PROBABILITY

Presented in the following section is a collision study for shallow water model and the deep water model conducted with retraction.

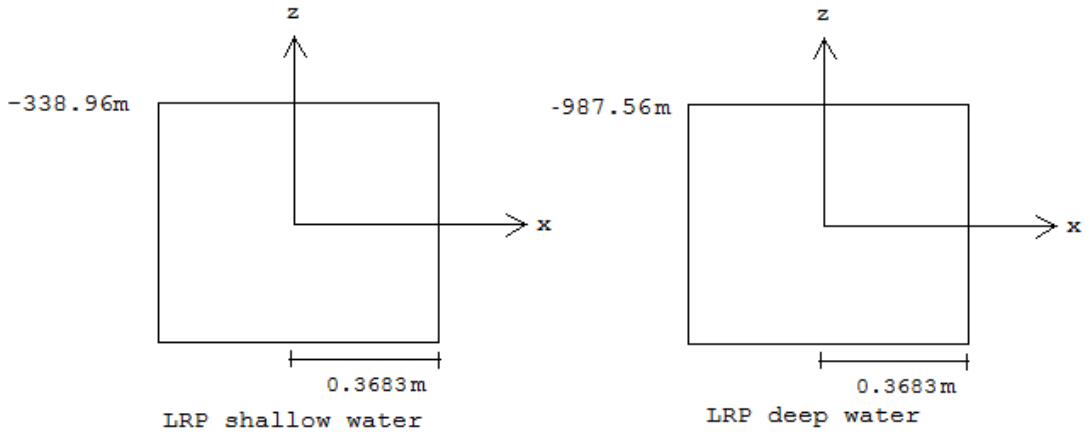

Figure 44: Dimensions LRP shallow and deep water

Figure 44 presents the limits for the LRP for both cases. The criterion for collision is that the EDP is within the limits of the LRP. The same MATLAB script as described in section 11 is applied to calculate the collision events in this case as well.

Shallow	0 [m] retraction			
Seed	No.hits	Total no. rows	Fraction hits	Percent hits
48160	97	1992	0.0486948	4.8694779
48161	1	1992	0.000502	0.0502008
48162	81	1992	0.0406627	4.0662651
48163	46	1992	0.0230924	2.3092369
48164	47	1992	0.0235944	2.3594378

Deep	0 [m] retraction			
Seed	No.hits	Total no. rows	Fraction hits	Percent hits
48160	50	1992	0.0251004	2.5100402
48161	0	1992	0	0
48162	54	1992	0.0271084	2.7108434
48163	62	1992	0.0311245	3.1124498
48164	49	1992	0.0245984	2.4598394

Table 16: Percent hits for shallow and deep water model, 0 m retraction

Table 16 contains information regarding number of times the EDP will collide with the LRP for the shallow and deep water simulations performed with no retraction. These results are calculated in the same way as in section 12.4. By comparing the two tables it is observed that number of hits is higher for the shallow water model than in the deep water model.

Shallow	1 [m] retraction			
Seed	No.hits	Total no. rows	Fraction hits	Percent hits
48160	39	1992	0.0195783	1.9578313
48161	22	1992	0.0110442	1.1044177
48162	19	1992	0.0095382	0.9538153
48163	0	1992	0	0
48164	0	1992	0	0

Deep	1 [m] retraction			
Seed	No.hits	Total no. rows	Fraction hits	Percent hits
48160	0	1992	0	0
48161	0	1992	0	0
48162	0	1992	0	0
48163	0	1992	0	0
48164	1	1992	0.000502	0.0502008

Table 17: Percent hits for shallow and deep water model, 0 m retraction

As for the zero retraction the results from the analyses conducted with 1 meter **Table 17**, show that the EDP collide with the LRP more frequent for the shallow water model. However it is observed that for this case the number of hits is significantly lower than for the case with zero retraction.

Shallow	2 [m] retraction			
Seed	No.hits	Total no. rows	Fraction hits	Percent hits
48160	0	1992	0	0
48161	0	1992	0	0
48162	0	1992	0	0
48163	0	1992	0	0
48164	0	1992	0	0

Deep	2 [m] retraction			
Seed	No.hits	Total no. rows	Fraction hits	Percent hits
48160	0	1992	0	0
48161	0	1992	0	0
48162	0	1992	0	0
48163	0	1992	0	0
48164	0	1992	0	0

Table 18: Percent hits for shallow and deep water model, 2 m retraction

Shallow	4 [m] retraction			
Seed	No.hits	Total no. rows	Fraction hits	Percent hits
48160	0	1992	0	0
48161	0	1992	0	0
48162	0	1992	0	0
48163	0	1992	0	0
48164	0	1992	0	0

Deep	4 [m] retraction			
Seed	No.hits	Total no. rows	Fraction hits	Percent hits
48160	0	1992	0	0
48161	0	1992	0	0
48162	0	1992	0	0
48163	0	1992	0	0
48164	0	1992	0	0

Table 19: Percent hits for shallow and deep water model, 4 m retraction

In **Table 18** and **Table 19** the results from the analyses performed with two and four meter retraction are presented. As seen in the tables when the EDP is lifted up two or four meters, the EDP is never within the limits of the LRP.

	Shallow	Deep
0[m] retraciton	2.730923695	2.1586345
1 [m] retraction	0.803212851	0.0100402
2 [m] retraction	0	0
4 [m] retraction	0	0

Table 20: Mean percent of time the EDP is within the limit of the LRP

Table 20 presents the mean percent of time the EDP is within the limits of the LRP for the different retraction events. It is observed that the deep water model has a lower mean percent of hits than the shallow water model. Furthermore, both the two and four meter retraction events have a mean percent of zero.

13. DISCUSSION

Several analyses have been completed to study the event of collision between the EDP and LRP. These analyses have been performed to gain a broad overview of the event. The results from these analyses are discussed in this section.

All the graphs presented show the vertical displacement at the bottom of the EDP. This is also the location of the top part of the LRP. If only considering the vertical displacement, the EDP will collide with the LRP if the displacement is below the initial position of the EDP. However the EDP will also have a horizontal displacement due to current. Moreover, the model applied in this Thesis is modelled without a heave compensation system. However, in the actual Workover System a heave compensation system is included. The reason for not introducing heave compensation system is due to the complexity of the system and thus uncertainties to how it should be modelled. Nevertheless, in the disconnection event the riser will lock-up to the platform simultaneously as disconnection is performed. Hence, the heave compensation system will not influence the vertical displacement after lock-up. It is therefore expected that this assumption is a suitable way of modelling the disconnection scenario.

In the first set of analyses the different disconnection events are studied, such as disconnection at heave displacement top, heave displacement bottom, random time incident and half way up the heave displacement. This is performed to study the displacement of the EDP after disconnection. It is expected that a displacement in negative z-direction immediately after disconnection will increase the probability for collision between the EDP and LRP. Further, the time length after disconnection will influence the probability for collision. The current may displace the EDP in positive x-direction when it is released, which will move the EDP away from the LRP. Thus if the time interval of the positive vertical displacement is long, this will provide more horizontal displacement before the EDP has a negative displacement.

By comparing the different scenarios it is seen that for the disconnection events at the heave displacement top, **Figure 23**, the EDP will have a displacement in negative z-direction immediately after disconnection. However, the disconnection at the heave displacement bottom shows the opposite, seen in **Figure 24**. Moreover, the disconnection at half way up the heave displacement, **Figure 25**, has a displacement in positive z-direction. After a certain time interval it has a displacement in negative direction. In terms of collision, these results show that the most critical event is disconnection at heave displacement top, and that the most optimal is disconnection at heave displacement bottom.

To avoid collision between the EDP and LRP, the best case scenario is if the trajectory of the EDP is above the LRP. Each time the vertical displacement of the EDP goes below its original position there is a risk of collision. Simultaneously as the EDP is disconnected,

the riser will be locked to the vessel at top. Where in the heave displacement this lock-up occur, will influence the mean vertical displacement. This is seen in the results for the different disconnection events in **Figure 23**, **Figure 24** and **Figure 25**. For the disconnection at the heave displacement top the riser lock-up will lead to longer effective riser length underneath the platform. The opposite is the case for the disconnection at the heave displacement bottom. Furthermore, disconnection half way up heave displacement will lead to no change in the length underneath the vessel. The consequence of riser lock-up, is a higher probability for collision when the EDP is disconnected at the heave displacement top and a lower probability when disconnected at the bottom.

A mean vertical displacement has been calculated from the results for the displacements, seen in **Figure 26**, **Figure 27**, **Figure 28** and **Figure 29**. Based on these results, the trends for the vertical displacement after disconnection are shown. The disconnection events done at the heave displacement top shows an immediate vertical displacement in negative z-direction after disconnection. In terms of collision this is an unfortunate scenario. However, the disconnections at the heave displacement bottom show the opposite trends. The vertical displacement after disconnection shows a direct displacement in positive z-direction. This is a good scenario in terms of collision. Furthermore, the random disconnection events show a small mean vertical displacement in positive z-direction followed by a vertical displacement in negative z-direction.

In RIFLEX, all components are modelled as circular cylinders. The criteria for collision between the EDP and LRP is set as a square in the probability study, shown in **Figure 30**. Due to the fact that the actual shape of the LRP is more like a square, it is expected to be an appropriate assumption. However this may lead to more conservative results. When the disconnection is done at the heave displacement top, the mean percent of time the EDP is within the LRP's limit is equal to 3.219, presented in **Table 12**. The random disconnect has the second highest mean percent, 2.053. When disconnected half way up the heave displacement, the mean percent is lower, 0.2664. Disconnection at heave displacement bottom has a mean percent of zero. Based on the results it is seen that the number of times the EDP is within the limits for the LRP is quite different for the different events. It is seen that the most critical scenario is disconnection at the top. Further, it is interesting that the second most critical scenario is the random disconnection event. The most optimal event is disconnection at the heave displacement bottom. These results illustrate that the disconnection timing leads to big differences in terms of probability for collision.

In the correlation study the vertical velocity 30 seconds in advance of disconnection and at the actual disconnection timing are calculated and plotted. The 30 seconds time interval was studied since this is the time it takes from the disconnection is initiated until it is performed. The purpose of the study was to try to find a relation between the two velocities. This was done for three different periods; T_p=8s, T_p=10 and T_p=15s. If a

relation exists, a linear pattern in the graphs is expected. Furthermore, it is expected a better correlation for higher periods. The results from the analyses showed that it does not exist a correlation for the velocities. In all three events the plot seems random and there is no clear pattern. Moreover, the correlation does not improve much for higher T_p as expected. This may be caused by the length of the time interval. If it was shorter, the correlation might be improved.

The last study performed, is the disconnection analyses done with riser lift-up. Simultaneously as the riser disconnects it is also lifted up at the top. It is raised minimum 2-4 meter at the top to prevent collision between the EDP and LRP. In order to study this event, four different random disconnection events have been completed and compared for both the shallow water and the deep water model. Even though the riser is lifted more than one meter in the actual disconnection, the analysis is included to be a base of comparison. The results from the example case show that when the riser is lifted either one or two meter, the vertical displacement of the EDP still has values below the location of the LRP. For the four meter lift-up, it is seen that the vertical displacement is significantly higher.

Based on the mean vertical displacement results, it is seen that the average value of the mean vertical displacement for all lift-up cases is above the location of the LRP. This is the case for both the shallow and deep water model. For the two and four meter lift-up there is a significant clearance between the EDP displacement and the initial positon of the EDP (LRP position). Based on the results from the displacement the percent of time the EDP is within the limits for the LRP is calculated. The mean percent of hits is lower for the deep water model than the shallow water model. The reason for this may be current. Both models are exposed to the same current. The current will act on the entire riser length in both cases. However the length is longer for the deep water model. Hence, the EDP will experience a higher horizontal displacement for the deep water model than the shallow water model. Finally, the results also show that the EDP will never collide with the LRP when the riser is lifted up either two or four meters. Thus, a riser lift-up of 2 meter should be sufficient.

14. CONCLUSION

The purpose of this Master Thesis is to study the critical event of collision between the EDP and LRP, and to propose a strategy to reduce this risk. The aspects which influence the risk of collision are as follows;

- The orientation of the vertical displacement of the EDP immediately after disconnection.
- The length of time after disconnect, in terms of how big horizontal displacement the EDP has.
- Where in the riser the lock-up occur, and riser lift-up.

From the different disconnection analyses it is seen that vertical displacement of the EDP after disconnection vary. The most critical scenario is disconnection at the heave displacement top. The EDP will have a vertical displacement in negative z-direction immediately after disconnect. Since this displacement occurs directly, the horizontal displacement will be small. Additionally, the riser is locked at a high point in the riser, which leads to a longer length underneath the vessel. The best disconnection scenario is disconnection at heave displacement bottom. Then, the EDP has a vertical displacement in positive z-direction. Additionally, the time before the orientation of the EDP changes is the longest out of the cases, which leads to a bigger horizontal displacement. Not to mention the lock-up occurs lower in the riser, leading to a shorter effective length of the riser underneath the vessel.

The results from the mean study also show that the disconnection at the heave displacement top is the most critical event , and that the disconnection at the heave displacement bottom is the most optimal event. The trend for the vertical displacement of the EDP after disconnect at heave top is that it moves directly in negative z-direction and the opposite for the disconnection at the bottom. The results from the disconnection half way up the heave displacement show that the trend is positive vertical displacement for a certain time interval, followed by a negative. The results from the probability are consistent and show that the disconnection event with the lowest mean percent of time the EDP is within the limit of the LRP is disconnection at the heave displacement bottom. The second lowest mean percent is disconnection performed half way up the heave displacement, followed by the random disconnection. The disconnection event at heave displacement top has the highest mean percent. Therefore it can be concluded that the optimal disconnection event is disconnection at the heave displacement bottom. The most critical is disconnection at the heave displacement top, and disconnection at a random time incident is the second worst.

The correlation study has been performed to check if it exists a relation between the vertical velocity at the disconnection timing and 30 seconds in advance. The results from

the analyses show that it does not exist a relation between the two velocities for the events studied for this time interval. Not even for the higher peak periods.

Furthermore, based on the results from the simulations conducted with riser lift-up, it can be concluded that the EDP will never hit the LRP if the retraction is two meters or above. The risk of the collision scenario is smaller in deep water than in shallow water due to current. For the retraction events, it is seen that there is a significant clearance between the EDP and LRP. It can therefore be concluded that critical event of collision will not happen if the riser is retracted a minimum of two meters.

15. FURTHER WORK

When working with this Thesis it has become apparent that the topic can be studied further. It has been challenging to determine a relation between the vertical velocity at the moment of disconnection and 30 seconds in advance. As presented in the results the correlation for the vertical velocity is poor. A set of suggestions for further work is therefore presented in this section.

In order to study this topic further different scenarios can be analyzed. One suggestion is to generate a long time series for a particular sea state. A constant time interval of 30 seconds can be studied through the entire sea state. Based on this the vertical velocity can be calculated for H1 and H2 in the same way as done in section 10. These results can then be further plotted in a scatter diagram to check for correlation.

It takes approximately 30 seconds for the signal to be sent from the vessel to the EDP. It is not possible to make this time interval shorter. However, a correlation study can be performed where the time interval is increased to 35, 40 and 45 seconds to check if this will improve the results. These results are plotted in the same way for H1 and H2 as described in section 10.

A third study could be to study the heave motion and find the moment with highest velocity in a wave. When this is determined the vertical velocity 30 seconds later where the actual disconnect will happen, can be calculated. By plotting these results in a scatter diagram it can be determined if it exists a relation between the two velocities.

Today the limitations lies with the system, the system is not capable of performing a disconnection in less than 30 seconds. However, this may change. If the time interval is reduced, will this improve the correlation for the vertical velocity? This is a scenario which can be further analyzed and of relevance if considering shortening the time interval.

The influence of the peak period is something that should be further studied. In the correlation study it was expected that when the peak period was higher, the correlation would improve. However, this was not the case. Therefore, a study where both the disconnection interval and the peak period are varied would be of interest.

REFERENCES

Aker Soltuions. (2013, August). Introduction Manual to the C/WO group, In-house document by Helene Kinge. Fornebu, Oslo, Norway: Aker Solutions.

Aker Solutions . (2008, 02 29). Workover for Dummies. Fornebu, Oslo, Norway: Aker Solutions.

Aker Solutions. (2014, October 17). Information received on email from Geir Magnus Knardahl. *Information WOS*.

Aker Solutions. (2014). Input provided by Kim Wold Christensen. *Personal comunicartion on email*.

Aker Solutions. (2014). Personal Communication with Geir Magnus Knardahl.

American Petroleum Institute. (1998). *Desing of Risers for Floating Production Systems and Tension-Leg Platforms.* Washington D.C.: American Petroluem Institute.

Bai, Y., & Bai, Q. (2012). *Subsea Engineering Handbook.* Amsterdam: Elsevier.

Den Norske Veritas. (2010). *DNV-RP-C203 Fatigue Design of Offshore Steel Structures.* Det Norske Veritas.

Det Norske Veritas. (2007). *DNV-RP-C205 Environmental Conditions and Environmental Loads.* Det Norske Veritas.

Det Norske Veritas. (2010). *DNV-OS-F201 Dynamic Risers.* Det Norske Veritas.

Det Norske Veritas. (2010). *DNV-RP-C203 Fatigue Design of Offshore Steel Structures.* Det Norske Veritas.

Faltinsen, O. (1990). *Sea Loads on Ships and offshore structures .* Cambrigde : The press syndicate of the university of Cambridge.

Grønevik, A. (2013, June). Simulations of drilling riser disconnection - Recoil Analysis. Trondheim: NTNU.

Hermanrud, L. (2014, june). Dynamic analysis of Workover Riser under unexpected conditions. Trondheim: NTNU-Norwegian University of Science and Technology.

ISO Technical commtee. (2009). *ISO/TR 13624-2 Petroleum and natural gas industries Drilling and production equipment, Part 2: Deep water drilling riser methologies operations and integrity technical report.* Geneva: ISO, International organization for standardization.

Kinge, H. (2014). *Global Analysis and Operation of Workover Risers.* Trondheim .

Kirkvik, R., & Berge, T. (2011). Integrity Management System for Work-Over Risers (WORs). *In The Twenty-first International Offshore and Polar Engineering Conference.* Maui, Hawaii: International Society of Offshore and Polar Engineers (ISOPE).

Knardahl, G. M. (2012). VORTEX INDUCED VIBRATIONS OF MARINE RISERS, Master Thesis. Trondheim: Norwegian Univeristy of Science and Technology, Department of Marine Technology.

Lang , D. W., Real, J., & Lane, M. (2009). Recent Developments in Drilling Riser Disconnect and Recoil Analysis for Deepwater Applications. *In ASME 2009 28th International Conference on Ocean, Offhsore Engineering, OMAE2009-79427* (pp. 305-318). Honolulu: American Society of Mechanical Engineers.

Larsen, C. M. (1990, December). Response Modelling of Marine Risers and Pipelines. *Response Modelling of Marine Risers and Pipelines*. Trondheim, Norway: The Norwegian University og Science and Technology.

Larsen, C. M. (2007). Finite Element Modelling lecture notes. Trondheim, Sør-Trøndelag, Norway: The Norwegian University of Science and Technology.

Larsen, C. M. (2008, January). Aspects of Marine Riser Analysis. Trondheim, Norway: Department of marine structures, Norwegian University of Science and Technology NTNU.

Larsen, C. M. (2008). Marine Riser Analysis. In C. M. Larsen, *Aspects of Marine Riser Analysis.* Trondheim: Norges Tekniske Naturvitenskaplige Universitet.

Larsen, C. M. (2012, January). TMR4182 Marin Dynamikk. Trondheim, Sør Trøndelag, Norway: Department of Marine Technology.

Larsen, C. M. (2013, August). Stochastic Analysis of Marine Structures, Lecture notes. Trondheim, Trondheim, Norway.

Larsen, C. M. (2014, October 28). Guidance Master Thesis. Trondheim.

MARINTEK. (2012). *RIFLEX Theory Manual.* Trondheim: MARINTEK.

MARINTEK. (2013). *Riflex user manual.* Trondheim: MARINTEK.

Microsoft Office. (2014, November 24). *Funksjon Korrelasjon*. Retrieved from Funksjon Korrelasjon: http://office.microsoft.com/nb-no/excel-help/funksjonen-korrelasjon-HP010062491.aspx?CTT=5&origin=HP010079190

Myrhaug, D. (2007, January). TMR 4180 Marin Dynamikk Uregelmessig Sjø. Trondheim, Norway: Departement of Marine Technology- Norwegian University of Science and Technolgy.

Norwegian Petroluem Directorate . (2014, 04 22). *Norwegian Petroluem Directorate* . Retrieved from http://www.npd.no/en/Publications/Resource-Reports/2014/Chapter-2/

Sævik, S. (2014, 3 10). Lecture Notes in Offshore Pipeline Technology. *Lecture Notes in Offshore Pipeline Technology*. Trondheim, Sør-Trøndelag, Norway: The Norwegian University of Science and Technology.

Sigbjörnsson, R., & Langen, I. (1979). *Dynamisk Analyse av Konstruksjoner.* Trondheim: Tapir.

Standard. (2014, 01 31). *standard.no*. Retrieved from standard.no: http://www.standard.no/en/sectors/energi-og-klima/petroleum/norsok-standards/#.U0usJVeU5Vk

Sten, R. (2012, june). Dynamic Simulations of Deep Water Driling Risers with Heave Compensation system, Doctoral thesis. Trondheim: NTNU-Norwegian University of Science and Technology.

T.Moan-N.Spidsøe-S.Haver. (1980, November). Analyse av usikkerhet. *Analyse av usikkerhet*. Trondheim, Norway: Department Of Marine Technology- The Norwegian University of Science and Techology .

Technical Comittee ISO/TC 67. (2005). *ISO 13628-7 Petroleum and natural gas industries- Design and operation of subsea production system- Part 7: Completion/Workover riser systems .* Brussel : International Organization for Standardization .

APPENDIX

A.1 CALCULATIONS

SHALLOW WATER MODEL

Component	External Area	Internal Area	Moment of inertia	Axial Stiffness	Bending Stiffness	Volume	Weight in air	Weight in Water	Buoyancy	Hydrodyna mic diameter	Mass per unit length	Mass per unit length s	Number of component	Effective weight
Unit	m^2	m^2	m^2	kN	kNm^2	m^3	kg	kg	N	m	Mg/m	kg/m		kN
Surface Flow Tree	0.15	0.03	0.0001	3.0048E+10	21248936.1	0.22436341	1761.25276	1531.28027	2256.03017	0.71912453	0.95151419	951.51419	1	8.10931718
Landing Joint	0.05	0.03	0.0000	1.0306E+10	1852791.02	0.35197806	2763.02777	2402.25026	3539.22739	0.35836676	0.18545055	185.450552	1	1.57518644
Tension joint section 3	0.05	0.03	0.0000	1.0306E+10	1704194.78	0.0588273	461.794276	401.496297	591.523171	0.34830736	0.16498545	164.985451	1	1.39999866
Tension joint section 2	0.23	0.03	0.0003	4.695E+10	52605814.8	0.05713331	448.496461	389.934821	574.489687	0.91450327	1.56816944	1568.16944	1	13.3678622
Tension Joint section 1	0.05	0.03	0.0000	1.0306E+10	1704194.78	0.08425817	661.426671	575.062042	847.237011	0.34830736	0.16498545	164.985451	1	1.39999866
Open Water Lubricator Valve	0.05	0.03	0.0000	9625016204	1374965.3	0.08840923	694.012439	603.39298	888.976888	0.32868375	0.13891362	138.913619	1	1.17763001
Safety joint	0.05	0.03	0.0000	9625016204	1374965.3	0.05393742	423.408709	368.122859	542.354194	0.32868375	0.13891362	138.913619	1	1.17763001
standard joint	0.05	0.03	0.0000	1.0127E+10	1590131.36	0.2284061	1792.9879	1558.87164	2296.68045	0.34157648	0.15480814	154.808142	27	35.4534609
Stress joint (tapered)	0.06	0.03	0.0000	1.1307E+10	2377571.07	0.32782255	2573.40705	2237.38893	3296.33774	0.38464903	0.22377453	223.774526	1	1.90205455
Non-circular cross sections														
EDP	0.37	0.03	0.0007	7.5725E+10	13834729	1.08123034	8487.65818	7379.39708	10872.0414	1.18424203	2.68342023	2683.42023	1	22.8803389
LRP	0.43	0.02	0.0009	8.7359E+10	18452441	0.92221572	7239.3934	6294.12228	9273.10961	1.27939913	3.15030174	3150.30174	1	26.8630751
XTAC	0.43	0.02	0.0009	8.7359E+10	18452441	0.42539106	3339.31984	2903.294	4277.41348	1.27939913	3.15030174	3150.30174	1	26.8630751
XMT	0.43	0.03	0.0009	8.7359E+10	18437892	1.14394816	8979.99306	7807.44619	11502.6847	1.2764929	3.12891744	3128.91744	1	26.6800187
WH	0.46	0.40	0.0003	9.3733E+10	52252688	0.14412185	1131.3565	983.631605	1449.1812	0.86354423	0.47081003	470.810028	1	3.91814703
sum=														172.767793

Table 21: Calculations shallow water model

DEEP WATER MODEL

Component	External Area	Internal Area	Moment of inertia	Axial Stiffness	Bending Stiffness	Volume	Weight in air	Weight in Water	Buoyancy	Hydrodynamic diameter	Mass per unit length	Mass per unit length	Number of components	Effective weight
Unit	m^2	m^2	m^2	kN	kNm^2	m^3	kg	kg	N	m	Mg/m	kg/m		kN
Surface Flow Tree	0.15	0.03	0.0001	3.0048E+10	21248936.1	0.22436341	1761.25276	1531.28027	2256.03017	0.71912453	0.95151419	951.51419	1	8.10931718
Landing Joint	0.05	0.03	0.0000	1.0306E+10	1852791.02	0.35197806	2763.02777	2402.25026	3539.22739	0.35836676	0.18545055	185.450552	1	1.57518644
Tension joint section 3	0.05	0.03	0.0000	1.0306E+10	1704194.78	0.0588273	461.794276	401.496297	591.523171	0.34830736	0.16498545	164.985451	1	1.39999866
Tension joint section 2	0.23	0.03	0.0003	4.695E+10	52605814.8	0.05713331	448.496461	389.934821	574.489687	0.91450327	1.56816944	1568.16944	1	13.3678622
Tension Joint section 1	0.05	0.03	0.0000	1.0306E+10	1704194.78	0.08425817	661.426671	575.062042	847.237011	0.34830736	0.16498545	164.985451	1	1.39999866
Open Water Lubricator Valve	0.05	0.03	0.0000	9625016204	1374965.3	0.08840923	694.012439	603.39298	888.976888	0.32868375	0.13891362	138.913619	1	1.17763001
Safety joint	0.05	0.03	0.0000	9625016204	1374965.3	0.05393742	423.408709	368.122859	542.354194	0.32868375	0.13891362	138.913619	1	1.17763001
standard joint	0.05	0.03	0.0000	1.0127E+10	1590131.36	0.2284061	1792.9879	1558.87164	2296.68045	0.34157648	0.15480814	154.808142	83	108.986565
Stress joint (tapered)	0.06	0.03	0.0000	1.1307E+10	2377571.07	0.32782255	2573.40705	2237.38893	3296.33774	0.3846903	0.22377453	223.774526	1	1.90205455
Non-circular cross sections														
EDP	0.37	0.03	0.0007	7.5725E+10	13834729	1.08123034	8487.65818	7379.39708	10872.0414	1.18424203	2.68342023	2683.42023	1	22.8803389
LRP	0.43	0.02	0.0009	8.7359E+10	18452441	0.92221572	7239.3934	6294.12228	9273.10961	1.27939913	3.15030174	3150.30174	1	26.8630751
XTAC	0.43	0.02	0.0009	8.7359E+10	18452441	0.42539106	3339.31984	2903.294	4277.41348	1.27939913	3.15030174	3150.30174	1	26.8630751
XMT	0.43	0.03	0.0009	8.7359E+10	18437892	1.14394816	8979.99306	7807.44619	11502.6847	1.2764929	3.12891744	3128.91744	1	26.6800187
WH	0.46	0.40	0.0003	9.3733E+10	52252688	0.14412185	1131.3565	983.631605	1449.1812	0.86354423	0.47081003	470.810028	1	3.91814703
											sum=			246.300897

Table 22: Calculations deep water model

A.2 RESULTS FROM RETRACTION ANALYSES

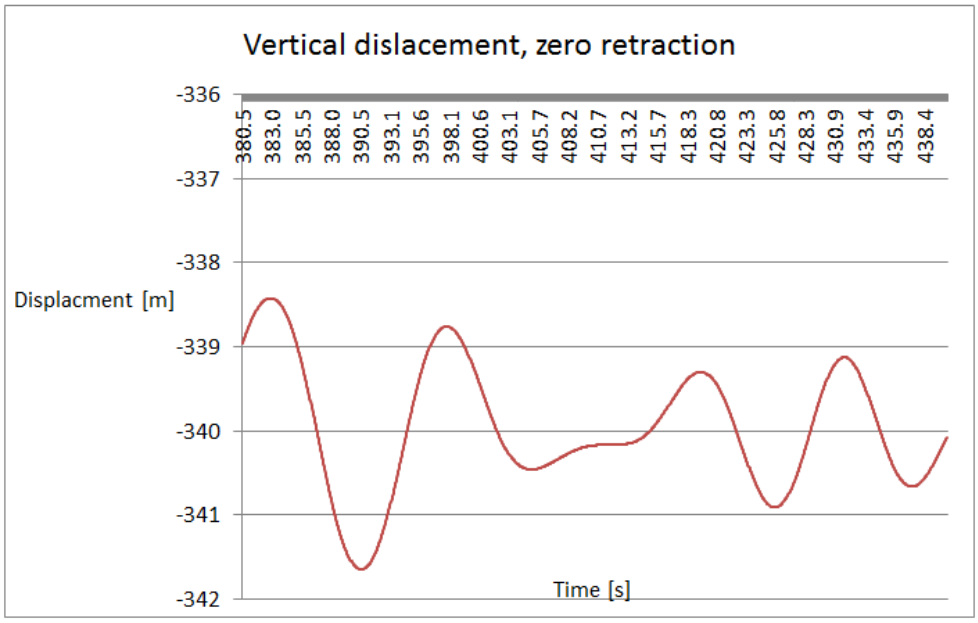

Figure 45: Single run, shallow water model with zero retraction

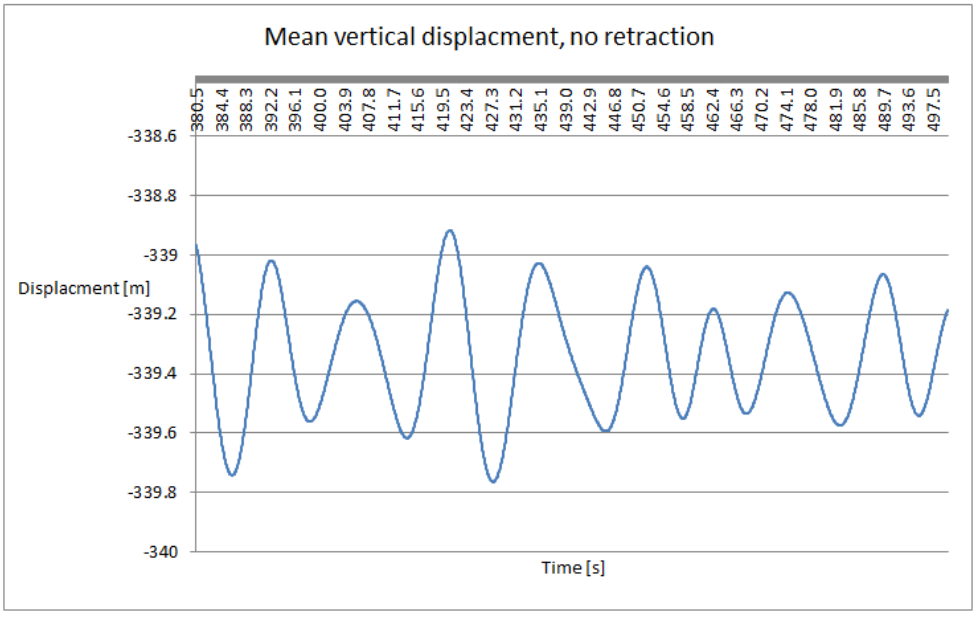

Figure 46: Shallow water model, mean vertical displacement retraction analyses

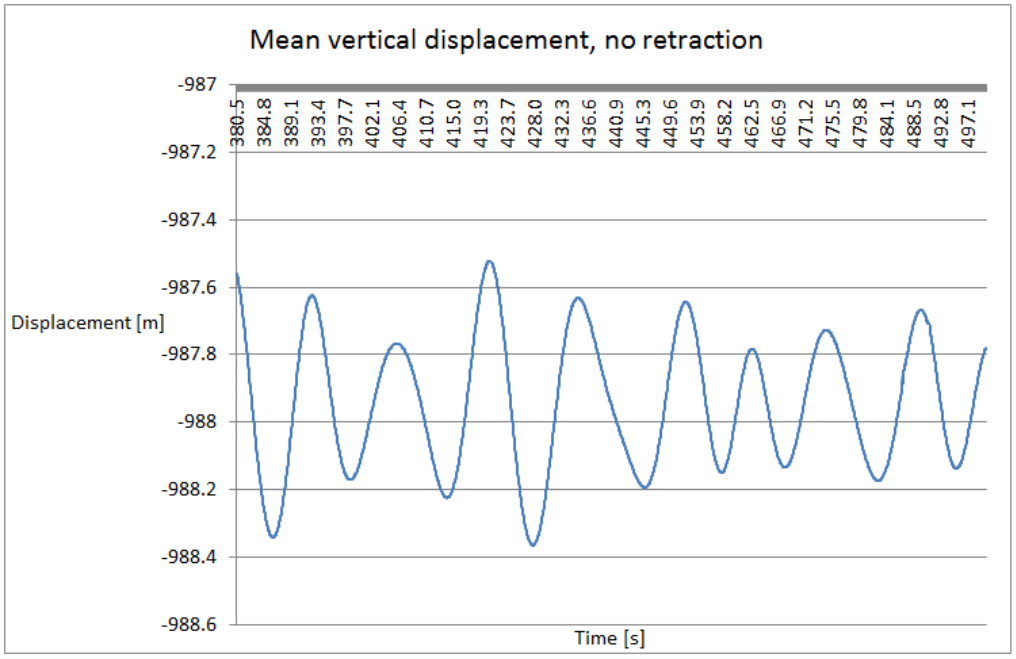

Figure 47: Deep water model, mean vertical displacement retraction analyses

A.3 CORRELATIONS RESULTS

H1	H2
0.02953211	-0.07692973
-0.13068517	-0.01309713
-0.16406377	0.12836456
0.0383695	0.25396347
0.05982717	0.24671555
0.4512469	0.00019073
0.04221598	-0.29738744
0.13122559	0.16558965
0.38324992	-0.15821457
-0.16527176	0.04224777
0.167497	0.0295639
0.15179316	-0.0591596
0.06252925	0.04243851
-0.43646495	0.44380824
0.12435913	-0.31725566
-0.16028086	-0.30975342
-0.09527206	0.13341904
0.10865529	-0.25307337
0.08592606	-0.15220642
-0.04355113	0.04688899
0.02393723	0.05280177
-0.07870992	0.04126231
-0.15481313	0.22042592
-0.23218791	0.10315577
-0.05200704	-0.00530879

Table 23: Vertical velocities Tp=8s

H1	H2
0.03973643	0.21276474
-0.21286011	0.15233358
-0.31531652	0.04008611
0.37730535	0.32513936
-0.12178421	-0.03782908
0.517114	-0.14940898
-0.02266566	-0.12076696
-0.44469833	-0.06847382
0.01856486	0.32838186
-0.4365921	0.04313787
0.12963613	0.29481252
0.1754125	-0.27160645
0.57624181	0.01525879
-0.38296382	-0.34898122
-0.13945897	-0.26601156
0.0439326	0.45671463
-0.21050771	0.01773834
-0.29335022	-0.36468506
-0.16050339	-0.09568532
0.36201477	-0.16447703
0.41615168	-0.050354
-0.02291997	0.39157867
-0.06306966	-0.07219315
0.39634705	0.28654734
-0.24159749	0.06011327

Table 24: Vertical velocities Tp=10s

H1	H2
0.05661647	0.31070709
0.01214345	-0.12435913
-0.4497846	0.0983874
-0.4612923	0.29233297
-0.0886281	-0.558122
-0.3207843	-0.01948675
-0.0651677	-0.3455162
-0.6283442	-0.22153854
0.41414897	-0.10557175
-0.2134959	-0.22080739
-0.3121058	0.09187063
0.11901855	0.23740133
0.05785624	0.16069412
0.42826335	0.06761551
0.34592946	0.05858739
-0.1550992	-0.89556376
-0.4944801	-0.20567576
0.27217865	0.27211507
0.1534462	0.17461777
0.13475418	0.09950002
-0.0449498	0.03824234
0.39345423	-0.04796982
-0.4739761	-0.04870097
-0.0224113	0.05785624
0.01935959	-0.1962026

Table 25: Vertical velocities Tp=15s

A.4 MATLAB SCRIPTS

CORRELATION SCRIPT

```
clear all
close all
%---------- Define number of files and create a storage matrix----------
numfiles=25;
mydata=zeros(8333,10,numfiles);

%---------- Open and store files----------------------------------------
for k=1:numfiles;
    shallow=sprintf('shallow%d.txt',k);
    mydata(:,:,k) = importdata(shallow);
end

%-------------Create speed matrix and start values---------------------
hiv_speed=zeros(25,2);
start1=3808;
start2=4308;
delta_t=0.03;

%------------------- Calculate the vertical velocity in all sea sates---
-
 for i=1:numfiles;

     hiv_speed(i,1)=(mydata(start1+1,7,i)-mydata(start1,7,i))/delta_t;
     hiv_speed(i,2)=(mydata(start2+1,7,i)-mydata(start2,7,i))/delta_t;
 end

 %--------------Plot in velocities in scatter diagram-----------------
 figure(1)
 scatter(hiv_speed(:,1),hiv_speed(:,2));
 xlabel('H1');
 ylabel('H2');
 title('Velocity at disconnection and 30 sec in advance');
```

COLLISION SCRIPT

```
clear all
close all
%----------------Reading the results into Matlab--------------------
fid=fopen('heave_random3.txt','r');
x0=textscan(fid,'%f %f %f %f %f %f %f %f %f %f', 8333);
fclose(fid);
%Definding constants and making matrix
x =
[x0{1,1},x0{1,2},x0{1,3},x0{1,4},x0{1,5},x0{1,6},x0{1,7},x0{1,8},x0{1,9},x0
{1,10}];

%---------------Definding the start point for the calculation--------
start=5000;
stop=8300;
collision_epd=0;
number_rows=8333;
number_rows_after=0;

for i=start:number_rows;
    if (x(i,10)~=-338.967987060550);
        number_rows_after=number_rows_after+1;

        if ((x(i,10)<=-338.967987060550)&&(abs(x(i,8))<0.3683));
            collision_epd=collision_epd+1;
        end
    end
end

 plot(x(:,1),x(:,10))
```

PLOTTING MOTION AND TIME

```
clear all
close all
%----------------Reading the results into Matlab--------------------
fid=fopen('wave_displacement1.txt','r');
x0=textscan(fid,'%f %f %f %f %f %f %f %f %f %f', 8333);
fclose(fid);
%Definding constants and making matrix
x =
[x0{1,1},x0{1,2},x0{1,3},x0{1,4},x0{1,5},x0{1,6},x0{1,7},x0{1,8},x0{1,9},x0
{1,10}];

total_time=zeros(8333,1);
heave_displacement=zeros(8333,1);
noe=0;
disconnect_motion=zeros(8333,1);
%----------------Define the heave motion and time----------------
for i=1:8333;
    total_time(i)=x(noe+i,1);
    heave_displacement(i)=(x(noe+i,7)-25);

end
%----------------Plot heave displacement vessel--------------------
figure(1)
plot(total_time,heave_displacement);
xlabel('t');
ylabel('Heave motion vessel');

%-----------------Define motion EDP-------------------------------
for j=1:8333;
    disconnect_motion(j)=x(noe+j,10);
end
%-----------------Plot motion EDP----------------------------------
figure(2)
plot(total_time,disconnect_motion);
xlabel('t');
ylabel('Motion z-direction EDP');
title('Motion EDP');
```

A.5 HANG-OFF MODE

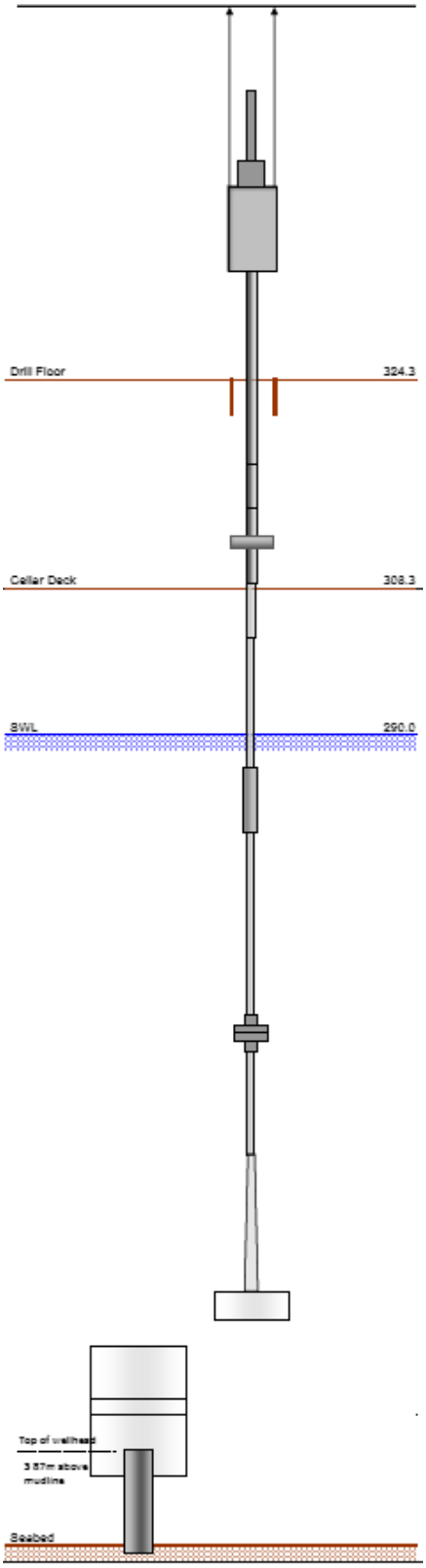

Figure 48: Hang-off mode (Aker Solutions, 2014)

A.6 EXCERPT FROM A CUSTOMER SPECIFCICATION FROM AKER SOLUTIONS

Design Codes and standards

The riser is to be designed according to ISO 13628-7 standard Ref./S.1/ and Statoil governing document TR3541, Ref./C.1/. The riser system has Statoil categorization type B. Certain aspects of categorization C will come into effect. In particular refer to TR3541, section D.4, Ref./C.1/.

The analysis methodology is according to ISO 13628-7 Ref./S.1/, TR3541 Ref./C.1/ and DNV recommendations for wellhead fatigue, Ref./E.1/. Consideration has also been given to inputs from ISO 13624-1 Ref./S.7/, ISO 13624-2 Ref./S.8/ and DNV-RP-H103, Ref./S.6/ with respect to drilling riser equipment, operations and marine operations.

Other supplementary references include the following:

- DNV-RP-C205 Environmental Conditions and Environmental Loads, Ref./S.2/.
- DNV-RP-F204 Riser Fatigue, Ref./S.3/.
- DNV-RP-C203 Fatigue Design of Offshore Steel Structures, Ref./S.5/.
- DNV-RP-H103 Modelling and Analysis of Marine Operations, Ref./S.6/.

The priority order is as follows:

1. NPD regulations and provisions
2. Statoil specifications
3. Project specifications
4. NORSOK standards
5. ISO standards
6. Other documents

A.7 INFORMATION PROVIDED BY AKER SOLUTIONS

Operating Mode	Tree and TH mode		TH mode, typical values	
	Significant wawe height [A] (m)	Static vessel offset range [B] % MSL	Marine riser top ball joint angle, (°)	Marine Riser bottom flex joint angle (°)
Running and retrieval [D]	5.5	NA	±3/±1 [C]	±3/±1 [C]
Running and suspending of spider [D]	7.5	NA	NA	NA
Landing and connecting [E]	5.5	±2	±4	±3
Over pull to verify lockdown, 20 metric tonnes overpull	5.5	±5	±3	±3
System Pressure test	5.5	±5	±4	±3
Normal operation, shut in surface	5.5	±5	±4	±3
Extreme shut in subsea	7.5	±9	±4	±
Planned / normal disconnect	5.5	±5	±3/±1 [C]	±3/±1 [C]
Quick disconnect	7.5	±18	±10	±10
Hang-off	10 year	NA	±7	NA
Overpull to release stuck TH/Tubing	5.5	±5	±3	±2
Tensioner failure – loss of one tensioner	7.5	±18	±4	±
Tensioner failure – loss of top compensator tension	7.5	±18	±4	±3
Excessive top tension – maximum breaking load of weak link/safety joint [F]	NA	±13	±7.5	±7.5
Disconnect failure (EQD connector, LMRP)	±TBD	±TBD	±TBD	±TBD
DP failure – drive off/drift off	7.5	±18	±10	±10
Loss of one anchor	7.5	13	7.5	7.5

A) Wave peak periode range covering 90% confidence interval from the wave scatter diagram shall be applied

B) Static (mean) vessel offset relative to the well centre in % of mean sea level (MSL). Dynamic vessel offset due to wave motion comes in addition.

C) ±1° applies when the landing string/tools is passing through, else ±3.

D) Includes normal running and pressure testing during.running. Note that Tree mode includes running/retrieval with EDP and/or LRP.

E) Maximum landing speed 0.5 m/s. Check connector stabilising/tilting moment to ensure zero connecting angle. Max/min set down weght to be established for EDP, LRP and LS as applicable.

F) Identify weak point above barrier elements and rank critical elements due to excessive top tension independent of cause. Check both upstroke and downstroke in case of stuck motion compensator. Shall be checked for subsea shut-in and zero pressure in riser. Static analysis may be performed.

G) For all above conditions, a one year current shall be applied.

H) Maximum equipment landing heave (i.e. max to min) is 2m

Figure 49: Requirements to the Workover System (Aker Solutions, 2014)

A.8 SEED NUMBERS RANDOM DISCONNECT

Tp=8s	Seed
1	98763
2	87634
3	31457
4	76833
5	34779
6	34589
7	15793
8	45380
9	79340
10	74389
11	76435
12	84610
13	88698
14	90742
15	91764
16	92275
17	92530
18	92658
19	92722
20	92754
21	92770
22	92778
23	92782
24	92784
25	92786

Table 26: Seed Tp=8sec

Tp=10s	Seed
1	50414
2	49126
3	48482
4	48160
5	47999
6	47919
7	47879
8	47859
9	47849
10	47844
11	47841
12	47839
13	46552
14	45908
15	45586
16	98763
17	87634
18	31457
19	76833
20	34779
21	34589
22	15793
23	45380
24	79340
25	74389

Table 27: Seed Tp=10s

Tp=15s	Seed
1	48160
2	48161
3	48162
4	48163
5	48164
6	86689
7	41398
8	89797
9	39434
10	17833
11	87364
12	63543
13	86543
14	92784
15	99025
16	105266
17	111507
18	117748
19	123989
20	130230
21	136471
22	142712
23	148953
24	155194
25	74934

Table 28: Seed Tp=15sec